THE ROLE OF MAMMALIAN TARGET OF RAPAMYCIN (mTOR) IN A MOUSE MODEL OF CEREBRAL PALSY

A Dissertation
Submitted to
the Temple University Graduate Board

In Partial Fulfillment
of the Requirements for the Degree
DOCTOR OF PHILOSOPHY

---

by
Isha N. Srivastava
May 2017

Examining Committee:
Dr. Peter Crino, M.D., Ph.D., Advisor, Shriners Hospital Pediatric Research Center
Dr. Michael Selzer, M.D., Ph.D., Shriners Hospital Pediatric Research Center
Dr. Dianne Soprano, Ph.D., Department of Medical Genetics and Molecular Biochemistry
Dr. Tanya Ferguson, Ph.D., Shriners Hospital Pediatric Research Center
Dr. Ignacio Valencia, M.D., External examiner, St. Christopher's Hospital for Children

ABSTRACT

The mammalian target of rapamycin (mTOR) is a serine/threonine kinase that governs cellular responses to various environmental stimuli, including nutrients, oxygen, energy, and growth factors. mTOR signaling, altered independently by hypoxia-ischemia and inflammation, plays a critical role in cell death following environmental stress. While the mTOR signaling cascade has been linked to several pediatric neurological disorders, a role for mTOR modulation in cerebral palsy (CP) has not been investigated. CP is a prevalent neurodevelopmental disorder characterized by a heterogeneous phenotype including impaired motor function accompanied by intellectual disability, blindness, and epilepsy. Both hypoxia-ischemia and inflammation are linked to CP, but the pathogenesis of CP remains unknown. Thus, I hypothesized that neuronal death in an animal model of CP is mTOR-dependent. Furthermore, inhibition of mTOR would diminish neuroinflammation and prevent neuronal death in a mouse model of CP

Post-natal day 6 (P6) mouse pups were subjected to hypoxia-ischemia and lipopolysaccharide-induced inflammation (HIL), an animal model of CP that causes neuronal injury within the hippocampus. Pups received rapamycin (an mTOR inhibitor; 5mg/kg) or saline immediately following HIL, and then for 3 subsequent days. Phosphorylation state and total expression of the mTOR effector proteins S6, S6K and 4EBP as well as upstream negative regulators, TSC1 and Redd1, were assessed as an *in vivo* measure of the mTOR signaling cascade. Expression of hypoxia inducible factor 1 (HIF-1α) was assayed as an indicator of hypoxia-mediated cellular injury. Neuronal cell death was defined with Fluoro-Jade C (FJC) and cleaved-caspase 3 (CC3), a marker of apoptosis. Autophagy was measured using Beclin-1 and LC3II expression. Lastly,

neuroinflammation following HIL was evaluated by examining Iba-1 labeled microglia number and morphology, as well as P-STAT3 expression.

Increased FJC staining and HIF-1α expression, which colocalized to areas of neuronal death, was observed in the hippocampus and cortex occurs within 48h of HIL exposure. Enhanced CC3, Iba-1 and HIF-1α expression was present in the periventricular white matter, a neuropathological hallmark of CP. Numerous Iba-1 labeled, activated microglia were evident at 24 and 48 hours following HIL. Basal mTOR signaling was unchanged by HIL at 24 and 48 hours. Coincident with persistent mTOR signaling, a decreased in Redd1 expression but not TSC1 was observed in HIL. Increased P-STAT3 expression was observed at 24 and 48 hours post-HIL. Rapamycin treatment following HIL significantly reduced neuronal death, decreased HIF-1α and P-STAT3 expression, and microglial activation, coincident with enhanced expression of Beclin-1 and LC3II, markers of autophagy induction. Increase in neuronal death was observed with concomitant administration of rapamycin and chloroquine, an autophagy inhibitor. Administration of a S6K inhibitor, PF-4708671, following HIL also decreased FJC staining further supporting an mTOR-dependent effect of HIL.

mTOR inhibition *following HIL* prevented neuronal death and diminished neuroinflammation in this model of CP. Decreased expression of Redd1, a negative upstream regulator of mTOR, likely contributes to constitutive expression of mTOR following HIL. Persistent mTOR signaling results in a failure of autophagy induction, which may contribute to neuronal death in CP. Rapamycin inhibited expression of HIF-1α and led to autophagy induction in association with diminished cellular injury. Rapamycin-mediated neuroprotection was reduced with concomitant administration of

chloroquine supporting that induction of autophagy promotes neuronal survival. Rapamycin was also associated with decreased P-STAT3 by glia coincident with a substantial decrease in microglial activation within the injured brain. Furthermore, this is the first evidence that treatment with S6KI following HIL is also neuroprotective, resulting in decreased neuronal death at levels similar to rapamycin. Collectively, these results provide pre-clinical evidence that mTOR signaling plays an integral role in promoting neuronal death following HIL. Furthermore, these results suggest that mTOR signaling may be a novel therapeutic target to reduce neuronal cell death in a subset of CP patients.

Dedicated to my amazing parents

– your unconditional love, support and

encouragement makes even the

impossible seem possible

ACKNOWLEDGEMENTS

I am deeply grateful for all those that have helped and guided me in one way or another during these three years of graduate work. Science is a collaborative effort and I am fortunate to be around so many talented and supportive individuals.

First and foremost, I'd like to thank my advisor and mentor, Peter Crino, for his unwavering support and guidance. I have the utmost gratitude and respect for Pete. He is a continuous source of inspiration for me and other young scientists. Pete is the kind of physician-scientist that I aspire to be when "I grow up" - innovative, brilliant, tenacious and approachable. I am eternally grateful that Pete gave me the independence to pursue my ideas and find my own way without ever letting me wander too far from the objective. It has truly been an honor learning from and working with Pete. Needless to say, this project would not have come to fruition without his help.

I am grateful for all my thesis advisory committee members, Dr. Michael Selzer, Dr. Dianne Soprano and Dr. Tanya Ferguson. I am thankful for their guidance throughout the process of transforming a handful of ideas into a completed project. I appreciate the time and effort they put in to attend my committee meetings. Their insightful feedback and perceptive comments about my results challenged me to evaluate my work more critically and helped me become a better scientist. I would also like to thank Dr. Ignacio Valencia for generously sharing his time to participate in my examining committee.

The Crino Lab is more like a family and I have enjoyed getting to know every single one of them. Xin-Ming's experience and useful comments during lab meetings were always helpful. Jennifer, with her positive attitude and optimism, was a delight to have in the lab, especially on those days where nothing went as planned. A special thank-

you to Jona – without her help, I may still be analyzing FJC data. I feel fortunate that I've been able to come to work alongside Marianna and MV, who have made this journey an enjoyable one. I truly appreciate their constant encouragement and continued support (and of course, I am especially thankful that Marianna did not "drown me at birth" ☺). Marianna was always willing to listen and help me with absolutely everything in my life, from immunostaining gone awry to dealing with all the "crazypants" in the world. I admire her independence and assertiveness, but also her enthusiasm for enjoying life. I hope in our time together some of these attributes have rubbed off on me! Whether it was our morning coffee time discussing and troubleshooting experimental mishaps or chatting about our lives, MV was always there to help me in any way she could. She is such a bright, fun, and caring person, who I am lucky to call my friend. She is amazing and I know that she will accomplish great things in her career!

Tanya deserves a special acknowledgement for teaching me the HIL surgeries, helping me with my mice related questions and all of her guidance relating to the lab and life along the way. Also, a special thank-you to Katherine, a former member of the Ferguson lab, for her patience while teaching me the microdissection technique.

I'd like to thank all the amazing people at Shriners Hospital Pediatric Research Center and the MD/PhD program for their support. I am especially grateful to Dr. Soprano, our program director, for her help and advice in navigating this process and the complicated transitions between medical and graduate school. Whether we were planning the APSA NERM, exploring my research interests or discussing my career goals, she has been a constant source of support and wisdom. She is a strong advocate for MD/PhD students and has always encouraged me to pursue my clinical and research interests.

Tracy Burton and Tracey Hinton deserve a huge thank-you for ensuring everything was completed in a timely manner without any glitches.

I am sincerely grateful for my MD classmates and my fellow MD/PhD students for their support. I'd like to thank Paul and Kaitlin for celebrating and commiserating with me throughout this process. Since that first summer research report that none of us knew we had to submit, I knew I had found two friends with whom I could share all aspects of the MD/PhD journey. I also have to thank Glenn and Lindsey for their advice about surviving medical and graduate school, support as I complained about my failed experiments and fun quizzo get-togethers! I want to acknowledge Ara, Rick, and Dina, my friends from medical school, for organizing fun outings and encouraging me to take a break from lab work.

I am so grateful for my college friends, Aparna, Sonia, Pooja, and Michelle. Their unwavering support and pep talks during our phone dates were essential in boosting my spirits during graduate school. My yearly reunion trips and mini-vacations with Sonia, Kamini and Deepika were always fun and provided some much needed R&R.

Through all the ups and downs, Ali has been my best friend and confidante. I admire his thirst for learning, thoughtfulness and patience. He inspires me to be the best version of myself. Ali has taught me to roll with the punches and given me the confidence to tackle challenges head on. I do not know how I would have done this without him.

Last but not least, I would like to thank my family (aka my fambam)! Everything I am I owe to my parents, Indresh and Ranjana, and my little brother, Sidharth. I do not know what I did to deserve such an amazing fambam. Through it all, they have been my

rock. Their unconditional love and support were a source of strength and comfort throughout this experience. They believed in me and saw my potential even when I did not. Whether it was organizing family phone dates, trekking down to Philly to visit me, patiently listening to me vent, planning a mini-vacation to relax or troubleshooting experiments with me, they were always willing to do anything to help. They mean the world to me and I would not have been able to reach this milestone without them!

TABLE OF CONTENTS

page

ABSTRACT iii

DEDICATION vi

ACKNOWLEDGEMENTS vii

LIST OF TABLES xiv

LIST OF FIGURES xv

LIST OF ABBREVIATIONS xvi

CHAPTER 1: INTRODUCTION 1

Classification and Sub-types of CP 1

Motor abnormalities 2

Associated Impairments 3

Neuroanatomical features 3

Etiology and Risk Factors 4

Maternal factors 5

Genetic factors 6

Prematurity and Low Birth Weight 7

Multiple births 8

Coagulation Disorders 8

Placental pathology 9

Hypoxia-ischemia and Perinatal Stroke 10

Intrauterine infection and inflammation 12

Multi-factorial etiology of CP 14

Animal Models of CP 15

Models induced by hypoxia-ischemia 16
Models induced by infectious agents 18
Models induced by combination of hypoxia-ischemia and infection..... 21
mTOR signaling cascade in the brain 23
mTOR in hypoxia-ischemia 28
mTOR in inflammation 30
Statement of Purpose 32
CHAPTER 2: MATERIAL AND METHODS 34
HIL Animal Model 34
Immunohistochemistry (IHC) and Immunofluorescence (IF) 35
Fluoro-Jade Staining and Quantification 37
Western Blotting 38
Statistical Analysis 40
CHAPTER 3: RESULTS 41
HIL Model 41
Changes in neonatal body temperature and body weight following HIL... 41
Constitutive mTOR signaling following HIL 44
Persistent phosphoactivation of S6 and S6K post-HIL 44
Constitutive phospho-inactivation of 4EBP1 following HIL 46
REDD1, but not TSC1, may contribute to mTOR activity following HIL 49
Enhanced HIF-1α associated with areas of neuronal death 49
Rapamycin is neuroprotective in HIL model of CP 51
Neuronal death is mTOR dependent 51

Rapamycin reduces neuronal death following HIL 55
Short course of rapamycin provides long-term neuroprotection 55
Neuroinflammation following HIL is mediated by mTOR 58
Rapamycin reduces microglia activation 58
P-STAT3 may contribute to mTOR-dependent microglia activation 60
Rapamycin results in transient autophagy induction 62
HIL results in failure of autophagy induction 62
Rapamycin-mediated neuroprotection is in part due to autophagy 66
CHAPTER 4: DISCUSSION 69
CHAPTER 5: FUTURE DIRECTIONS AND IMPLICATIONS 75
Potential mechanisms of decreased Redd1 expression 75
Differential effects and regulation of S6K and 4EBP1 76
The role of mTOR in microglia function and polarization 77
mTOR-mediated neuronal death may promote white matter damage in CP 79
Clinical application of rapamycin as a therapeutic intervention in CP 80
REFERENCES 83

LIST OF TABLES

page

Table 1. Avg body temperature (°C) and avg change in body weight (grams) post-HIL 43

LIST OF FIGURES

page

Figure 1. mTOR signaling cascade 25

Figure 2. The HIL animal model of CP and treatment scheme 35

Figure 3. Neuronal and periventricular white matter injury following HIL. 42

Figure 4. P-S6 and P-S6K following HIL and HIL+Rapamycin 45

Figure 5. DAPK and P-DAPK expression is not changed following HIL. 47

Figure 6. P-4EBP1 following HIL and HIL+Rapamycin. 48

Figure 7. Expression of upstream regulators, TSC1 and Redd1, following HIL. 50

Figure 8. Increased HIF-1α expression localizes to areas of neuronal death. 52

Figure 9. mTOR inhibition during period of maximal injury is protective. 54

Figure 10. Analysis of neuronal death in HIL model of CP. 56

Figure 11. Neuropathological sequelae of HIL at 1 week and 1 month. 57

Figure 12. Rapamycin treatment ameliorates neuroinflammation following HIL 59

Figure 13. Microglia activation following HIL is mTOR dependent. 61

Figure 14. P-STAT3 activation following HIL localizes to microglia. 63

Figure 15. Schematic representation of autophagy. 64

Figure 16. Rapamycin treatment post-HIL results in transient autophagy induction. 65

Figure 17. Inhibiting autophagy reduces rapamycin-mediated neuroprotection. 67

Figure 18. Reduced microglia activation following autophagy inhibition. 68

LIST OF ABBREVIATIONS

4E-BP1	Eukaryotic translation initiation factor 4E-binding protein
5’-TOP	5’-terminal oligopyrimidine
CA1	Cornu ammonis area 1
CA3	Cornu ammonis area 3
CC3	Cleaved-caspase 3
Chq	Chloroquine
CP	Cerebral palsy
DAPI	4',6-diamidino-2-phenylindole
DAPK	Death associated protein kinase
FJC	Fluoro-Jade C
HI	Hypoxia-ischemia
HIF-1α	Hypoxia inducible factor 1
HIL	Hypoxia-ischemia LPS-induced inflammation
iNOS	Inducible nitric oxide synthase
LPS	Lipopolysaccharide
mTOR	Mammalian target of rapamycin
OD	Optical density
P-4EBP1	Phosphorylated eukaryotic translation initiation factor 4E-binding protein
P6	Post-natal day 6
P-DAPK	Phosphorylated death associated kinase
PRTE	Pyramidine-rich translational element
P-S6	Phosphorylated ribosomal protein S6

P-S6K	Phosphorylated ribosomal protein p70 S6 kinase
P-STAT3	Phosphorylated signal transducer and activator of transcription 3
PVL	Periventricular leukomalacia
Rapa	Rapamycin
REDD1	Regulated in development and DNA damage 1
ROI	Region of interest
S6	Ribosomal protein S6
S6K	Ribosomal protein p70 S6 kinase
S6KI	Ribosomal protein p70 S6 kinase inhibitor, PF-4708671
SR/L/M	Strata radiatum, lacunosum, moleculare
STAT3	Signal transducer and activator of transcription 3
TLR4	Toll-like receptor 4
tMCAO	Transient middle artery occlusion
TOR1/2	Target of rapamycin 1/2
TSC1	Tuberous sclerosis complex 1

CHAPTER 1: INTRODUCTION

Cerebral palsy (CP) is among the most common neurodevelopmental disorders, affecting 2-3 out of every 1,000 live births in the United States[1]. The most recent definition of CP describes it as a "a group of permanent disorders of the development of movement and posture, causing activity limitation, that are attributed to non-progressive disturbances that occurred in the developing fetal or infant brain. The motor disorders of CP are often accompanied by disturbances of sensation, perception, cognition, communication, behavior, by epilepsy and by secondary musculoskeletal problems"[2]. This definition emphasizes 5 core components of CP: 1) it is an umbrella term, describing a diverse group of disorders; 2) it is a disorder of movement and/or posture and motor function; 3) it results from an abnormality/lesion in the brain; 4) this lesion is acquired early in life; and 5) the condition is permanent, but may not be static [2–4].

Classification and Sub-types of CP

Due to the heterogeneous group of disorders encompassed in the definition, CP is further classified into subtypes to facilitate description of the deficits, management/treatment of children with CP, comparison of cases, and evaluation of changes in clinical manifestations over time[2]. The classification is based on the motor abnormalities (nature, localization and severity of the abnormality), associated impairments, and neuroanatomical features[2,3].

Motor abnormalities

CP can be divided into spastic, dyskinetic (further classified into dystonic or choreoathetoid) and ataxic depending on the predominant type of motor disorder present. A second method of classification based on physiology divides CP into pyramidal (spastic) or extra-pyramidal (non-spastic). Pyramidal, or spastic CP, is characterized by stiff or unyielding muscle tone (hypertonia), increased reflexes (hyperreflexia), and a scissor or tiptoe. It is thought that spastic CP results from damage to the motor cortex or corticospinal tracts in the brain resulting in upper motor neuron type of lesions. Spastic CP accounts for 75-80% of children with CP[5–7]. Spastic CP can be sub-divided to hemiplegia, diplegia, or quadriplegia based on localization of abnormal motor function.

Extrapyramidal CP, which includes both dyskinetic and ataxic CP, is thought to result from lesions outside of the pyramidal tracts, e.g. the basal ganglia, thalamus and/or cerebellum. Dyskinetic CP is defined by involuntary, uncontrolled movements of either the extremities or the trunk, which are especially noticeable when an individual attempts to move. These movements can be slow, writhing, and repetitive (athetoid) or irregular, jerky, and dance-like (chorea) or a mix (choreoathetoid). When the involuntary movements are accompanied by an abnormal or sustained posture, it is classified as dystonic CP. The muscle tone in dyskinetic CP can vary with emotion, stress and attempted movement.

Lastly, ataxic CP is characterized by problems with coordinated movements and fine motor control. Balance and posture are commonly affected, often manifesting as a wide and irregular gait. Mixed CP is used to describe cases where impairments in some limbs are spastic whereas other limbs display non-spastic motor abnormalities.

The severity and functional consequences of motor deficits are classified using objective scales. The Gross Motor Function Classification System (GMFCS) groups individuals with CP into levels based on mobility and activity limitation[8]. Other scales that are used include the Functional Mobility Scale (FMS), to evaluate gait, and/or the Manual Ability Classification System (MACS), to assess hand and arm function[9,10].

Associated Impairments

In addition to motor impairments, individuals with CP often have associated conditions such as cognitive disability and epilepsy that can contribute to activity limitations. These conditions are believed to result from similar processes as the motor deficits[2]. A systematic review of case studies involving 886 children with CP demonstrate that the most common associated impairments include intellectual disability (52%), epilepsy (45%), ophthalmologic defects (28%), speech and language disorders (38%) and hearing impairments (12%)[11].

Neuroanatomical features

Neuroimaging, especially magnetic resonance imaging (MRI), provides an important tool to visualize pathogenic abnormalities during brain development. In a systematic review by the American Academy of Neurology and the Child Neurology Society, imaging abnormalities are noted in 89% of children with CP[11]. The most common abnormalities observed in neuroimaging are periventricular white matter injury (19-56%), diffuse gray matter injury (14-18%), cerebral vascular accident (11-16%) and

cerebral malformations (9-11.3%) in children with CP[12–14]. Grey matter involvement in CP includes injury to cortical and subcortical areas, such as the hippocampus, basal ganglia and thalamus[15,16]. Isolated white matter lesions are most common in bilateral spastic or athetoid CP, whereas a combination of white and grey matter lesions are most common in hemiplegic spastic CP[17]. Isolated grey matter lesions are a rare imaging finding across CP subtypes[17]. Thalamic abnormalities are often noted in children with periventricular white matter injury, a neurological hallmark of CP, and may contribute to long-term cognitive deficits in these children[18]. Furthermore, the presence of lesions in the cortical or subcortical grey matter is associated with more severe functional impairments in CP[12,16,19].

Since regions of the brain that are susceptible to injury change throughout development, the type of brain lesion that is present may provide insight to the timing of the insult. Cerebral malformations are most prevalent during the first 20 weeks of gestation[20]. The brain is vulnerable to periventricular white matter damage during weeks 28-32, and grey matter damage and neonatal stroke after week 34[20]. Thus, a majority of CP results from insults in the late second and third trimester of pregnancy.

Etiology and Risk Factors

An English orthopedic surgeon Dr. William Little first described CP, unnamed at the time, in a series of lectures from 1830-1850, culminating in his seminal paper where he asserted that brain damage related to preterm birth and birth asphyxia was associated with spasticity and paralysis, clinical manifestations of cerebral palsy[21]. Dr. Little was

one of the first clinicians to suggest that complications leading to birth asphyxia could result in adverse outcome later in life. The term "cerebral palsy" was introduced by Sir William Osler in 1889, when he provided an extensive classification of the motor deficits in CP[22]. Sigmund Freud further expanded the conceptualization of CP emphasizing that that the causes of CP were not limited to complicated delivery[23,24]. In fact, Freud asserted that prenatal factors (e.g. factors during early pregnancy and fetal brain development), in addition to perinatal factors (e.g. difficult pregnancy), contribute to neurological deficits of children with CP [23,24]. And, thus began the controversy surrounding the pathogenesis of CP, which remains elusive even today.

A population based study demonstrated that complicated births account for less than 10% of cerebral palsy cases[25], supporting Freud's assertion. Though a single precipitating event has not been identified, 70-80% of CP cases are associated with antenatal injuries[26]. Several risk factors in the antenatal, perinatal or postnatal periods of development, alone or in combination, including maternal thyroid disease, placental pathology, prematurity, low birth weight, multiple gestations, coagulation disorders, hypoxia-ischemia, and fetal exposure to maternal infection or inflammation[27,28] are highly associated with the pathogenesis of CP.

Maternal factors

There are certain pre-existing maternal conditions that can enhance the risk of CP. Advanced maternal age (> 35 years) is associated with a 2-fold increase in the risk for CP[27,29]. Furthermore, maternal obstetric history of stillbirth and neonatal death, as well as greater than 3 miscarriages, were strongly associated with increased risk of CP[27]. A systematic review of children with CP and their parents demonstrated that mothers with a

history of seizures, intellectual disability or thyroid disease significantly increased the risk of CP[27]. Family histories of epilepsy or neurological diseases are associated with over a 2.5 fold increase in risk of newborns with neurological complications, like CP[30,31]. Interestingly, *in utero* exposure to magnesium sulfate, commonly prescribed for maternal seizures, has been shown to reduce the risk of white matter damage in neonates[32]. Women with thyroid disease were over 9 times more likely to have a newborn with moderate to severe "encephalopathy"[30], a condition which can precede a CP diagnosis[33], than those without.

Another maternal risk factor is the use of in vitro fertilization (IVF), which is associated with a 3.7 times increased risk of CP[34], in part, due to the increased frequency of multiple gestations, prematurity and low birth weight[34,35] with IVF, which are all independent risk factors for CP (see below).

Genetic factors

There is evidence that familiar forms of CP exist, although genetic forms of CP account for less than 2% of all CP cases[36]. The rate of CP is higher in monozygotic twins compared to dizygotic twins[37]. Furthermore, parents with one affected child are at 4.8-fold increased risk of having another child with CP[36]. Consanguineous families have an increased risk of CP compared to outbred families[38,39]. Monogenic forms of CP have been identified. Genetic linkage studies have missense mutations in *GAD1* (glutamate decarboxylase 1, important for the production of GABA from glutamate) and deletions in *KANK1* (KN motif and ankyrin repeat domains 1, integral in protein-protein interactions and regulates actin polymerization) in familial forms of CP[40,41]. More recently, several

genetic variants in potentially pathogenic genes have been identified in children with CP[42,43]. Whole exome sequencing identified *de novo* mutations in three previously identified disease genes, *TUBA1A, SCN8A* and *KDMSC*, as well as six novel candidate genes *AGAP1, JHDM1D, MAST1, NAA35, RFX2* and *WIPI2*[42]. Additionally, copy number variation (CNV) analysis demonstrated a rare variation in 10 (20%) of the 50 CP cases studied[43]. Of the 14 CNV's identified, 8 were inherited from an unaffected mother, 3 from an unaffected father and 3 with unknown inheritance[43]. However, further studies are necessary to determine whether these genes contribute to CP pathogenesis or are merely biomarkers for CP risk. Hereditary forms of CP may help identify pathways or proteins that may predispose an individual to sporadic CP.

Prematurity and Low Birth Weight

Prematurity is an important risk factor for CP. In children born at term (37-42 weeks gestation), the prevalence of CP is approximately 2-3 out of 1000 live births[1], but increases to 40/1000 in children born at 28-31 weeks gestation and 76.6/1000 in children born before 28 weeks gestation[44]. Furthermore, though infants born prematurely account for less than 5% of all births, they account for approximately 43% of all CP cases[45]. Similar to prematurity, there is a step wise increase in the incidence of CP among children with low birth weight – from 6.7/1000 live birth in infants with birth weights of 1500-2500g to 84/1000 in infants weighing less than 1000g[44]. The association of prematurity and CP is of significant importance in developed nations, which have increased survival of premature and low birth weight neonates.

Multiple births

Babies resulting from multiple births (e.g. twins, triplets, etc.) are at increased risk of CP – the prevalence of CP among twins is 12.6 in 1,000 live births and 44.8 in triplets[46] compared to 2-3 in 1000 live births for singletons[1]. Furthermore, antenatal death of twin markedly increases the risk of CP in the surviving twin[46,47]. The association between CP and multiple births is in part due to the higher rate of prematurity and low birth weight among multiple births, which are both risk factors for CP[46,48].

Coagulation Disorders

Children with CP had increased levels of antibodies against coagulation factors, such as antithrombin III, mutated factor V Leiden and to proteins C and S [49]. Studies investigating a direct link between inherited thrombophilias and CP have had mixed conclusions. Though there is increased frequency of mutations in *Factor V Leiden* (FVL) in children with CP and their mothers[49,50], it alone is not directly associated with an increased risk of CP[50,51]. A case-control study from 443 CP cases established that among common polymorphisms in hereditary thrombophilias mutations in methylenetetrahydrofolate reductase (MTHFR), alone or in combination with prothrombin gene mutation (PGM), confer a slight increased risk of CP in all gestational ages[51]. However, a recent systematic review of hereditary thrombophilia and CP literature failed to establish a direct correlation to CP[52]. Though single thrombophilias may not increase risk of CP, combinations of two or more hereditary thrombophilias or the combination of thrombophilias and other risk factors for CP have additive effects[51,52].

Inherited or acquired thrombophilias disorders can predispose children to vascular injury in either placental or fetal blood vessel, which may lead to complications during antenatal and perinatal period[49]. Thus, it is likely that coagulation disorders alone may not be sufficient to result in neurological damage, but in combination with other genetic or acquired risk factors, may contribute to the pathogenic sequence leading to CP.

Placental pathology

The placenta serves as the sole supply of substrates necessary for fetal wellbeing; thus disruption of maternal-placenta or placenta-fetal vasculature has been associated with adverse neurological outcomes. For example, separation of the placenta from the uterine wall (abruptio placentae), which can result in reduced blood flow to the fetus, has been associated with up to an 8-fold increased risk for CP[28,53]. One or more severe fetal placental lesions, including fetal thrombotic vasculopathy, villitis of unknown cause with obliterative fetal vasculopathy, chorioamnionitis with severe fetal vasculitis and meconium-associated fetal vascular necrosis, were found in 52% of placentas from infants with CP compared to only 10% in control placentas[54]. Furthermore, the risk of neurological impairment, such as CP, increases as a function of the number of placental lesions present[55]. Rather than directly affecting placental vasculature, placental lesions may also decrease the reserve capacity of the placenta, or the ability of the placenta to compensate for adverse or stressful insults during the pregnancy and labor. Abnormally small placentas have decreased surface area for gas exchange and, thus, may have diminished reserve capacity[56]. These placentas might account, in part, for the association of in utero growth restriction and CP[57].

As a direct link between mother and fetus, the placenta is subjected to the same processes as the fetus in utero. Thus, in addition to identifying placental lesions contributing to CP pathogenesis, examination of the placenta may provide insights into the antenatal environment and may help causal or contributing factors, such placental malformations, presence of infection, maternal or fetal thromphilias, placental infarction and maternal hypoperfusion, that increase risk of fetal brain injury.

Hypoxia-ischemia and Perinatal Stroke

Hypoxic-ischemic insults can be groups into global hypoxia-ischemia (such as reduced blood flow to the fetus due to obstetric complications) and tissue specific oxygen deprivation (cerebral hypoxia-ischemia or stroke). Birth asphyxia and obstetric complications, representing global hypoxic-ischemic insults, have been implicated in the pathogenesis of CP since it was first described[21]. Of these obstetric complications, tight nuchal cord and abruption of the placenta have consistently been associated with an increased risk of CP[25,28,53].Though there has been some variation in the extent of association between birth asphyxia and CP, a recent multivariate analysis confirmed previous findings that intrapartum or obstetric hypoxia account for approximately 10% of CP cases[58–60]. The use of indirect measures to identify birth asphyxia is attributed, in part, to the varying association to CP[60]. The International Cerebral Task Force outlined specific criteria that are necessary and sufficient to establish that intrapartum events caused CP, which included metabolic acidosis in fetal, umbilical arterial cord or early neonatal blood (defined as pH <7, base deficit ≥ 12nmol/L), early onset of severe or moderate neonatal encephalopathy ≥ 34 weeks gestation, and CP of the spastic quadriplegic or dyskinetic type[61]. Other clinical signs of fetal distress, such as low Apgar

scores, passage of meconium, and abnormal fetal heart rate, are often used as measures of intrapartum hypoxia, but not necessarily specific to intrapartum hypoxia[60–63]. Indeed, infection related events such as maternal fever during labor or chorioamnionitis are a common antecedent of low Apgar scores and respiratory depression in the neonate[62,63].

Though obstetric hypoxia may account for a very small portion of CP cases, perinatal strokes, representing cerebral hypoxic-ischemic insults, are the most common cause of hemiplegic CP[64]. Of children with perinatal arterial ischemic strokes, 58-78% develop CP [65–67]. Several studies have demonstrated that arterial infarction of a large vessel was predicative of developing CP later in life[66–68] and results in damage to the parietal, temporal and frontal lobes as well as basal ganglia. Indeed, cerebral vascular infarcts and damage to watershed regions, or regions between vascular territories, were identified in some CP cases[12–14]. CP is also associated with intraventricular hemorrhage, and subsequent central venous infarction, resulting in damage to the periventricular white matter damage[69,70]. Of children with intraventricular hemorrhage, 84% with parenchymal involvement progressed to CP compared to 20% without [69]. 67% of children with a cerebral venous infarct had CP[70]. CP is strongly associated with a delayed presentation of hypoxic-ischemic insult, in which children appear neurologically normal and present with deficits after 1 month of age, but not neonatal presentation, in which children present within 1 month of birth with seizures, apnea and neurobehavioral changes[66,67]. Of note, children with normal motor outcomes had predominantly neonatal presentations[66]. Thus, perinatal hypoxic-ischemic brain injury may account for one, but not the only, mechanism of cerebral injury in CP.

Intrauterine infection and inflammation

In the 1950's, it was first reported that maternal fever during labor resulted in a 7-fold increase in CP[71]. An extensive review of over thirty years of literature spanning from 1972 to 1998 presented a strong argument that both neonatal (positive blood culture, clinically diagnosed sepsis and presence of cytokines) and maternal infection (urinary tract infection, chorioamnionitis , clinical sepsis, placental infection and presence of cytokines) can contribute to white matter injury and CP[72]. Since then, several studies have demonstrated that exposure to infection or inflammatory processes in utero increases the risk of CP in both preterm[28,53,73,74] and term infants[28,64,74,75].

Maternal infection, such as urogenital infection, chorioamnionitis, were associated with increased risk of CP, specifically spastic CP[75]. One or more clinical indicators of maternal infection were present in 22% of children with CP, compared to 2.9% of control children[62]. Maternal fever or clinical diagnosis of chorioamnionitis, as well as evidence of placental infection, are associated with almost a 9-fold increased risk of CP[62]. A prospective study demonstrated that histological evidence of placental inflammation and recovery of microorganisms in the placenta was predictive of CP, as well as periventricular leukomalacia, a neuropathological hallmark of CP[76]. Moreover, maternal infection is associated with low Apgar scores, seizures, newborn resuscitation and meconium aspiration syndrome[62].

In addition to maternal infection, exposure to infectious processes as neonate can increase the risk of CP[73,75,77]. Neonatal infection, including congenital infection (TORCH: toxoplasmosis, rubella, cytomegalovirus, and herpes simplex virus), pneumonia, septicemia, meningitis, encephalitis, neonatal urinary tract infection or

ventriculitis, results in a 15-fold increase in the risk of CP[75]. Furthermore, preterm infants with CP and white matter injury had increased culture-positive infections of the blood, cerebrospinal fluid, and trachea during the neonatal period[77]. Even in the absence of sepsis, inflammation can contribute to the development of CP[78]. In a prospective study of preterm infants without signs of sepsis, persistent and recurrent elevations of pro-inflammatory markers in the blood during the first 2 weeks of life was significantly associated with the diagnosis of CP later in life[78]. School aged children with CP had increased proinflammatory molecules in an unstimulated state and an exaggerated inflammatory response following LPS stimulation than their counterparts[79]. In children with CP, the activation of inflammatory pathways during fetal or neonatal life can promote a persistent proinflammatory state[79].

Cytokines are believed to play an integral role in the pathophysiology of infection-mediated brain injury resulting in CP[76,79–84]. The inflammatory hypothesis postulates that maternal infection results in the release of proinflammatory cytokines , such as IL-1, IL-6, TNF-α, into the fetal circulation leading to neuronal and white matter damage, such as that observed in CP[72,80,85]. Children with CP had increased levels of proinflammatory cytokines in their amniotic fluid[81], blood[49] and brain[82]. 88% of children with PVL had IL-1, IL-6, or TNF-α present in their tissue compared to 18% found in controls[82]. The primary source of these pro-inflammatory cytokines are activated microglia[83,84]. In autopsy samples of children with CP and white matter injury, activated microglia and proinflammatory cytokines were observed within the periventricular white matter[83,84]. These activated microglia can also produce reactive oxygen and nitrogen

species, which combined with the cytokines, can cause significant injury to the immature oligodendrocytes in the fetal brain resulting in PVL[83,84,86].

Multi-factorial etiology of CP

There is increasing evidence suggesting that CP arises from a combination of multiple risk factors. A recent analysis of 241 children with CP demonstrated that there is an increased risk of CP with increasing number of risk factors; though few children had the same combination of risk factors[87]. This finding supports previous work, demonstrating that the presence of multiple risk factors confers an additive risk for developing CP[25,55,64,88,89]. The presence of multiple placental pathologies present higher risk than a single pathology[55]. In addition, many children who had experience birth asphyxia had a combination of risk factors present, such as maternal/fetal infection, coagulation abnormalities or extended family member with CP, rather than a single event[90].

Inflammatory processes may also have a synergistic effect with other CP risk factors, such as premature birth and hypoxia-ischemia. Intrauterine infection has a strong association with preterm birth from both ruptured and intact membranes[91,92]. Thus, the development of CP subsequent to intrauterine infection in preterm infants may be the combination of prematurity due to infection and the fetal inflammatory response elicited by the infection[93]. Inflammation resulting from maternal or fetal infection dramatically increases the risk for CP, especially if superimposed on prenatal or perinatal hypoxia-ischemia[25,64,88,89]. The incidence of chorioamnionitis in CP was 17-fold greater in children with neuroradiologic evidence of hypoxic-ischemic injury than in children with

other findings[64]. Moreover, in a study of 457 preterm infants with CP, the combination of hypoxic-ischemic events, including birth resuscitation, patent ductus arteriosus ligation, and chronic lung disease, with infectious events, such as sepsis, resulted in a greater risk of CP than either insult alone[89]. Collectively, these findings suggest a multifactorial pathogenic mechanism for CP involving hypoxia-ischemia and inflammation, and should be reflected in animal models emulating the disorder.

Animal Models of CP

Based on the various risk factors, several different animal models of CP have been developed. These animal models strive to emulate the most common histopathological findings in CP, which include periventricular white matter and diffuse cortical/subcortical grey damage[12–14], and accompanying neurobehavioral deficits, which include spasticity and sensorimotor deficits[5–7]. Using ultrasound, varying degrees of periventricular white matter injury were detected in approximately 50-70% of pre-term infants with CP[94–96], supporting MRI findings[12–14] that PVL is a common neuropathological occurrence in CP. Infants at 23-32 weeks gestation are most vulnerable to periventricular white matter injury due to the predominance of oligodendrocyte progenitors[97], which are more susceptible to damage than mature oligodendrocytes[98]. Thus, many animal models of CP target this period of vulnerability, which is equivalent to post-natal day 5-7 (P5-7) in rodents[98,99], gestational day 20-28 in rabbits [100]and gestational day 93-95 in sheep[101,102] in term of CNS development and maturation.

Based on the risk factors of CP discussed above, several animal models of CP have been developed and can be grouped into those using hypoxic-ischemic insult, those utilizing infectious agents, and those using a combination of the two to induce injury characteristic of CP.

Models induced by hypoxia-ischemia

Hypoxic-ischemic (HI) models in sheep and rabbits were developed since these animals have gyrencephalic brains and the period of white matter vulnerability occurs in utero, similar to humans. In sheep, HI induced by bilateral ligation of fetal carotid arteries in utero resulted in periventricular white matter injury accompanied by lesions in the cortex and basal ganglia with prolonged ischemia[103]. Furthermore, these models demonstrated that cerebral ischemia, in addition to hypoxia, is necessary to induce PVL since white matter injury was infrequently observed with hypoxemia alone[104]. In rabbits, HI models of placental insufficiency, induced by transient uterine artery ischemia, resulted in multiple stillbirths[100,105]. In survivors, damage to the cortex, basal ganglia, thalamus, hippocampus and white matter was observed[100,105]. In addition, rabbit kits exposed to ischemia had significant motor and sensory deficits resembling children with CP[100]. However, there is substantial cost and technical challenges with both ovine and rabbit models of HI. Thus, rodent models are more commonly utilized due to cost efficiency and transgenic animals available.

Rodent models of intrauterine hypoxia have been developed[106]. However, this model replicates an insult that occurs extremely early during development since

embryonic day 9-10 in rats is equivalent to 7-8 weeks in human gestation. Due to small proportion of CP cases associated with birth asphyxia and the extremely preterm insults, these animal models have limited relevance to CP pathogenesis.

The most common and widely used model of hypoxic-ischemic injury is the Rice-Vannucci model, which combines unilateral ligation or cauterization of the common carotid artery with systemic hypoxia in P7 rats resulting in damage to both grey and white matter, specifically the cortex, striatum, hippocampus and the periventricular area[98,107], similar to the rabbit and sheep HI models. Modifying the duration of the systemic hypoxia, from 8% O_2 for 3.5 hours to 6% O_2 for 1 hour in P7 rat pups, results in selective white matter injury in the periventricular white matter[108]. Due to the variety of transgenic mice available, the Rice-Vannucci model of HI injury was modified for mice, which required shorter duration of hypoxia (40-70 minutes) to produce injury[109,110]. There were some strain variations in susceptibility to HI[110]. Following hypoxic-ischemic brain injury, several developmental motor and cognitive deficits were observed in the mice. At 24h following HI, mice demonstrated not only impaired sensorimotor reflexes, including right, geotaxis and cliff aversion reflex[111]. HI not only impaired, but also significantly delayed the appearance of these reflexes in HI animals compared to control[112] resembling the delayed onset of deficits in CP. Diminished sensorimotor reflexes significantly correlated with long-term neurofunctional deficits assessed at 4 weeks post-HI in mice[111]. Despite early motor impairment observed in animals exposed to HI, the persistence of this impairment is controversial with some studies reporting functional recovery at 6 weeks post-injury while others observe continued functional impairment [111–113]. Compensation from the undamaged hemisphere, contralateral to the ischemia, in

combination with other unknown factors may contribute to the spontaneous recovery and, thus, more long-term behavioral studies are needed in this model. Overall, this well characterized model reproduces lesions and many of the deficits associated with CP.

Transient middle cerebral artery occlusion (tMCAO) at various stages during development (at P7 and P14-P18) in rodents is another common model of perinatal hypoxic-ischemic injury[114,115]. Comparison of the tMCAO and HI animal models demonstrate that the tMCAO models produce focal injury primarily in the distribution of the middle cerebral artery and less white matter injury more representative of neonatal stroke, whereas the HI model results in a more white matter injury with diffuse grey matter damage[116]. Thus, the HI animal models may be superior to the tMCAO model with respect to CP, which is characterized by both white matter damage and diffuse grey matter injury.

A full discussion of the mechanisms of hypoxic-ischemic brain injury including glutamate excitotoxicity, oxidative stress and apoptosis is beyond the scope of this dissertation but has been comprehensively reviewed in (see [117]).

Models induced by infectious agents

In infection-mediated brain injury, there is considerable variability in the timing of the insult, mode of delivering the infectious agent, and what type of infection it models. Most infection or inflammation animal models use live cultures of E. coli or lipopolysaccharide (LPS), a component of most gram negative bacteria that is a strong inducer of the immune system. In a rabbit model of intrauterine infection, intracervical

exposure to *E. coli* resulted in kits with evidence of intrauterine infection, all of whom also had periventricular white matter damage, demonstrating that ascending intrauterine inflammation can contribute to CP[118]. In addition, rabbit intrauterine infection models using live bacteria or LPS have also demonstrated motor deficits such as spasticity and impaired reflexes, evidence of neuroinflammation in the white matter, and some gray matter injury to the cortex and hippocampus accompanying white matter injury[119–121]. A sheep model of intrauterine infection by fetal exposure to a single, repeated or chronic dose of LPS resulted in periventricular white matter injury and increased neuroinflammation, as well as accompanying cortical and subcortical damage in some animals[101,102,122,123]. Though the ability to simulate *in utero* insults similar to those during human gestation is a huge advantage with rabbit and sheep animal models, the high rate of fetal mortality and the high cost associated with these models is a significant drawback.

Maternal or intrauterine infection models have also been developed in rodents[124,125]; however, similar to intrauterine models of HI discussed earlier, these models translate to an insult during a very premature stage of human development and thus may have limited relevance to CP.

Since the white matter in rodents develops postnatal, many models induce white matter injury with neonatal LPS exposure. In the first model of *ex utero* endotoxin mediated encephalopathy, exposure to LPS (i.p.) resulted in damage in the thalamus, caudate and white matter in new born cats but minimal to no damage in rodents[126]. Though a single peripheral exposure to LPS does not result in severe injury[126,127], it does initiate a pro-inflammatory response evidenced by increased expression of pro-

inflammatory cytokines and activated microglia[128,129]. Examination of global gene expression following LPS exposure (0.3 mg/kg, i.p.) at P7 demonstrated significant changes in genes associated with inflammation and immune function, including IL- 1β, IL-6 [129]. Repeated administration of LPS (0.3 mg/kg, i.p.) from P3 to P11, modeling a chronic subclinical infection, resulted in hypomyelination of the subcortical white matter and reduced gray matter volume following insult[130]. Direct intracerebral injection of LPS (1mg/kg) at P5-7 results in damage to the periventricular white matter and ventricular enlargements in animals[131,132].

Since exposure to LPS was associated with decreased cerebral blood flow and/or decreased blood pressure, LPS-mediated brain injury was initially thought to be the result of hypoperfusion[133,134]. However, it was demonstrated that repeated doses of LPS exposure resulted in significant white matter damage, though only a transient change in hemodynamics was observed shortly following LPS[101]. Thus, reduction in blood pressure or cerebral blood flow was not a critical factor in mediating brain injury following LPS exposure. LPS brain injury are mediated by its interaction with toll-like receptor 4 (TLR4)[135], which is able to recognize foreign infectious pathogens and initiate the production of pro-inflammatory mediators and cytokines, like IL-1β, IL-6. In animal models, intra-uterine or neonatal LPS- induced inflammation leads to increases in pro-inflammatory cytokines, such as IL- 1β, IL-6, and/or TNF-α, in fetal or neonatal tissue and blood[120,121,124,128–131] that can cause injury to oligodendrocytes and neurons directly or indirectly by activating microglia. Activated microglia can release cytotoxic substrates

such as proinflammatory cytokines, excitotoxic substances and reactive oxygen and nitrate species that result in neuronal and oligodendrocyte damage and death (reviewed in[136]).

Models induced by combination of hypoxia-ischemia and infection

One of shortcomings of the models discussed thus far is the focus on a single inciting event using interruption of intrauterine blood supply to model placental complications, perinatal hypoxic-ischemic injury to model neonatal cerebral ischemia, or infectious agents to model intrauterine/fetal infection and inflammation, but this does not recognize the multiple etiologies that contribute to pathology. Thus, most widely accepted animal models of CP combine hypoxia-ischemia plus lipopolysaccharide-induced inflammation (HIL) exposure during development.

Several groups have demonstrated that LPS exposure sensitizes the brain to subsequent HI brain injury. In rats, the combination of repeated prenatal LPS exposure (200μg/kg, i.p., from E17-gestation) with post-natal HI (common carotid ligation, hypoxia with 8% O2 for 3.5 hours) at P1 resulted in increased cerebral lesions, such as hypereosinophilic nuclei, pyknotic nuclei and dissolution of cellular membranes, and severe motor deficits compared to either insult alone [137,138]. Furthermore, damage to the white matter in the corpus callosum, internal and external capsules was accompanied by damage to gray matter in the cortex and striatum, as well as increased astrocytes and microglia adjacent to lesions[138]. Of note, lesions were observed in both ipsilateral and contralateral to the carotid ligation, though lesions were more severe on the ipsilateral hemisphere[138]. The synergistic effects of LPS and HI were evident with neonatal exposure. LPS (0.3mg/kg, i.p.) enhanced vulnerability of the immature brain when

administered 4-6h or 72h prior to HI (common carotid ligation followed by hypoxia with 7.7% O_2 for 20 min), but not 2 h prior [127,139]. Since a preconditioning effect has been reported when LPS is administered 24h prior to HI (common carotid ligation followed by hypoxia with 7.7% O_2 for 20 min) through an unknown mechanism, it appears that LPS has a biphasic sensitizing effect acutely (at 4-6h) and chronically (at 72h) prior to HI[139]. The combination of LPS and HI resulted in permanent injury to the cortex, hippocampus, striatum and thalamus ipsilateral to the ligation, which persists for at least 2 weeks post-injury[140]. In addition to gray matter injury, the combination of LPS and HI exacerbates subcortical white matter damage, demonstrated by decreased myelin basic protein (MBP) reactivity, [141] and evokes a inflammatory response, with increased IL-1β, IL-6 and TNF-α[141,142].

More recent studies have demonstrated that the synergistic effects of LPS and HI are not dependent on LPS-mediated sensitization since reversing the order still exacerbates damage than either insult alone[143,144]. The combination of HI (carotid ligation, hypoxia at 6% O_2 for 30 min) followed by LPS (1 mg/kg, i.p.) in P6 mice resulted in greater injury in the periventricular white matter, demonstrated by decreased expression of oligodendrocyte markers MBP and O1, and damage to myelinated axons than HI alone[143,145]. In addition to white matter injury, diffuse areas of gray matter damage in the hippocampus and cortex, were observed. Increasing the duration of hypoxia to 45 minutes or dose of LPS to 3mg/kg resulted in increased injury, characterized by focal areas of severe infarction in the hippocampus and cortex, resembling neonatal stroke rather than CP[143,145]. Increased microglia activation and reactive astrogliosis was also observed within 72 hours following HIL[143,144]. Injury was

observed exclusively ipsilateral to the ligation[143,144]. Furthermore, the combined exposure of HIL resulted in more substantial motor and behavioral deficits than either insult alone[138].

Although the exact mechanism of HIL pathogenesis is unknown, it is thought be associated with the pathways involved in HI and LPS-mediated brain injury. Mice lacking either TLR4 or MyD88, a TLR4 adaptor protein, have reduced, but not complete absence of, damage compared to wild-type littermates subjected to HIL[141,146]. These finding suggest that both TLR4 and MyD88 contribute, in part, to the damage following HIL.

mTOR signaling cascade in the brain

Rapamycin was chemically isolated from a soil bacteria (*Streptomyces hygroscopicus*) found on Easter Island (named after indigenous peoples' name for the island, Rapa Nui) in the 1970's[147]. Rapamycin was originally introduced as a macrolide antifungal agent[147,148]. Later, rapamycin was also discovered to have immunosuppressive effects via inhibition of T-cell proliferation and anti-cancer properties demonstrating that its anti-proliferative effects extend to mammalian cells[149,150]. These findings prompted the investigation into the cellular targets mediating the effects of rapamycin.

Mutations in the target of rapamycin (TOR) genes in yeast, TOR1 and TOR2, were identified in a drug screen for rapamycin-resistance in yeast. TOR is an evolutionarily conserved serine/threonine protein kinase, with approximately 42% similarity between yeast TOR1/2 and mammalian TOR (mTOR)[151,152]. Unlike yeast where the genes TOR1 and TOR2 encode proteins Tor1 and Tor2[153], a single gene FRAP1 (also known as RAFT1) encodes mTOR in mammals[151,152,154]. The human, rat

and mouse mTOR share a > 95% homology (reviewed in[155]). mTOR, found primarily in the cytoplasm, is ubiquitously expressed throughout the body, including the central nervous system.

mTOR signaling is executed by two ternary complexes, mTORC1 and mTORC2, which are defined by the regulatory proteins bound to mTOR. mTORC1 is comprised of mTOR, raptor, DEPTOR and mLST8, while mTORC2 consists of mTOR, rictor, sin1, mLST8, DEPTOR and protor (reviewed in[156]). Rapamycin selectively inhibits mTORC1 by binding FKBP1, an mTOR binding protein and required co-factor of rapamycin toxicity[151,152,154]. The FKBP1-rapamycin-mTOR complex allosteric inhibits mTORC1 by destabilizing the binding of mTOR to mTORC1-specific component raptor thereby uncoupling mTORC1 from its substrates[151,152,154]. mTORC2 is largely insensitive to rapamycin, though chronic rapamycin treatment has been shown to diminish mTORC2 activity in some cell lines[157]. *In vivo* chronic rapamycin administration (daily i.p. administration for 2-4 weeks) resulted in decreased mTORC2 in the tissues examined (liver, skeletal muscle and adipose tissue)[158]. This is thought to be due to decreased availability of unbound mTOR to bind to mTORC2-specific rictor and promote assembly of the mTORC2 complex over time[157]. Due to its sensitivity to rapamycin, mTORC1 (referred to as mTOR herein) is a clinically actionable pathway and, thus, it will be the focus for the remainder of this section.

mTOR acts as a critical integration step between external cues and internal signaling cascades regulation cell proliferation and growth. mTOR is essential for normal cell size and proliferation since homozygous mice lacking the mTOR kinase domain are embryonic lethal due to impaired cell proliferation[159,160]. Upstream regulators of mTOR

ensure that cell proliferation is activated under appropriate environmental conditions. mTOR is regulated by several well-characterized proteins, including PI3K (phosphoinositide-3 kinase) and Akt (also known as protein kinase B) in response to growth factors, AMPK (AMP kinase) in response to cellular energy and Redd1 (regulated in development and DNA damage 1) in response to intracellular oxygen levels, which signal through tuberous sclerosis complex 1 and 2 (Tsc1 or Tsc2), negative upstream regulators of mTOR (reviewed in [156,161,162]; Figure 1).

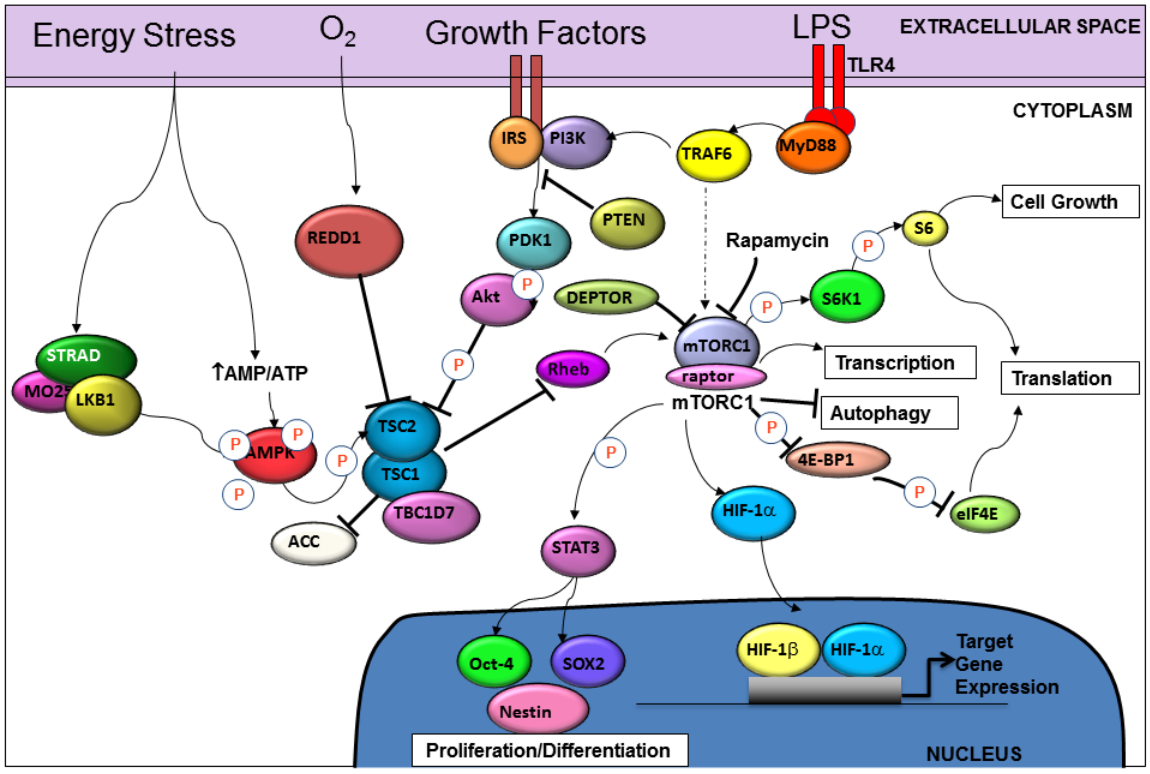

Figure 1. mTOR signaling cascade

Activated mTOR phosphorylates downstream targets and regulates processes related to transcription, translation, cell growth and proliferation/differentiation(reviewed in [156,161,162]). The best characterized downstream effectors of mTOR are ribosomal protein p70 S6 kinase (S6K) and eukaryotic translation initiation factor 4E-binding protein (4E-BP1), which act in parallel to ultimately promote translation and cell growth. S6K phosphorylates ribosomal protein S6, a component of the 40S ribosomal subunit, which promotes protein translation. mTOR can phosphorylate S6K1 at multiple sites, but of these the phosphorylation of Thr389 is critical for S6K activation[163]. Activated S6K1 can phosphorylate S6 at Ser 240/244 and Ser 235/236, the latter of which is also phosphorylated by other kinases in a mTOR- independent manner[164,165]. Phosphorylated S6 recruits ribosomal machinery and promotes mRNA translation. Phosphorylation of S6K (P-S6K) and S6 (P-S6) are robust markers of mTOR activation and are commonly used as a measure of mTOR activity. The 4E-BP1 facet of the mTOR signaling cascade also affects translation. When phospho-inactivated by mTOR, phospho-4E-BP1 (P-4EBP1) releases eukaryotic initiation factor 4E (eIF4E), which then binds to 7-methylguanosine cap of mRNA and enhances global translation[166]. Like S6K, 4E-BP1 can be phosphorylated at multiple sites (Thr 37/46, Ser 65, Thr 70) by mTOR[156,167]. Phosphorylation of Thr 37/46 by mTOR primes 4E-BP1 for phosphorylation at other sites resulting in maximum inactivation[167]. In addition to promoting global translation, mTOR, via phosphorylated S6 and 4E-BP1, specifically enhances the translation of mRNA's with 5'-terminal oligopyrimidine (5'-TOP) and pyrimidine-rich translational element (PRTE) [168–171]. 89% of mTOR-responsive genes have either a 5'-TOP or a PRTE[171]. 5'-TOP mRNA's are a small, but abundant subset of mRNA's consisting of approximately 90

mRNA's that encode for ribosomal proteins and translation initiation and elongation factors (for review see [172]).

In addition to translation, mTOR also affects transcription of genes by influencing the activity and expression of several transcription factors. The activation of mTOR is sufficient to induce transcription of genes involved in glycolysis, pentose phosphate pathway and lipid and sterol synthesis[173]. The metabolic processes of glycolysis and lipogenesis are regulated via mTOR-dependent induction of hypoxia inducible factor 1α (HIF-1α) and sterol regulatory element binding protein (SREBP), respectively[173]. These results confirm the previously established role of mTOR as an environmental nutrient sensor. In addition, mTOR may affect cell proliferation via phosphorylation of signal transducer and activator of transcription 3 (STAT3), a transcriptional activator, at Ser 727[174]. STAT3, typically phosphorylated in response to cytokines and growth factors, can induce genes involved in growth, survival and differentiation. In cells with constitutively activated mTOR, there is increased phosphorylated STAT3 (P-STAT3) at Ser 727 and this is required to promote proliferation and survival of these cells[175,176]. The mTOR-STAT3 may be integral in linking the inflammatory response with environmental cues. Lastly, phosphoproteome analysis demonstrated that mTOR stimulates de novo pyrimidine synthesis by phosphorylating CAD (carbamoyl-phosphate synthetase 2, aspartate transcarbamylase, and dihydroorotase), an enzyme that catalyzes the first three steps of pyrimidine synthesis[177,178]. This is yet another avenue by which mTOR regulates the capacity of protein biosynthesis and cell growth.

There is a delicate regulation of the mTOR signaling cascade to ensure cell growth and proliferation is appropriately activated in response to environmental cues.

Augmented mTOR plays a critical role in regulating cell death following environmental stress. Enhanced mTOR activity, due to TSC2 knockdown or Rheb overexpression, results in more DNA damage and increased susceptibility to oxidative stress[179,180]. Thus, inappropriate mTOR activity in the context of an environmental stress, such as hypoxia-ischemia or inflammation, results in an imbalance in the metabolic supply and demand, ultimately leading to cell damage and death.

mTOR in hypoxia-ischemia

In vitro and *in vivo* models of hypoxic-ischemic injury have demonstrated that activated mTOR in a limited nutrient and energy environment is detrimental. Cells with constitutively active mTOR, due to TSC1 or TSC2 knock out, had poor survival following glucose deprivation[181]. Furthermore, inhibiting mTOR in these cells reduced both cell death and energetic stress demonstrating that constitutive mTOR activation increases energetic burden during conditions of nutrient deprivation[182]. In an adult animal model of stroke, similar results were observed. Enhanced mTOR activity, via suppression of the upstream mTOR inhibitors Tsc1 or Tsc2, increases vulnerability of neurons to hypoxic-ischemic injury[183,184]. Conversely, decreasing mTOR activity via overexpression of Tsc1 fosters resistance to ischemia-induced damage[184]. Ischemic preconditioning, a potent inducer of ischemic tolerance, 24h prior to cerebral ischemia results in decreased mTOR phosphorylation and reduced damage[185]. The neuroprotective effects of ischemic preconditioning were potentiated by rapamycin[185]. Furthermore, in a neonatal model of hypoxic-ischemic injury, mTOR inhibition with rapamycin treatment prior to injury reduces neuronal death[186–188].

Other reports suggest that increased mTOR activity following cerebral ischemia is neuroprotective[189–192]. Ischemic post-conditioning mediated neuroprotection by increasing phosphorylation of S6K1, S6, and 4EBP1 and these effects were abolished with rapamycin[189]. Furthermore, enhanced mTOR signaling, by PRAS40 overexpression or PTEN deletion, was neuroprotective while decreased mTOR signaling was not[190,192]. However, it should be noted that both PRAS40 overexpression and PTEN deletion affected other proteins upstream of mTOR, and thus possible other pathways[190,192]. Therefore, whether increased mTOR is mediating the injury or an associated finding in these models of adult cerebral ischemia needs to be further investigated. Furthermore, it may seem counterintuitive that both increasing and decreasing mTOR activity is neuroprotective. However, there may be different optimal amounts of mTOR activity necessary to balance the rate cellular energy demand with induction of pro-survival responses, such as autophagy, depending on the timing, duration and severity of injury.

Macroautophagy (hereafter referred to as autophagy) is an evolutionary conserved process for degrading and recycling cellular components. mTOR signaling cascade is a negative upstream regulator of autophagy related genes (ATG) and regulates autophagy in response to growth factors, nutrients and cellular stress[193–196]. There is evidence that induction of autophagy may be an adaptive cellular response during conditions of bioenergetic stress to promote cell survival [184,186,187,197]. The absence of autophagy in the context of cellular stress may leave cells without a means to maintain energy homeostasis, and vulnerable to cell death. Rapamycin-induced autophagy has been demonstrated as a potential mechanism of mTOR-dependent neuroprotection following cerebral ischemia in adults and neonates[183–187]. Constitutive activation of mTOR can

result in impaired autophagy and promote damage following hypoxic-ischemic injury *in vitro*[183]. Pre-injury administration of rapamycin increases autophagy, and results in decreased cell death and brain damage 24h following neonatal hypoxia-ischemia[186]. Enhancing autophagy with rapamycin reduces infarct size and improves neurological outcome at 48h following injury in permanent and slow reperfusion stroke models[198]. The addition of inhibitors of autophagy, 3-methyladenine, eliminates rapamycin-mediated neuroprotection[187]. Thus, induction of autophagy is one mechanism of rapamycin mediated neuroprotection following hypoxia-ischemia.

mTOR in inflammation

In addition to the potent anti-fungal effects, rapamycin is also FDA approved for use as an immunosuppressant demonstrating that mTOR has an integral role in regulating the immune system[199]. Specifically, mTOR is thought to contribute to a pro-inflammatory state by promoting the proliferation and differentiation of immune cells. mTOR promotes T-cell proliferation in response to cytokine stimulation[200]. More recently, it was demonstrated that mTOR is crucial in effector T cell fate determination, especially of pro-inflammatory Th1 and Th17 cells[201,202]. Furthermore, inhibition of mTOR promoted regulatory T-cells, which restrain the immune system under physiological and pathological conditions[203–205]. Though not as well characterized as T-cell differentiation, mTOR also plays a crucial role in promoting differentiation and activation of B-cells, which are key components in adaptive immunity (for review see [204]). In addition to its role in orchestrating the peripheral immune response, there is growing interest recently in the role of mTOR in neuroinflammation, or inflammation within the brain.

As the resident immune cells in the brain, microglia act as "first responders" to injury. Microglia are in a constitutive resting state, characterized by a small cell body with long, fine processes, and actively survey the surrounding environment under physiological condition (e.g. in the absence of infection or injury). In response to certain stimuli, e.g. LPS or hypoxia, microglia transform through a spectrum of morphological changes from a resting state to an activated state, characterized by an enlarged, spherical cell body with retracted processes[206,207]. Following neonatal hypoxia-ischemia, activated microglia were present within hours of injury and persisted for several days[208]. These activated microglia can initiate and maintain neuroinflammatory response. In patients with CP, activated microglia were found in the periventricular white matter and determined to be the primary source of pro-inflammatory cytokines that contribute to CP pathogenesis[83,84].

Both *in vivo* and *in vitro* studies have demonstrated that mTOR activity may contribute to activation of microglia[209–213,205]. Exposure of microglial cultures to hypoxia resulted in increased mTOR signaling, which regulated production of inflammatory mediator iNOS (inducible nitric oxide synthase)[210]. Rapamycin decreased microglia activation, indicated by decreased expression of iNOS[210]. Furthermore, mTOR is critical in microglia activation and proliferation in response to pro-inflammatory cytokines, as rapamycin was able to reduce iNOS activity[209]. Of note, though mTOR activity was increased in microglia stimulated with both LPS and cytokines, rapamycin had little effect on microglia proliferation in response to LPS stimulation *in vitro*[209]. These results suggest that LPS-stimulated microglia activation may have a different temporal sequence or involvement of another pathway. An *in vivo* model of spinal cord injury a biphasic

increase in mTOR activity was observed in both neurons and microglia at the site of injury[211]. In a traumatic brain injury animal model, increased phosphoactivation of S6 was noted in both neurons and microglia[212]. Inhibiting the mTOR signaling pathway was neuroprotective resulting in improved motor and cognitive deficits, and decreased microglia activation[212,213]. Furthermore, rapamycin treatment following cerebral ischemia in adult rats resulted in a significant decrease in production of pro-inflammatory cytokines, improved motor deficits and enhanced activity of regulatory T-cells[205]. Collectively, these results demonstrate that mTOR plays an important role in neuroinflammation, specifically microglia activation, but has not been investigated in animal model of CP.

Statement of Purpose

From a public health perspective, CP is one of the most costly chronic disorders of children[214]. The Center for Disease Control (CDC) estimates that the total lifetime costs for all individuals with cerebral palsy is $11.5 billion (in 2003 dollars)[215]. The lifelong implications of CP for patients and families are substantial. Despite many studies to define CP risk factors, no new therapies have been established in recent years.

The mTOR pathway has been implicated in cellular responses to hypoxia and inflammation. CP is often linked to hypoxic and inflammatory injury to the brain. While the mTOR signaling cascade has been linked to several pediatric neurological disorders[216–220], manipulation of the mTOR signaling cascade as a pre-clinical therapeutic strategy in CP has not been investigated. Thus, I hypothesize that neuronal death following the combination of hypoxia-ischemia and LPS-induced inflammation is mTOR dependent. Unlike previous studies in neonatal hypoxia-ischemia model, I demonstrate

that mTOR inhibition with rapamycin following HIL reduces neuronal death and neuroinflammation in a mouse model of CP. This approach provides a new potential therapeutic intervention for a subset of infants at high risk for CP.

CHAPTER 2: MATERIAL AND METHODS

HIL Animal Model (Figure 2)[145]

On post-natal day 6 (P6), C57BL/6 pups were anesthetized using indirect cooling on ice to the point of unconsciousness. The pup was considered fully anesthetized when it was not responsive to pain (foot-pinch test), and reached a body temperature of 10-11^{o}C. Unilateral permanent ischemia was induced by right common carotid artery occlusion using a small vessel cauterizer (Fine Science Tools). The average total surgery time was approximately 6 minutes. Once fully recovered, i.e. an active pup with a body temperature of 28^{o}C or greater, the pup was returned to the dam for 1 hour followed by 35 minutes in a hypoxia chamber (BioSpherix) pre-equilibrated to 6% O_2 with N_2. Next, LPS (Escherichia coli, 0111:B4, Sigma; 1mg/kg) was injected intraperitoneally (i.p.) immediately following hypoxia. Following LPS, pups received either vehicle or rapamycin treatment (LC laboratories; 5 mg/kg i.p), which was continued once a day for the next 3 days. A subset of animals received the autophagy inhibitor chloroquine (60mg/kg, i.p.) immediately prior to ischemia and a second dose (30mg/kg, i.p.) immediately following LPS, in conjunction with rapamycin. Another group of animals received S6K inhibitor PF-4708671 (Tocris, 75mg/kg i.p.) immediately following LPS.

The body temperature of pups were monitored throughout the surgery using an infrared thermometer, including immediately after anesthesia, prior to returning pups to dams, prior to hypoxia, immediately after LPS administration and prior to experimental end-point. Following the surgery procedures, pups were returned to the dam, and housed with littermates until the experimental end-point. Sham surgeries (exposure of the carotid

but no ligation, no hypoxia, and no LPS injection) served as controls. Pups were euthanized at 24 hours, 48 hours, 1 week and 1 month post-injury

Animals were housed under temperature and humidity control on a 12:12 light: dark cycle. Animals were not subject to water or food restrictions. All experiments were approved by Institutional Animal Care and Use Committee (ACUP – 4260, 4094) and were in accordance with institutional guidelines at Temple University School of Medicine.

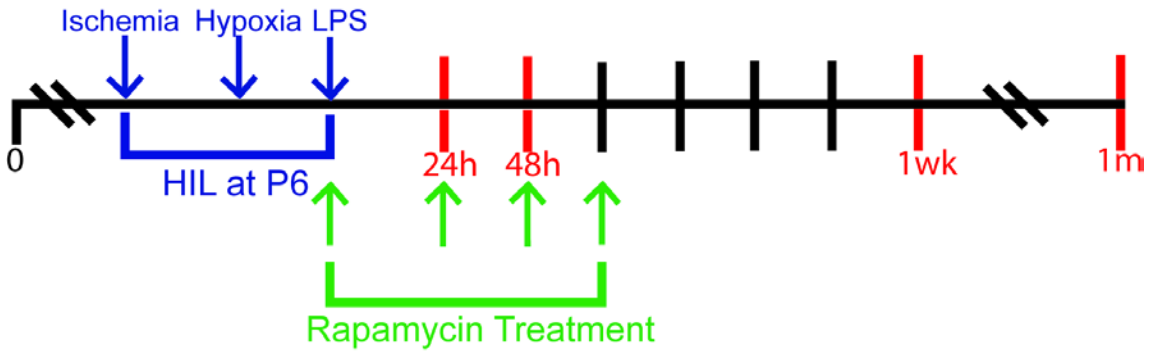

Figure 2. The HIL animal model of CP and treatment scheme
Schematic of HIL animal model and rapamycin treatment paradigms. At post-natal day 6 (P6), pups were subjected to a combination of ischemia, hypoxia and LPS-induced inflammation indicated by blue lines. Red lines represent time-points when animals were euthanized. Green lines indicate rapamycin treatment (5mg/kg, i.p.).

Immunohistochemistry (IHC) and Immunofluorescence (IF)

Animals were euthanized using isofluorane anesthesia followed by transcardial perfusion with ice-cold 4% buffered paraformaldehyde. Brains were removed and cryoprotected in 30% sucrose. 14 µm sections were cryostat sectioned through the entire brain. Antigen unmasking was performed using antigen unmasking solution (Vector

Labs), according to manufacturer's instructions, when necessary. Sections were incubated for 1 hour at room temperature in blocking buffer (5% Fish Gelatin, 0.02% Sodium Azide, 0.1% Triton X-100), followed by overnight incubation at 4°C with primary antibodies recognizing phospho-S6 (Ser 235/236; Cell Signaling, 1:1000, anti-rabbit), HIF-1α (Abcam, 1: 1000, anti-mouse), phospho-STAT3 (S727; Biorbyt, 1:100, anti-rabbit) and Iba1 (Wako, 1:2000, anti-rabbit; Novus Biologicals, 1:500, anti-goat).

For IHC, appropriate biotinylated secondary antibodies (Vector Labs) were applied to sections followed by avidin-biotin-complex (Vectastain ABC Kit, Vector Labs). Immunoreactivity was visualized using 3,3'-diaminobenzidine (Sigma-Aldrich). To aid with regional analysis, cells were labeled using cresyl violet acetate (Sigma-Aldrich) or the nuclear stain 4',6-diamidino-2-phenylindole (2μg/mL; DAPI, Cell Signaling) as indicated. Slides were cover slipped and mounted using Permount (Fisher Scientific) and imaged using a Nikon Eclipse 80i microscope with Nikon DS-Ri1 color camera.

For IF, appropriate fluorescent secondary antibodies (Life Technologies) were applied to sections. Slides were mounted using fluorescence mounting media with DAPI (Vector Laboratories), cover slipped and imaged using a Nikon Eclipse 80i microscope attached to CoolSNAP EZ monochrome camera.

Resting and activated microglia were distinguished based on cell body area, which was calculated in digital images (Nikon Eclipse 80i microscope attached to CoolSNAP EZ monochrome camera) utilizing area measurement function in ImageJ. Activated microglia were defined as Iba1 labeled cells with cell body area $\geq$ 80 μm^2, which consistently corresponded with activated microglia morphology based on our cell

body area quantification. For microglia quantification, Iba-1 labeled cells were quantified from 3 randomly selected microscope fields in both the strata radiatum/ lacunosum/ moleculare (SRLM) and the stratum pyramidale of the CA3 region of the hippocampus. Three sections were analyzed for sham, HIL and HIL + rapamycin treated pups (n = 3-4 animals/condition). Values are expressed as average number of cells in region of interest.

Fluoro-Jade Staining and Quantification

Fluoro-Jade C (FJC) was used to identify necrotic and apoptotic neuronal death in tissue sections as described previously[221,222], with minor modifications. Briefly, slides were immersed sequentially in basic ethanol (0.2% sodium hydroxide in ethanol), 70% ethanol, distilled water, 0.06 % potassium permanganate (Sigma-Aldrich), 0.001% Fluoro-Jade C (FJC, Histo-Chem Inc.) in 0.1% acetic acid, 2ug/mL DAPI (Cell Signaling) in 0.1% acetic acid, followed by dehydration in xylene and cover-slipped using DPX mounting medium (VRW International).

For triple labeled sections, sections were incubated for 1 hour at room temperature in blocking buffer (5% Fish Gelatin, 0.02% Sodium Azide, 0.1% Triton X-100), followed by overnight incubation at 4°C with cleaved caspase-3 (CC3, Cell Signaling). Alexa-fluor 647 goat-anti-rabbit secondary antibody (Life Technologies) was added for 1 hour at room temperature. The sections were then labeled with FJC and DAPI as described above.

Neuronal cell death was quantified in the CA1 and CA3 subfields of the hippocampus, since these areas are affected in our animal model of CP, using a Nikon Eclipse 80i microscope attached to CoolSNAP EZ monochrome camera. Using ImageJ, a

1000 x 300 region of interest (ROI) was operationally defined in the CA1 pyramidal cell layer above the blades of the dentate gyrus, and the CA3 pyramidal cell layer adjacent to the hilus of the dentate gyrus. Cells co-labeled with FJC and DAPI, as well as cells triple labeled FJC, DAPI and CC3, within the ROI were counted using ImageJ (NIH). 3 sections of the dorsal hippocampus, spaced at least 42μm apart, were counted per animal for sham, HIL and HIL + rapamycin treated pups (n = 5/condition) at 24 hours, 48 hours, 1 week and 1 month following injury.

To evaluate severity of neuronal cell death, 4 evaluators blinded to conditions rated images of FJC and DAPI labeled sections on a 6 point scale (0 – no cell death; 1-minimal cell death, primarily outside regions of interest; 2 – cell death in < 25% of hippocampus; 3 - cell death covering 25%-50% of hippocampus; 4 – cell death present throughout the hippocampus, covering ≥ 50% of hippocampus; 5 – cell death present in the hippocampus, as well as non-hippocampal structures such as cortex, thalamus, etc.). Scores from evaluators were averaged for each section. Multiple sections were averaged and rounded to the nearest whole number to determine cell death score for each animal. 2-3 sections were evaluated per animal for sham, HIL, HIL + rapamycin, and HIL + rapamycin + chloroquine treated pups (n = 5-7/condition) at 24h and 48h post-injury.

Western Blotting

Hippocampal samples from the ipsilateral hemisphere and analogous areas of the contralateral hemisphere were micro-dissected, and homogenized in RIPA buffer (50mM Tris pH 8.0, 150mM NaCl, 1% NP-40, 0.5% Na-Deoxycholate, 0.1% SDS) containing 2mM phenylmethlysulfonyl fluoride (PMSF, Thermo Scientific), 1X protease inhibitors

(complete protease inhibitor cocktail, Roche) and 1X phosphatase inhibitors (Halt Phosphatase Inhibitors, Thermo Scientific). Lysates were centrifuged at 14,000 RPM for 20 minutes at 4^{o}C, and protein concentration of supernatants was calculated using bicinchoninic acid (BCA) protein assay (Bio-Rad Laboratories, Inc.). 2X SDS-PAGE loading buffer (125mM Tris-HCl pH 6.8, 20% Glycerol, 4% SDS, 0.1% bromphenol blue, 0.2M dithiothreitol) was added to lysates, followed by incubation at 95^{o}C for 5 minutes. 30μg of protein was electrophoresed and transferred to PVDF membranes. Membranes were blocked for 1 hour in blocking buffer (0.3X Odyssey blocking buffer, Li-cor Biosciences) then incubated with antibodies recognizing Beclin 1 (Abcam, 1:2000, anti-rabbit), LC3 (Cell Signaling, 1:1000, anti-rabbit), HIF-1α (Abcam, 1:500, anti-mouse), total S6 (Cell Signaling, 1:500, anti-mouse), total S6K (Abcam, 1:1000, anti-rabbit), total 4E-BP1 (Cell Signaling, 1:1000, anti-rabbit), phospho-S6 (S235/236; Cell Signaling, 1:1000, anti-rabbit), phospho-S6K (T389; Novus, 1:1000, anti-rabbit), and phospho-4EBP1 (T36/47, Cell Signaling, 1:500, anti-rabbit) at 4^{o}C overnight. After washing in washing buffer (blocking buffer, 0.1% Tween), membranes were incubated with IRDye-conjugated anti-mouse or anti-rabbit secondary antibodies (Li-cor Biosciences).

Blots were analyzed using an Odyssey Imaging System (Li-cor Biosciences). densitometric analysis was performed using Image Studio (Li-cor Biosciences). Protein levels normalized to respective GAPDH values and expressed relative to average sham values.

Statistical Analysis

Results are expressed as mean ± SEM. Differences between treatment groups were determined using a one-way ANOVA with Tukey post-hoc analysis or Tukey-Krammer analysis, if groups had differing number of samples. $P < 0.05$ was considered statistically significant.

CHAPTER 3: RESULTS

HIL Model

A consistent finding in MRI analyses and post-mortem human brain tissue in CP is injury to the periventricular white matter (periventricular leukomalacia, PVL)[13,15,223]. Similar to rat[224] and rabbit[105] models of CP, the HIL mouse model of CP is characterized by PVL, accompanied by cell death in the hippocampus ipsilateral to the carotid ligation, as well as selective areas of the cortex and thalamus[145] (Figure 3A). We observed enhanced expression of HIF-1α, a marker of hypoxic cellular stress, Iba-1, a microglia marker, and cleaved-caspase 3 (CC3), an indicator of apoptotic cell death, in morphologically identified oligodendrocytes in the periventricular white matter at 24h (Figure 3B) post-injury in HIL, but not in shams. The effects were more severe ipsilateral to the carotid ligation and served to confirm previously reported findings of periventricular injury in HIL animal models[145]. Treatment with rapamycin reduced cellular injury demonstrated by decreased HIF-1α, CC3 and Iba-1 immunoreactive cells in the periventricular white matter (Figure 3B).

Changes in neonatal body temperature and body weight following HIL

To eliminate the confounding effects of neonatal fever in our animal model of CP, the body temperature of pups was taken prior to euthanization. There was no significant difference observed in body temperature among sham, HIL and HIL + rapamycin treated animals at 24h or 48h following surgery (Table 1).

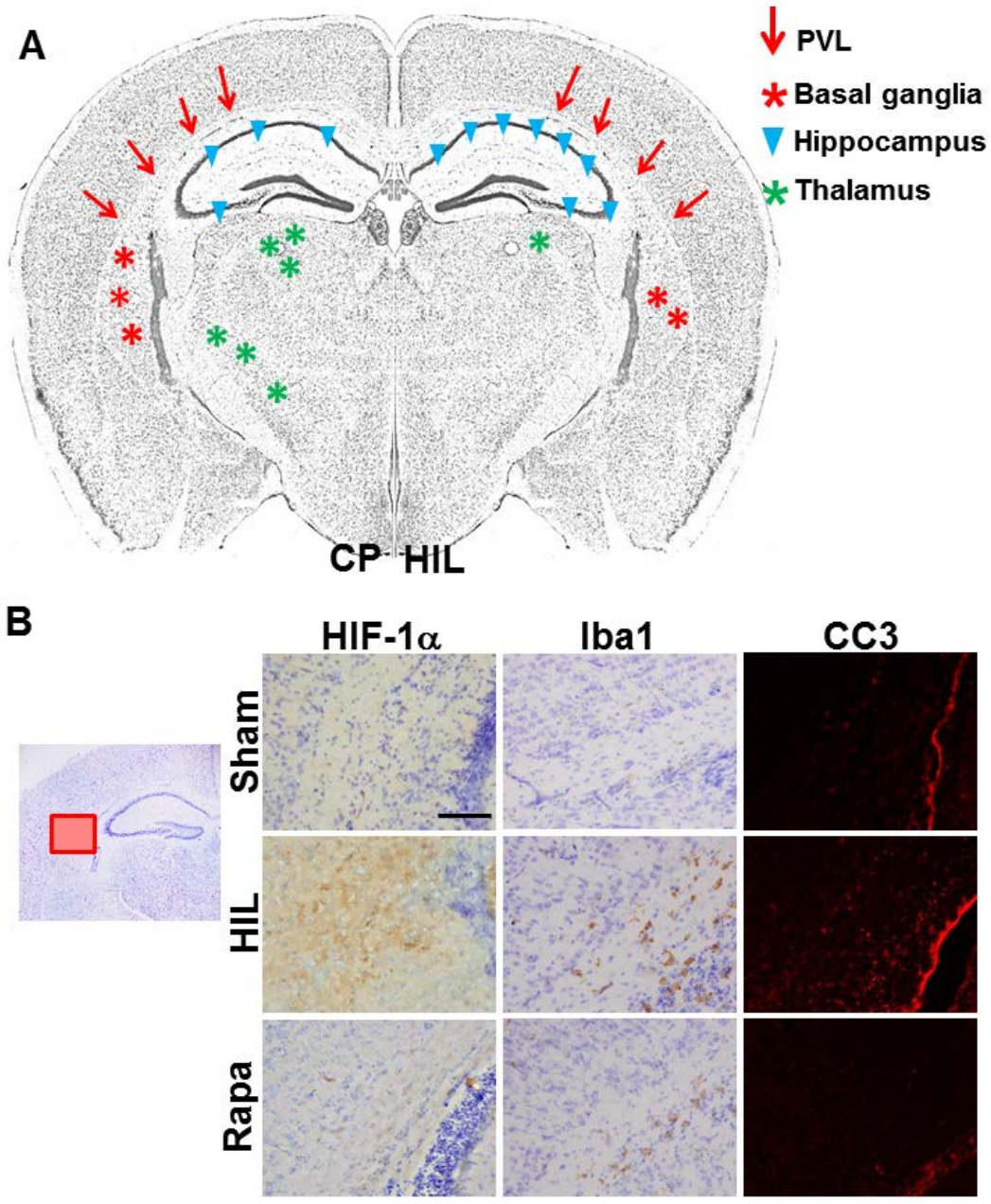

Figure 3. Neuronal and periventricular white matter injury following HIL.
A: Similarities between cellular damage observed in human cerebral palsy (CP, left)[13,15,16] and our animal model (HIL, right) on a section from Allen Brain Atlas[225]. PVL (see text) and injury to the basal ganglia, hippocampus, and thalamus are observed in human CP and the HIL model. In CP, more severe injury is often seen in the dorsal and ventral thalamus and basal ganglia; hippocampal injury is common to both but may be more severe in HIL. B: Red box demarcating periventricular white matter area imaged. Increased HIF-1α, Iba-1 and cleaved-caspase 3 (CC3) labeling seen in HIL animals at 24h post-injury is significantly reduced with rapamycin treatment. Scale bar = 100μm.

Previous work has demonstrated that the mTOR signaling pathway is an important regulator of body size[226,227]. Furthermore, while some studies have demonstrated that chronic rapamycin treatment can affect body weight and growth in animals[228], others report no effect on body weight[226]. To investigate whether rapamycin adversely affected growth of mice, pups were weighed prior to ischemia and at the time of euthanization to determine a change in body weight. HIL and HIL + Rapa treated animals exhibited significant weight loss at 24 and 48 hours post-surgery compared to shams, but no difference was observed at 1 month post-injury (Table 1).

Table 1. Average body temperature (°C) and average change in body weight (grams) post-HIL

Condition	Body Temperature (°C)	n	Change in body weight (g)	n
24h				
Sham	27.48°C ± 0.53	8	0.49 ± 0.06	33
HIL	27.01°C ± 0.49	9	-0.14 ± 0.05*	34
HIL + Rapa	27.07°C ± 0.53	13	-0.31 ± 0.06*,†	27
48h				
Sham	27.06°C ± 0.59	5	1.03 ± 0.14	18
HIL	26.77°C ± 0.65	9	0.40 ± 0.16*	32
HIL + Rapa	27.25°C ± 0.64	11	-0.50 ± 0.22*,†	24
1wk				
Sham	N/A		3.26 ± 0.25	15
HIL	N/A		2.76 ± 0.20	25
HIL + Rapa	N/A		1.02 ± 0.31*,†	10
1 month				
Sham	N/A		12.23 ± 1.18	14
HIL	N/A		11.32 ± 0.79	13
HIL + Rapa	N/A		15.55 ± 1.22	8

Values expressed as mean ± SEM. N/A – not assessed
*Statistically significant difference (P< 0.05) compared to sham treated pups.
†Statistically significant difference (P< 0.05) compared to HIL treated pups.

Constitutive mTOR signaling following HIL

Persistent phosphoactivation of S6 and S6K post-HIL

Our lab was particularly interested in the effects of mTOR inhibition on neuronal death, and thus focused our analysis on the hippocampus due to its vulnerability to hypoxic-ischemic damage in animals[229–232] and humans[233–235], and because hippocampal injury has been observed in children with CP[16]. Levels of phospho-S6K (P-S6K) and phospho-S6 (P-S6), known downstream effectors of mTOR, were not altered by HIL compared with sham animals in hippocampal lysates at both 24 and 48h (Figure 4A-B). Immunohistochemical analysis confirmed these results and revealed P-S6 immunoreactive cells in the CA1 and CA3 subfields of the hippocampus at 24h (Figure 4C) and 48h (Figure 4D) in both sham and HIL treated animals. Unlike sham animals, P-S6 labeled cells in the pyramidal neuronal layer showed severe disorganization in both subfields in HIL animals. Thus, HIL does not alter S6K or S6 phosphorylation and there are constitutive levels of mTOR signaling.

Since mTOR signaling normally persists in conditions favorable for cell growth, I hypothesized that persistent mTOR signaling following HIL was deleterious and thus, treated animals following HIL with rapamycin. Rapamycin administration (HIL+Rapa) dramatically reduced the number of P-S6 immunoreactive cells in the hippocampus at both 24h and 48h (Figure 4C-D) and reduced the levels of P-S6, but did not affect total S6 protein expression in hippocampal lysates (Figure 4A-B). Moreover, laminar disorganization seen following HIL in the hippocampus was not observed in HIL + Rapa animals.

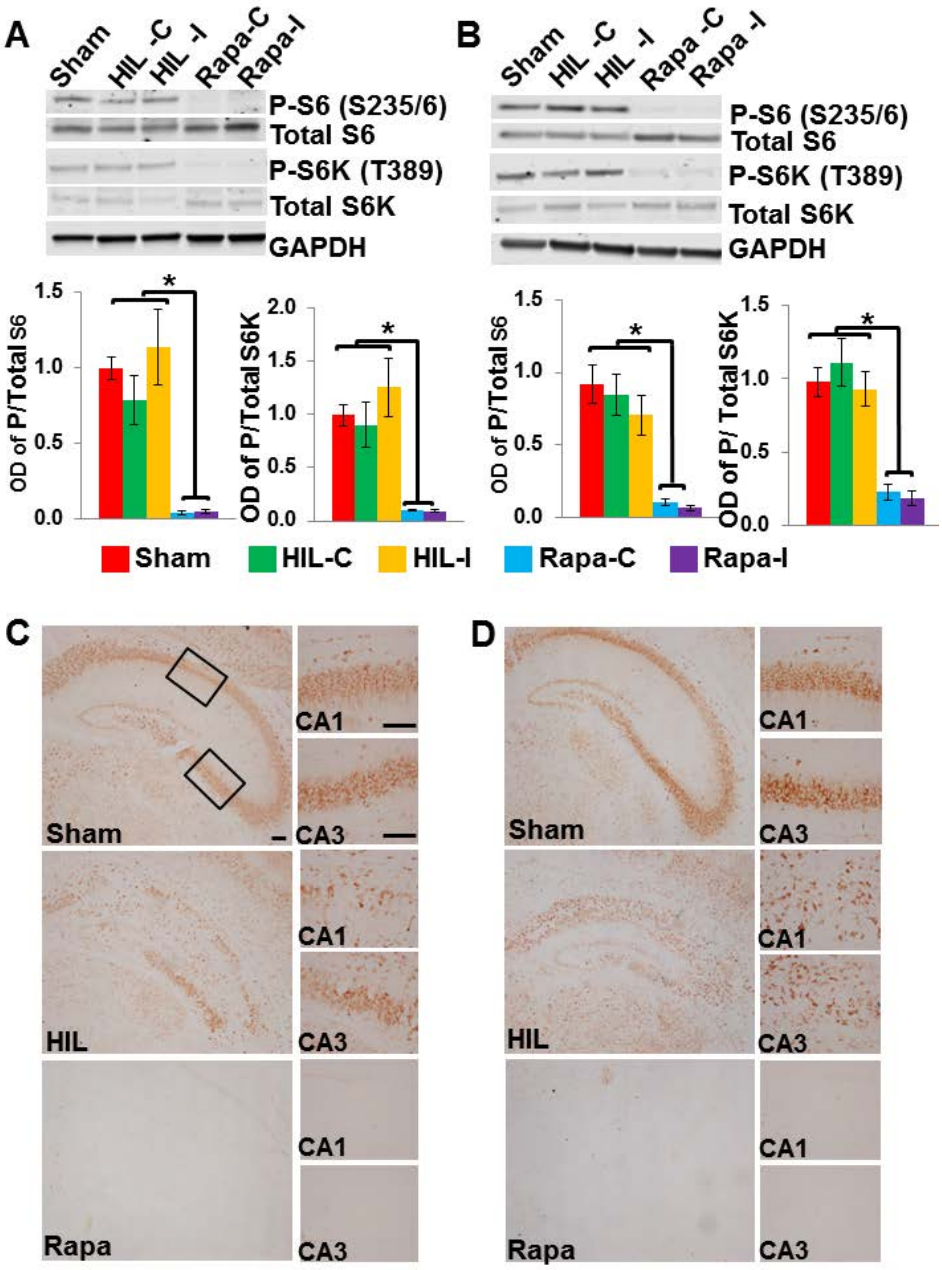

Figure 4. P-S6 and P-S6K following HIL and HIL+Rapamycin

A,B: Western blot analysis of phospho-S6 (P-S6) and phospho-S6K (P-S6K) at 24 hours (A) and 48 hours (B) post-HIL. Note no change in P-S6 and P-S6K following HIL but significant reduction in both following rapamycin (Rapa). Data are expressed as optical density (OD) of phospho- to total (non-phosphorylated) isoform, relative to sham values and are mean±SEM. One way ANOVA with post-hoc analysis was performed and $P< 0.05$ (*) was considered significant. C: contralateral, I: ipsilateral to common carotid occlusion. C,D: Phospho-S6 at 24 hours (C) and 48 hours (D) in the ipsilateral hippocampus. Note near complete absence of phospho-S6 following Rapa. Black boxes indicate CA1 and CA3 areas. Scale bar = 100μm

In addition to mTOR, death associated protein kinase (DAPK) can also phospho-activate S6[236]. DAPK, which is phospho-inactivated, regulates apoptosis in response to a death inducing signals, e.g. TNF-α, IFN-ɣ, and growth factor signaling, e.g. MAPK/ERK (reviewed in [237]). The phosphorylation state and total expression of DAPK was investigated since increased activity of DAPK following HIL may contribute to the persistent phospho-activation of S6 observed following HIL. Neither total DAPK expression nor the phospho-isoform (P-DAPK) was altered in response to HIL at 24h post-injury (Figure 5). Furthermore, there was no change in P-DAPK or DAPK expression following rapamycin treatment (Figure 5). These data supports the hypothesis that persistent P-S6 expression is mediated by constitutive mTOR signaling, not by enhanced DAPK activity.

Constitutive phospho-inactivation of 4EBP1 following HIL

In addition to the S6, the 4E-BP facet of the mTOR signaling cascade was also investigated. Similar to P-S6 and P-S6K, levels of phospho-4EBP1 (P-4EBP) were not altered by HIL compared with sham animals in hippocampal lysates at either 24 or 48h (Figure 6A-B). There was a modest increase in total 4E-BP1 levels ipsilateral to the ischemia and in rapamycin treated animals at 48h, which was not observed at 24h following HIL (Figure 6B). Rapamycin administration reduced the levels of P-4EBP at both 24h hours and 48h (Figure 6A-B). Of note, the effect of rapamycin on the phosphorylation state of 4EBP1 was less dramatic than the effect on S6. Collectively, these data demonstrate that HIL results in constitutive activation of the mTOR signaling cascade, which is significantly inhibited by rapamycin.

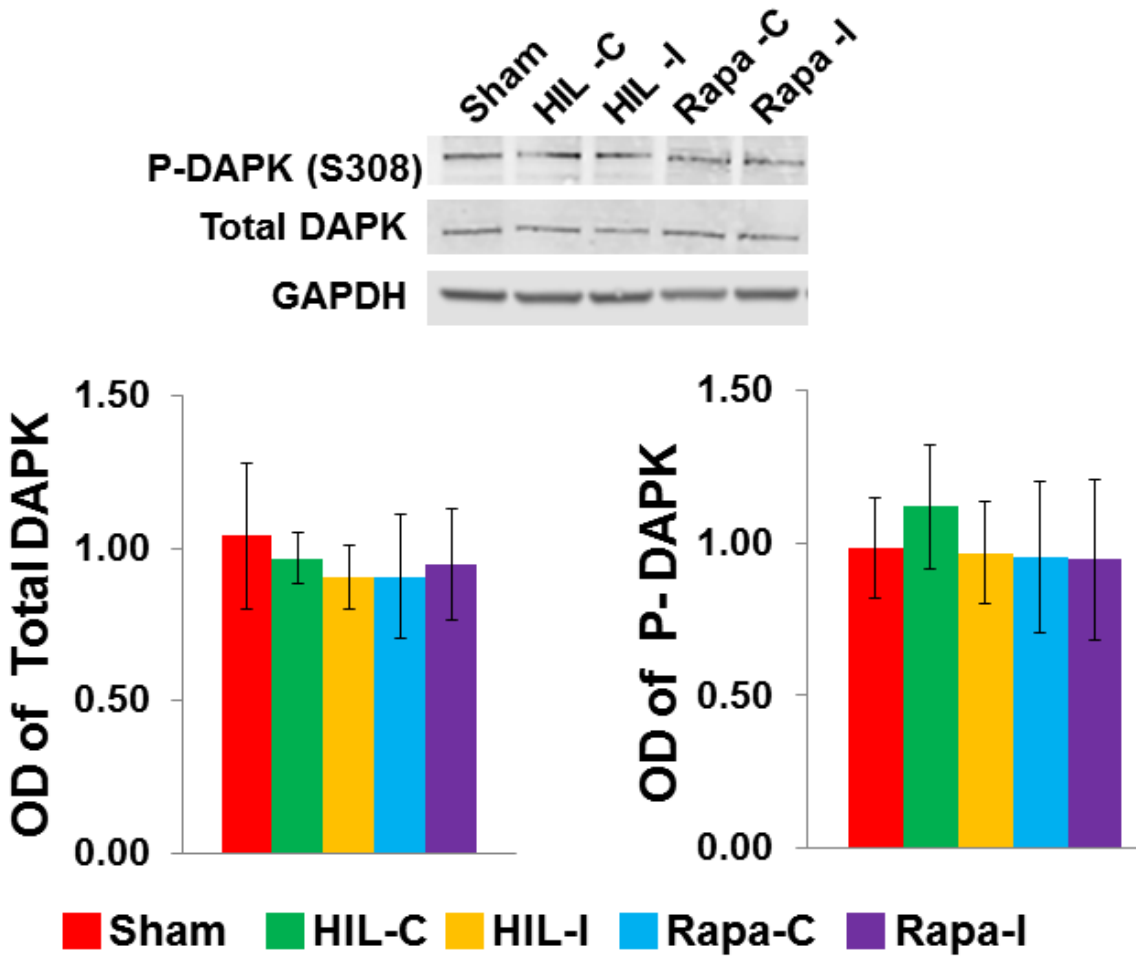

Figure 5. DAPK and P-DAPK expression is not changed following HIL.
Western blot and densitometric analysis of total (non-phosphorylated) and phospho-DAPK (P-DAPK) at 24 hours post-HIL. Note no change in P-DAPK or DAPK following HIL or with rapamycin treatment. Data are expressed as optical density (OD) of phospho- or total (non-phosphorylated) isoform relative to sham values and are mean±SEM.

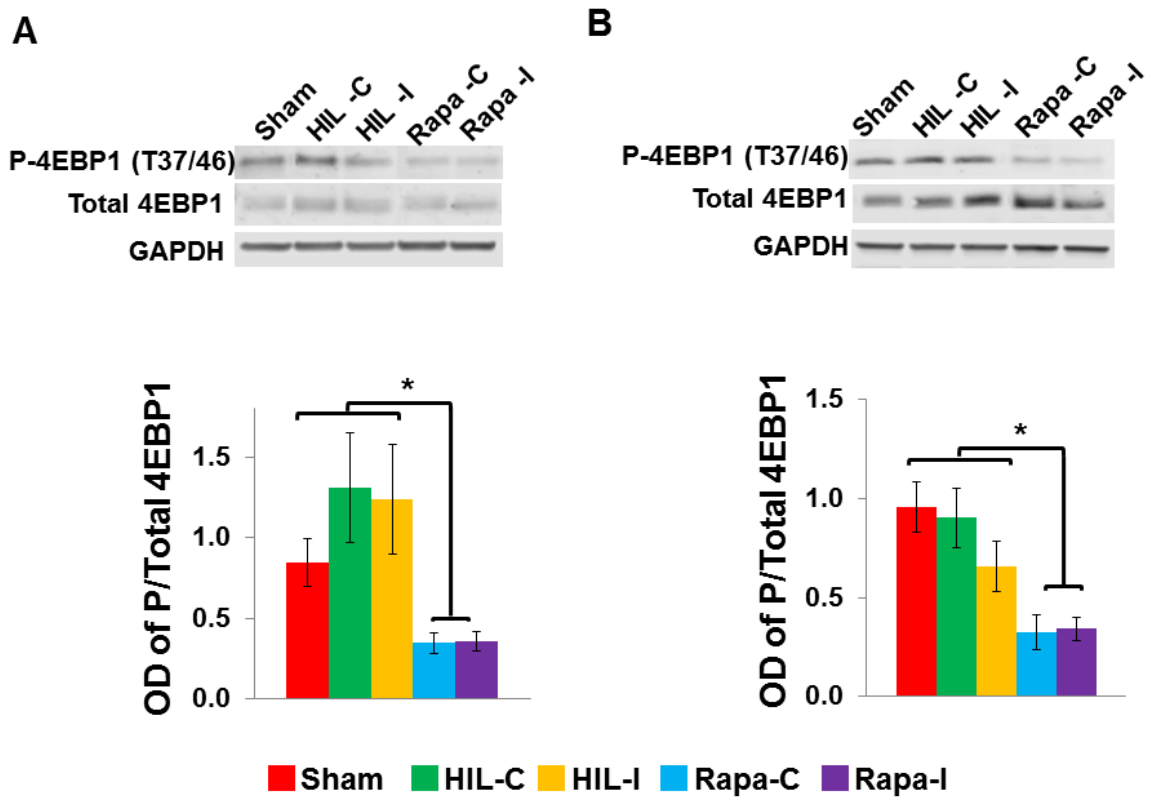

Figure 6. P-4EBP1 following HIL and HIL+Rapamycin.

A,B: Western blot analysis of phospho-4EBP1 (P-4EBP1) and total (non-phosphorylate) 4EBP1 at 24 hours (A) and 48 hours (B) post-HIL. Note no change in P-4EBP1 following HIL but significant reduction following rapamycin (Rapa) at 24 and 48 hours. At 48 hours, a modest increase in total 4EBP1 was observed following rapamycin treatment and in HIL ipsilateral to ischemia. Data are expressed as optical density (OD) of phospho- to total (non-phosphorylated) isoform, relative to sham values and are mean±SEM. One way ANOVA with post-hoc analysis was performed and $P< 0.05$ (*) was considered significant. C: contralateral, I: ipsilateral to common carotid occlusion.

REDD1, but not TSC1, may contribute to mTOR activity following HIL

Previous work has demonstrated that suppression of TSC1 following ischemia results in increased mTOR activity and enhanced neuronal damage in the hippocampus[184]. In addition, regulation of mTOR activity following hypoxia requires induction of Redd1 (regulated in development and damage 1), and overexpression was protective in hypoxic conditions[238]. Since TSC1 and Redd1 have been suggested as potential mechanisms of mTOR-dependent damage following hypoxic-ischemic insults[184,238], we hypothesized that dysregulation of one or both of these negative upstream regulators may result in persistent mTOR signaling and examined the expression of both TSC1 and Redd1 following HIL .

At 24h post-injury, there was no change in TSC1 expression in hippocampus lysates following HIL (Figure 7A). However, HIL resulted in a significant decrease in Redd1 expression in the hippocampus as compared to shams (Figure 7B). Furthermore, this decrease was only observed ipsilateral to carotid occlusion, which is the site of greatest neuronal death (discussed below). Thus, these findings demonstrate that dysregulated Redd1 expression contributes to constitutive activity of mTOR following HIL.

Enhanced HIF-1α associated with areas of neuronal death

In addition to the canonical signaling nodes of the mTOR pathway, we assessed the expression of HIF-1α, which is modulated by mTOR and orchestrates cellular responses to low oxygen tension[239,240], in the hippocampus of sham, HIL and Rapa

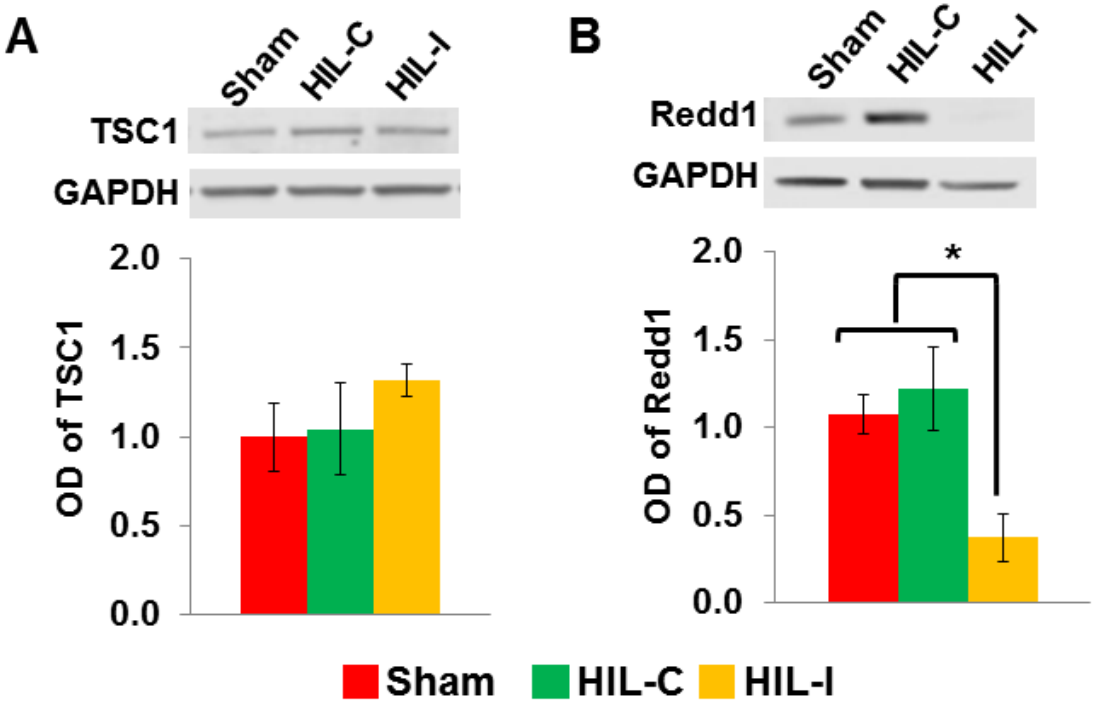

Figure 7. Expression of upstream regulators, TSC1 and Redd1, following HIL. Western blot analysis of TSC1 (A) and Redd1 (B) at 24 hours post-HIL. Note, there is no change in TSC1 following HIL. There is a significant reduction in Redd1 ipsilateral to carotid occlusion (HIL-I), but no change in Redd1 contralateral to occlusion compared to sham animals. Data are expressed as optical density (OD) relative to sham values and are mean±SEM. One way ANOVA with post-hoc analysis was performed and $P< 0.05$ (*) was considered significant. C: contralateral, I: ipsilateral to common carotid occlusion.

treated pups. Though undetectable due to constant degradation in normal oxygen tension, HIF-1α is stabilized and robustly expressed in the nucleus following hypoxia.

Enhanced HIF-1α expression was detected throughout the hippocampus ipsilateral to the carotid ligation of HIL animals at 24h (Figure 8A) and 48h post-injury (Figure 8B), as well as the ipsilateral periventricular white matter (Figure 3B), cortex and thalamus (data not shown). There were very few HIF-1α labeled cells observed in the contralateral hippocampus and cortex in HIL mice and none detected in the sham animals. Western blot analysis of hippocampal lysates demonstrated significantly increased HIF-1α expression compared shams at both 24h (Figure 8C) and 48h (Figure 8D), confirming immunohistochemical findings. Furthermore, rapamycin reduced HIF-1α expression at 24h (Figure 8A,C) and 48h post-injury (Figure 8B,D). Interestingly, HIF-1α immunoreactive cells observed in the hippocampus at 24h and 48h localize to areas of neuronal cell death indicated by FJC (Figure 8).

Rapamycin is neuroprotective in HIL model of CP

Neuronal death is mTOR dependent

Fluoro-Jade C was used to label degenerating neurons at 24h, 48h, 1 week and 1 month post-injury as a strategy to define neuronal injury following HIL and a potential response to rapamycin. The maximal period for neuronal death occurs within the first 48h following HIL (Figure 9A). Though there was some animal-to-animal variation, the hippocampus consistently exhibited extensive FJC labeling demarcating areas of cell

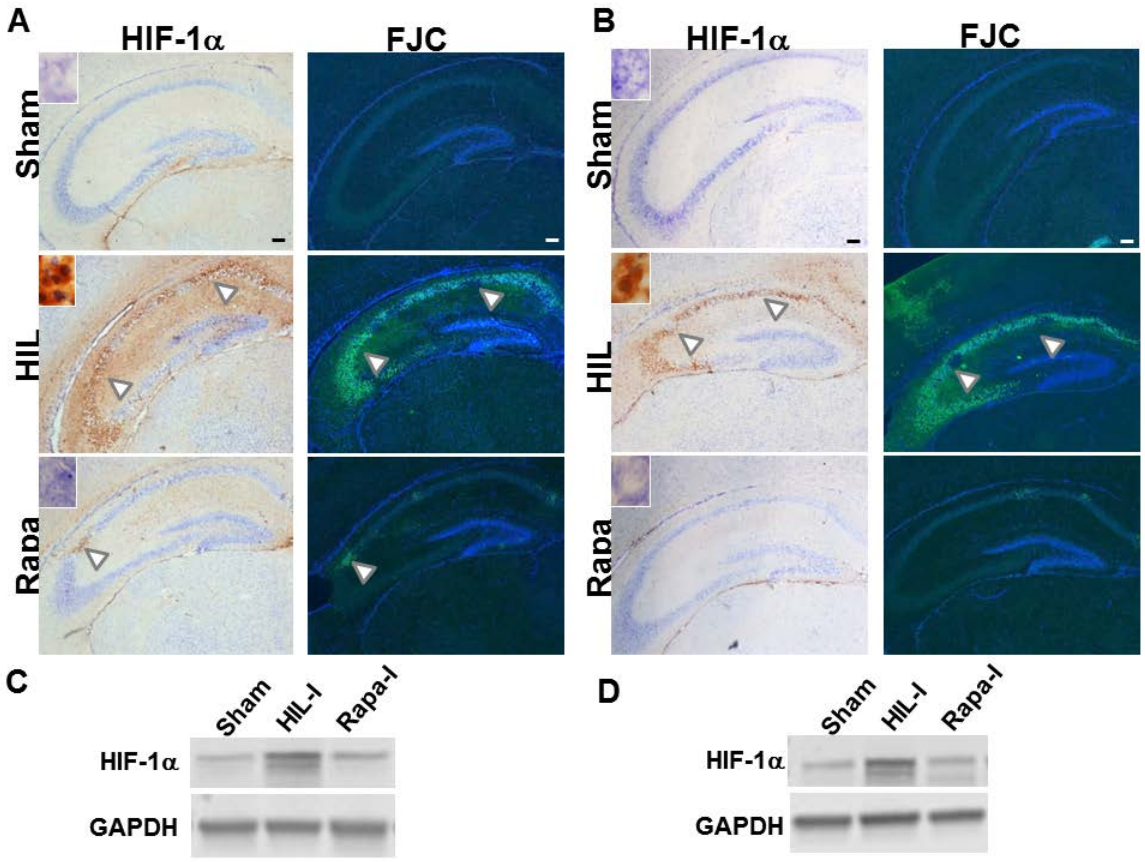

Figure 8. Increased HIF-1α expression localizes to areas of neuronal death.
A,B: HIF-1α expression with cresyl violet counterstain and FJC labeling with DAPI in the hippocampus at 24 hours (A) and 48 hours (B);. Insets: HIF-1α immunoreactive neurons at 60X magnification. Note increase in HIF-1α following HIL and that the pattern of HIF-1α expression localizes with the areas of neuronal death (arrowheads) indicated by FJC at 24 hours (A) and 48 hours (B). Rapa reduced HIF-1α expression and diminished neuronal death at both time points. FJC: Fluoro-Jade C, Rapa: Rapamycin. Scale bar = 100μm. C,D: Western blot analysis of HIF-1α expression in hippocampal lysates at 24 (C) and 48 hours (D). Note increase in HIF-1α expression in HIL animals, which is drastically reduced by rapamycin treatment. I: ipsilateral to common carotid occlusion.

death following HIL (Figure 9A). Neuronal cell death in the hippocampus occurred exclusively ipsilateral to the carotid ligation with no cell death in the contralateral hemisphere.

A 6-point cell death scale (0-5) was devised to assess the global severity of neuronal death in the hippocampus, thalamus, and cortex following HIL. In this scale, a score of 0 corresponded to no cell death, whereas a score of 5 represented cell death present throughout the hippocampus, as well as non-hippocampal structures such as cortex, thalamus, etc. The average cell death score for HIL was 4/5 at 48h reflecting cell death in >50% of the hippocampus (Figure 9B) and in some HIL animals, neuronal cell death extended to the ipsilateral cortex and areas of the thalamus, (a 5/5 on the scale). Following rapamycin treatment, the average injury scores were diminished to 0.8/5 at 24h and 1/5 at 48h reflecting near absence of cell death across the hippocampus, thalamus, and cortex (Figure 9B-C).

We utilized an S6K inhibitor (PF-4708671, 75 mg/kg, i.p.) to confirm that the mTOR signaling cascade contributes to neuronal death following HIL. Similar to rapamycin treatment, animals treated with S6KI immediately following HIL exhibited significant decrease in neuronal death demonstrated by FJC staining and decreased average injury score (Figure 9B). Following S6KI treatment, the average injury scores were reduced to 1/5 at 24h hours following HIL (Figure 9B). This was statistically similar to animals treated with rapamycin and sham animals, but drastically less than HIL without any treatment. In concert with the neuroprotective effects of rapamycin, these data further demonstrate that the mTOR signaling cascade mediates neuronal death following HIL.

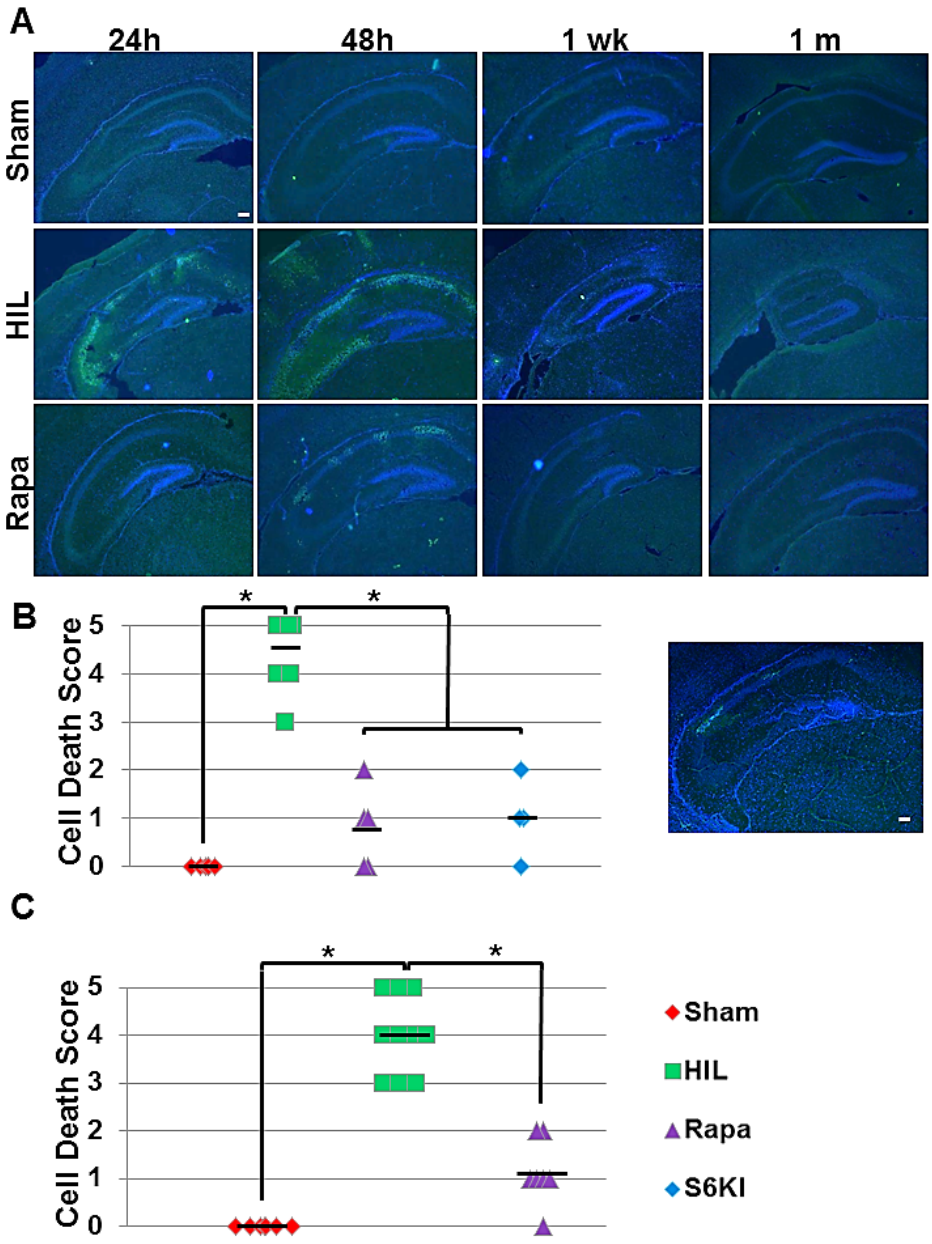

Figure 9. mTOR inhibition during period of maximal injury is protective.

A: Representative images of Fluoro-Jade C (FJC, green) and DAPI (blue) labeled sections demonstrate substantial neuronal death at 24 and 48 hours following HIL. No new cell death is seen at 1 week and 1 month following HIL. Scale bar = 100μm. B,C : Neuronal death score (see text) of sham, HIL, HIL+ Rapa at 24h (B) and 48h (C) post-HIL. B: In addition, representative image of neuronal death HIL+ S6K inhibitor (S6KI) at 24h. Note, HIL had significantly greater injury scores than sham and Rapa animals at both time points. S6KI significantly reduced neuronal death to levels equivalent to sham and rapamycin treated animals. Black bars represent mean scores for each condition. One way ANOVA followed by post-hoc analysis was performed and $P < 0.05$ (*) was considered significant.

Rapamycin reduces neuronal death following HIL

Analysis of FJC labeling demonstrated extensive neuronal cell death in the hippocampal CA1 and CA3 subfields following HIL at both 24h (Figure 10A,C) and 48h (Figure 10B,D) compared to shams. There were significantly more FJC labeled neurons seen in the CA1 region of interest than CA3 at 24h following HIL (Figure 10C); however, by 48h FJC labeling was similar in both subfields (Figure 10D). Furthermore, 90% of the FJC labeled neurons were also immunoreactive for CC3 (Figure 10) suggesting that the primary mechanism of cell death following HIL is apoptosis. Rapamycin reduced neuronal cell death in the CA1 and CA3 subfields to levels similar to sham operated animals at 24h (Figure 10A,C) and 48h (Figure 10B,D) following HIL. At 24h, rapamycin treatment significantly reduced the average number of FJC labeled cells in the CA1 (from 93.80±17.50 to 19.87±11.07) and CA3 regions (from 38.67±13.73 to 2.67±2.58) (Figure 10C). Similar findings were observed at 48h (Figure 10D). Of note, there was no significant difference between rapamycin and sham treated animals.

Short course of rapamycin provides long-term neuroprotection

To determine long term effects of rapamycin treatment, neuronal death was evaluated following the conclusion of rapamycin administration (1 week and 1 month). There was no ongoing cell death e.g., no FJC labeling at these time points (Figure 9A), at 1 week or 1 month post-injury but obvious permanent injury to the hippocampus evidenced by atrophy and loss of cells in the CA subfields (Figure 11). In rapamycin treated animals, there was no evidence of delayed or permanent hippocampal injury (Figure 11), and no FJC labeling was seen at 1 week or 1 month (Figure 9A).

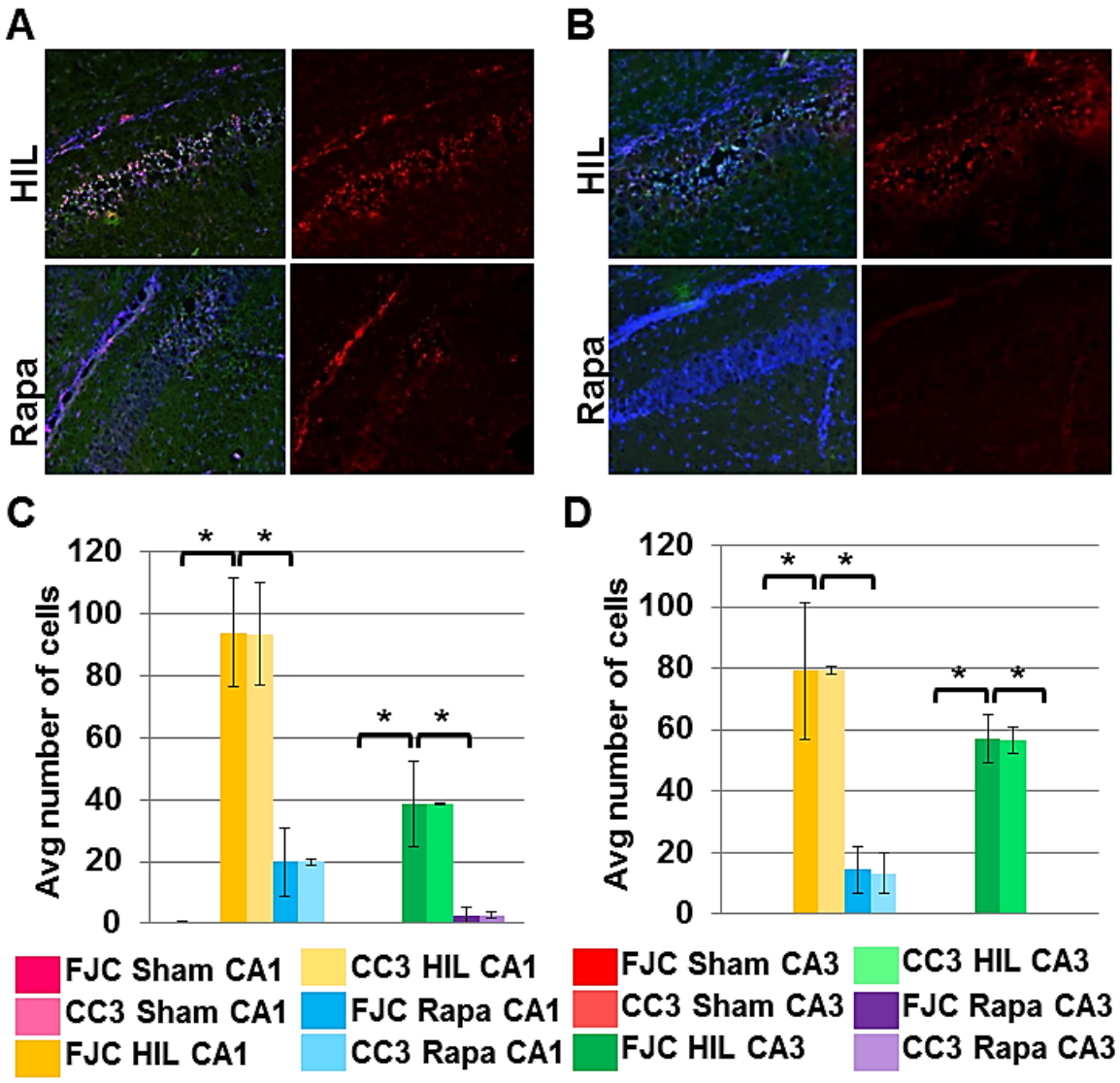

Figure 10. Analysis of neuronal death in HIL model of CP.

A,B Representative FJC (green), DAPI (blue) and cleaved caspase 3 (red, CC3) triple labeled CA1 sections at 24h (A) and 48h (B). Scale bar = 100μm. C,D: Quantification of FJC labeled cells in the CA1 and CA3 regions of the hippocampus at 24 (C) and 48h (D) hours post-HIL. FJC (FJCSham) and CC3 (CC3Sham) labeling was not detected in sham CA1 or CA3. Note significant reduction in FJC and CC3 labeled neurons following HIL+Rapa in CA1 and CA3. One-way ANOVA followed by Tukey post-hoc analysis was performed to determine significance and $P < 0.05$ (*) is considered significant.

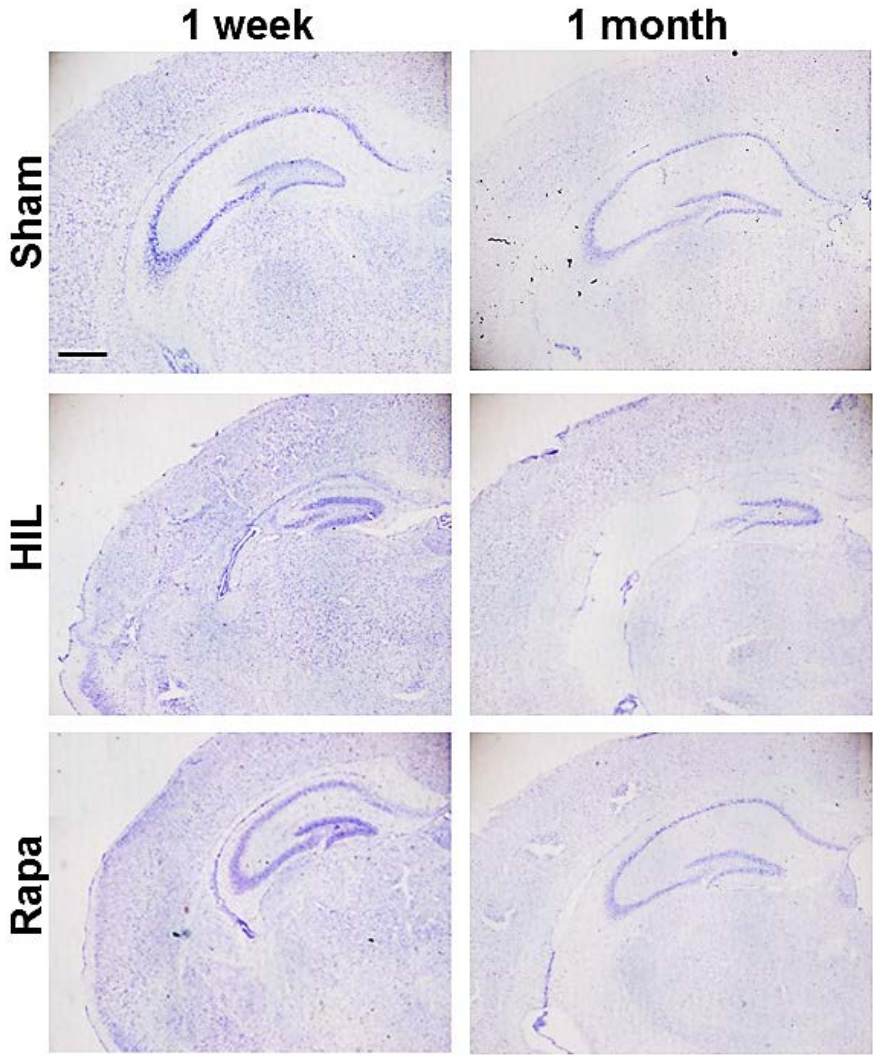

Figure 11. Neuropathological sequelae of HIL at 1 week and 1 month.
Representative images of cresyl violet stained sections demonstrating atrophic hippocampi at 1 week and 1 month post-HIL. Note normal size and morphology of hippocampus at 1 week and 1 month following rapamycin (Rapa) treatment. Scale bar = 500μm

The cytoarchitecture of the hippocampus 1 week and 1 month following HIL+Rapa was intact (Figure 11) compared with HIL at these time points. Collectively, these results demonstrate that rapamycin treatment provided long-term neuroprotection since it eliminated, rather than delayed, neuronal cell death.

Neuroinflammation following HIL is mediated by mTOR

Rapamycin reduces microglia activation

Microglia transform through a spectrum of morphological changes from a resting state, characterized by a small cell body with long, fine processes, to an activated state, characterized by an enlarged, spherical cell body with retracted processes, in response to stimuli such as LPS or hypoxia[206,207]. Activated microglia are widely believed to be the primary source of pro-inflammatory cytokines contributing to the pathogenesis of CP[83,84]. Thus, the morphology of microglia was examined following HIL and in response to rapamycin treatment. Activated microglia were present in the hippocampus (Figure 12), periventricular area (Figure 3C), thalamus and cortex (data not shown) ipsilateral to the carotid ligation of HIL animals at 24h post-injury. In the pyramidal cell layer of the hippocampus, the microglia were located primarily surrounding areas of neuronal cell death (Figure 12A). However, activated microglia were present throughout the strata radiatum, lacunosum and moleculare (SR/L/M) in the ipsilateral hippocampus (Figure 12B). Microglia in an intermediate activation state, characterized by a larger soma and thick processes, were observed on the contralateral side whereas resting microglia were observed throughout the hippocampus in sham animals (Figure 12B).

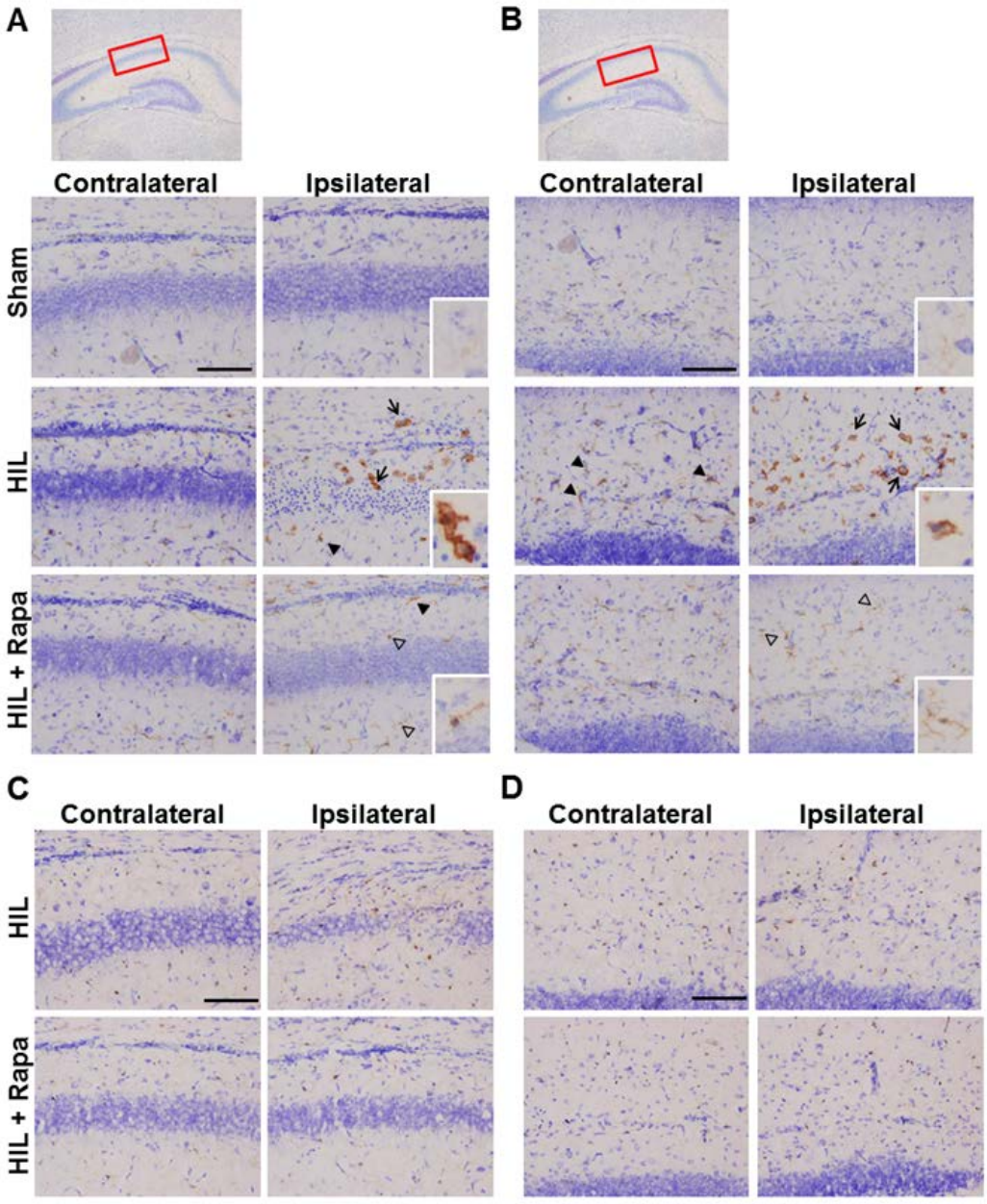

Figure 12. Rapamycin treatment ameliorates neuroinflammation following HIL. Iba-1 labeled microglia in the stratum pyramidale (A,C), and strata radiatum and lacunosum-moleculare (SR/L/M; B,D) at 24h (A, B) and 1 wk (C,D) post-HIL. Red boxes demarcate respective areas of the hippocampus. A, B: At 24h, the number of activated Iba-1 labeled microglia is increased following HIL and reduced following HIL+Rapa. Insets: Iba-1 immunoreactive microglia at 60X magnification. Arrow: activated morphology, closed arrowhead: intermediate morphology, open arrowhead: resting morphology. C,D: At 1 week following HIL, no activated microglia are observed in either HIL or Rapa treated animals. Of note, more Iba-1 microglia are present in HIL than rapamycin treated animals. Scale bar = 100μm.

Resting or intermediately activated microglia were primarily observed in rapamycin treated animals (Figure 12A).

At 1 week post-HIL, there were no activated microglia observed in HIL or HIL + Rapa conditions demonstrated by a lack of enlarged, spherical Iba-1 labeled microglia observed at earlier time points (Figure 12C-D). However, there are more resting microglia observed in HIL compared to HIL+Rapa, especially in the SR/L/M of the hippocampus (Figure 12D). Since mTOR signaling is increased in activated microglia[209,210], the effect of mTOR inhibition on the number and morphology of Iba-1 labeled microglia was quantified in the hippocampus post-HIL. Both the number of total and activated Iba-1 labeled microglia was significantly increased in HIL in the strata radiatum, lacunosum and moleculare and CA3 stratum pyramidale (Figure 13A-B). Activated microglia coincided with robust increase in phospho-S6 labeling (Figure 13A).

Rapamycin treatment significantly reduced both the number of total and activated Iba-1 labeled microglia (Figure 13B), which coincided with decreased phospho-activation of S6 (Figure 13A), demonstrating that rapamycin treatment ameliorates microglial activation following HIL.

P-STAT3 may contribute to mTOR-dependent microglia activation

Signal transducer and activator 3 (STAT3) is a latent cytoplasmic transcription factor that translocates to the nucleus to induce transcription of target genes when phospho-activated. STAT3 can be activated in response to growth factor and cytokine signaling via phosphorylation at T705. In addition, STAT3 can be phospho-activated by

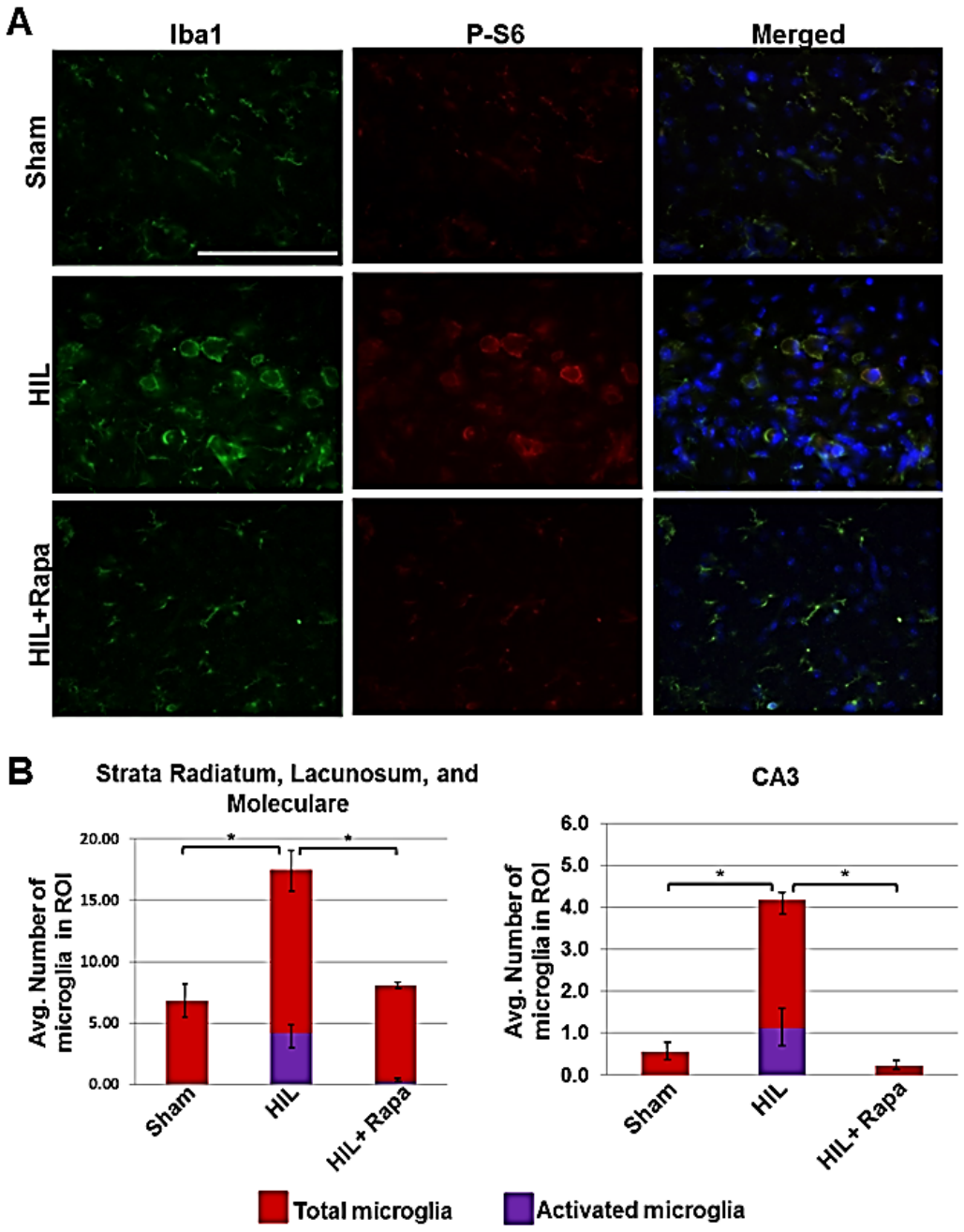

Figure 13. Microglia activation following HIL is mTOR dependent.

A: Iba-1 and phospho-S6 (P-S6) co-labeled microglia in SR/L/M in sham, HIL and HIL+Rapa conditions at 24 hours. Note reduction in microglia activation and S6 phosphorylation following Rapa. Scale bar = 100μm. B: Quantification of Iba-1 labeled in SR/L/M and CA3. Red bars depict total Iba-1 labeled microglia, purple bars represent activated microglia. Note reduction in both total and activated microglia following Rapa. One-way ANOVA followed by Tukey post-hoc analysis was performed to determine significance and $P < 0.05$ (*) is considered significant.

mTOR at S727, which is required for maximal transcriptional activity [174,241]. When activated, P-STAT3 can regulate various processes, such as cell growth and proliferation, Since STAT3 is regulated in response to growth conditions and inflammatory cytokines, mTOR mediated phospho-activation of STAT3 was examined to determine whether it contributes to neuroinflammation following HIL. Western blot analysis of P-STAT3 demonstrates an increase in P-STAT3 expression ipsilateral to carotid ligation as compared to sham and rapamycin treated animals (Figure 14A). No change in total (non-phosphorylated) STAT3 levels was observed (Figure 14A). Phospho-STAT3 (P-STAT3) immunoreactive cells were observed in the hippocampus ipsilateral to carotid ligation at both 24h and 48h following HIL (Figure 14C-D). No P-STAT3 cells were observed contralateral to carotid occlusion or in sham animals. Of note, P-STAT3 labeling was primarily observed in the strata radiatum, lacunosum and moleculare, but not in the stratum pyramidale layer of the ipsilateral hippocampus suggesting a glial expression pattern of P-STAT3 (Figure 14C-D). Rapamycin resulted in significant reduction in P-STAT3 immunoreactivity at both 24 (Figure 14C) and 48h (Figure 14D) post-HIL.

Rapamycin results in transient autophagy induction

HIL results in failure of autophagy induction

Macroautophagy (hereafter referred to as autophagy) is an evolutionary conserved process for degrading and recycling cellular components. mTOR signaling cascade is negative upstream regulator of autophagy related genes (ATG) and regulates autophagy

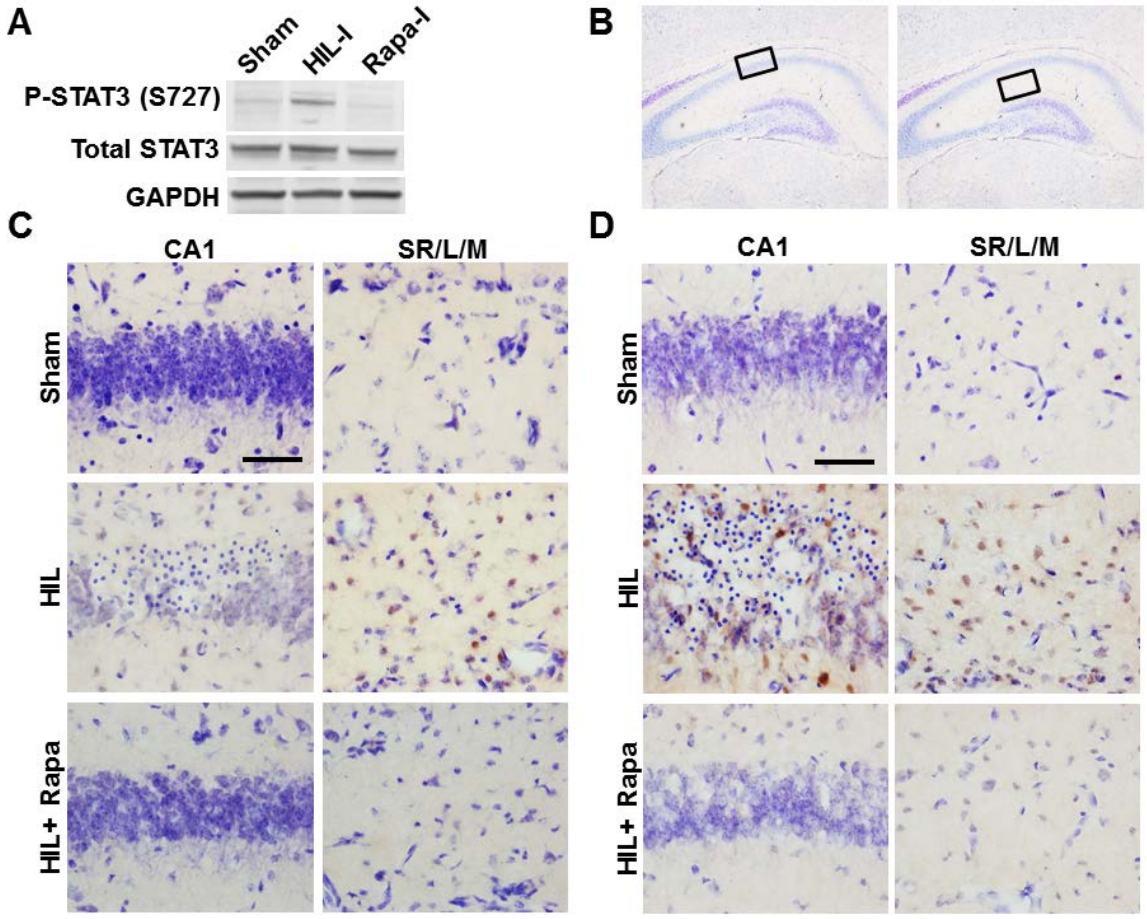

Figure 14. P-STAT3 activation following HIL localizes to microglia.

A: Western blot analysis of hippocampal lysates at 24h demonstrating increased P-STAT3 expression following HIL, which is significantly reduced with rapamycin treatment. Of note, there is no change in total STAT3 expression. I: ipsilateral to the carotid ligation. B: Black boxes demarcate CA1 and strata radiatum and lacunosum-moleculare (SR/L/M) subfields of the hippocampus imaged. C,D: Representative images of phospho-STAT3 (P-STAT3) labeling with cresyl counterstain in sham, HIL and HIL+Rapa conditions at 24h (C) and 48h (D) post-HIL. Note increased P-STAT3 immunoreactive cells in the SR/L/M in HIL treated animals at both time-points. In the CA1 subfield, P-STAT3 immunoreactive cells are present but do not localize with cresyl staining and likely represent gliosis surrounding dying or injured neurons. Rapamycin treatment significantly reduced immunoreactivity of P-STAT3 to sham levels at both 24 and 48h. Scale bar = 100μm.

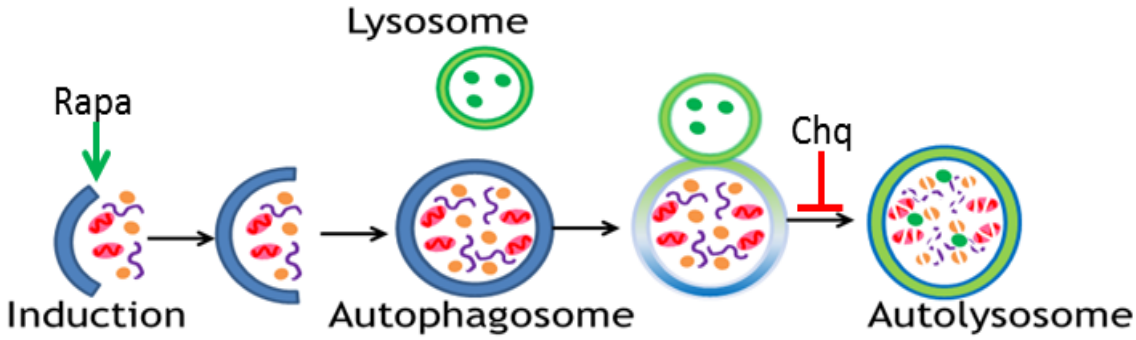

Figure 15. Schematic representation of autophagy.
Rapamycin leads to induction of autophagy and formation of functional autophagosome. Fusion with a lysosome leads to the autolysosome for protein degradation, a process blocked by Chq.

in response to growth factors, nutrients and cellular stress[195,196]. As such, mTOR inhibition would foster autophagy induction. There is evidence that induction of autophagy may be an adaptive response to promote cell survival during conditions of bioenergetic stress [242–244]. Thus, the absence of autophagy in the context of cellular stress may leave cells vulnerable to cell death. The expression of Beclin-1, a marker of autophagy induction, and LC3II, a marker of autophagosome formation, (Figure 15) was evaluated to test the hypothesis that persistent activation of the mTOR signaling cascade following HIL results in impaired autophagy induction. There was no change in expression of either autophagy marker between sham and HIL treated animals at 24 (Figure 16A) and 48h (Figure 16B) post-injury. In contrast, rapamycin treatment resulted in transiently increased autophagy induction evidenced by increased Beclin-1 and LC3II expression at 24h (Figure 16A) suggesting that autophagy induction may aid with neuronal survival. No change in autophagy induction was seen in rapamycin treated animals at 48h (Figure 16B).

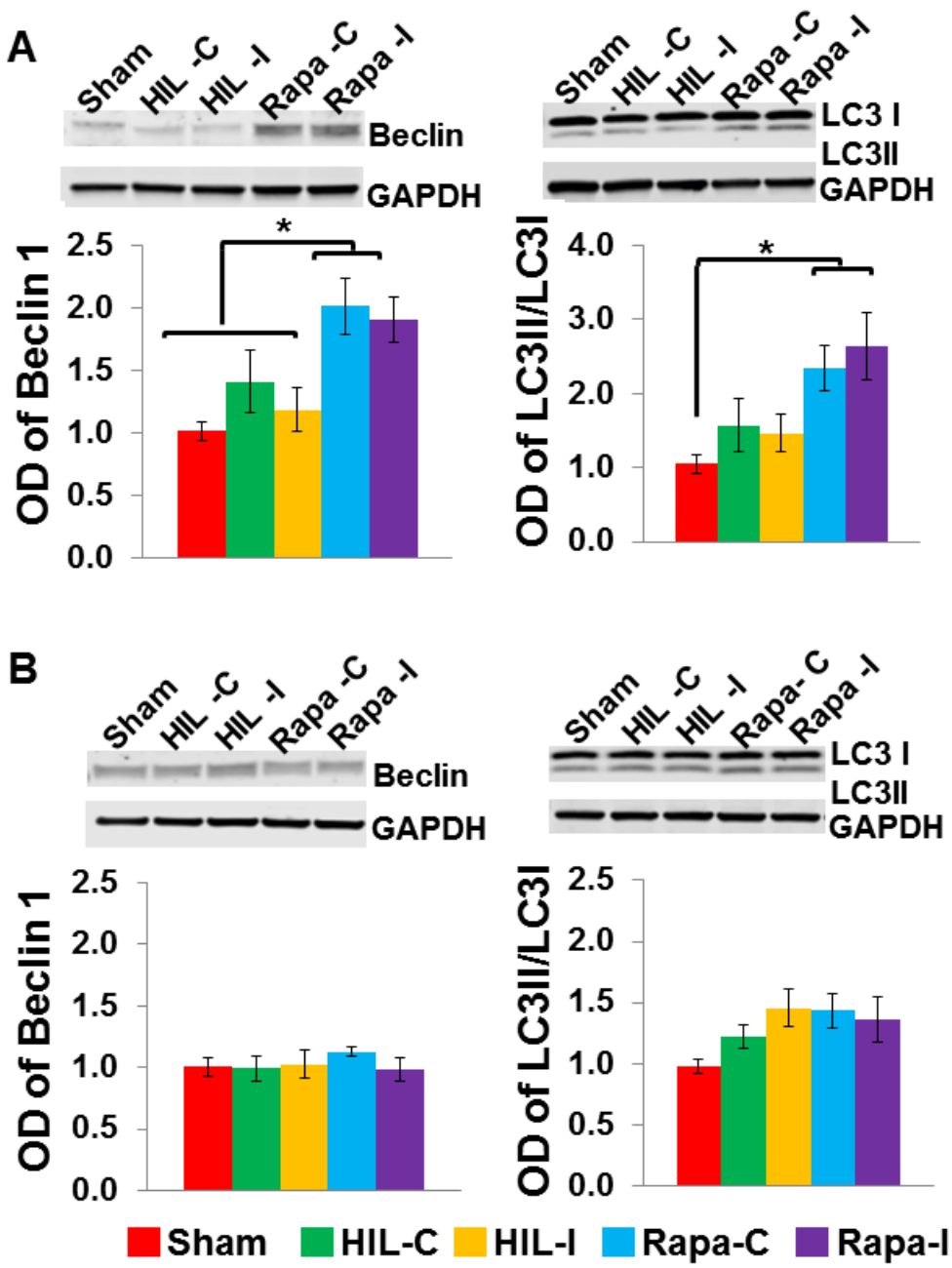

Figure 16. Rapamycin treatment post-HIL results in transient autophagy induction. Western blot analysis of hippocampal lysates at 24h (A) and 48h (B) following HIL. Note, increased expression (induction) of autophagy markers, Beclin-1 and LC3II (lower band, 14kD) at 24 hours. No change in either autophagy marker was observed at 48h. GAPDH was used as a loading control. Data are expressed as optical density (OD) relative to sham values and are mean ± SEM. One way ANOVA followed by post-hoc analysis was performed and $P < 0.05$ (*) was considered significant. C: contralateral, I: ipsilateral to common carotid occlusion

Rapamycin-mediated neuroprotection is in part due to autophagy

In support of these results, I next demonstrated that inhibiting autophagy diminishes rapamycin-mediated neuroprotection following HIL. Mice were treated with chloroquine, a known autophagy inhibitor, in addition to rapamycin. Indeed, the combination of HIL+ rapamycin + chloroquine (Rapa+Chq) increased severity of neuronal cell death to an average injury score of 2.77 versus 0.8 ($P<0.05$) in Rapa+Chq and HIL+Rapa mice respectively (Figure 17A-B). In addition, chloroquine treatment resulted in more cell death in regions outside of the hippocampus e.g., cortex and thalamus (Figure 17C). These results suggest that rapamycin may abrogate cell death by initiation of autophagy, as a cell survival response to hypoxia, ischemia, and LPS.

Of note, concurrent rapamycin and chloroquine treatment following HIL still reduced neuroinflammation as evidenced by few activated microglia present at 24h in Rapa+Chq treated mice (Figure 18). A predominance of intermediately activated microglia was noted in the SR/L/M (Figure 18). These results suggest that chloroquine does not affect the anti-inflammatory effects of rapamycin.

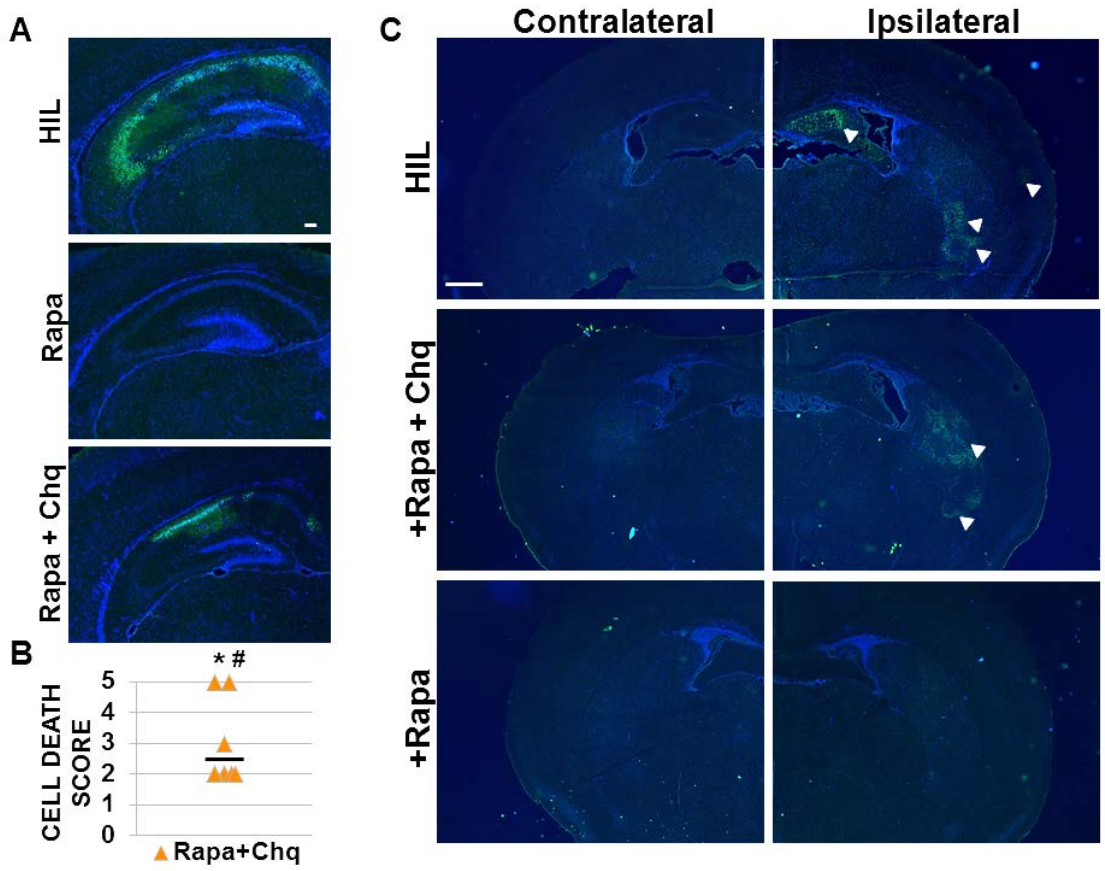

Figure 17. Inhibiting autophagy reduces rapamycin-mediated neuroprotection. A: Representative images of Fluoro-Jade C (FJC, green) and DAPI (blue) labeled sections from HIL, HIL + Rapa (Rapa) and HIL + Rapa + Chq (Rapa + Chq) treated animals at 24 hours post-HIL. Chq reverses neuroprotective effects of Rapa, likely through inhibition of autophagy, resulting in increased cell death. Scale bar = 100μm. B: Neuronal death score of Rapa+ Chq animals at 24 hours. A score of "0" corresponds to no injury whereas a "5" indicates neuronal death in hippocampus, cortex, and thalamus. Black bars represent mean scores for each condition. One way ANOVA followed by post-hoc analysis was performed and $P< 0.05$ (*) was considered significant. C: Representative images of FJC and DAPI sections demonstrating increased FJC labeling (neuronal death) in non-hippocampal regions in Rapa+Chq compared with Rapa alone. Arrowheads point to areas of cell death. Rapa: HIL + rapamycin; Rapa + Chq: HIL + Rapamycin + Chloroquine. Scale bar = 500μm.

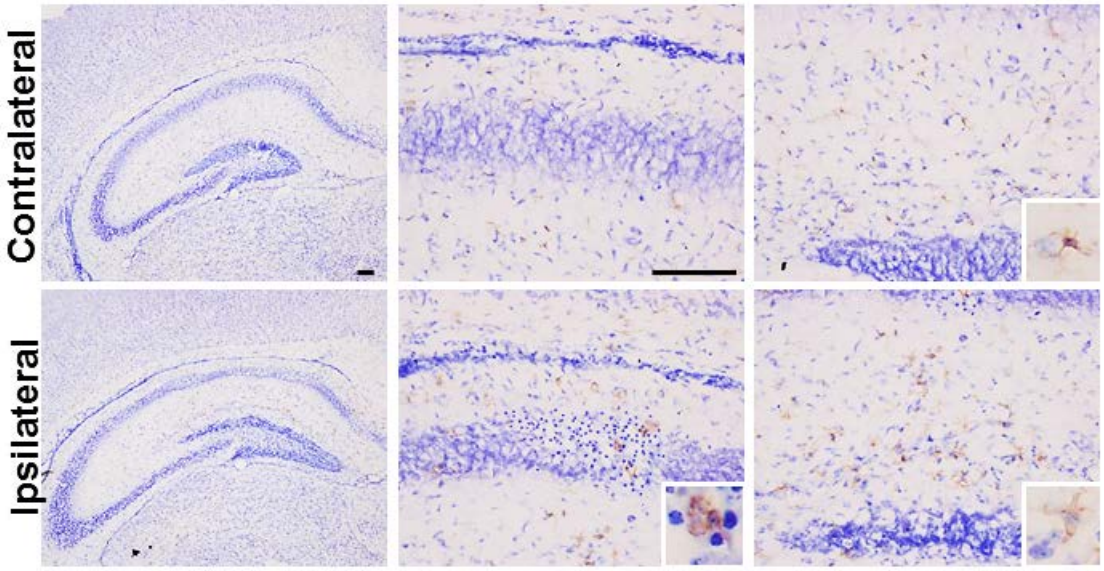

Figure 18. Reduced microglia activation following autophagy inhibition.
Iba-1 labeled microglia in the stratum pyramidale, and strata radiatum and lacunosum-moleculare (SR/L/M; B,D) at 24h following HIL in HIL + Rapa + Chq treated animals. Of note, few activated microglia observed ipsilateral, but not contralateral to carotid ligation. Primarily, resting or intermediately activated microglia were observed in sections. Insets: Iba-1 immunoreactive microglia at 40X magnification. Scale bars = 100μm

CHAPTER 4: DISCUSSION

The data presented provide the first evidence that cell death in an HIL animal model of CP can be prevented with the mTOR inhibitor rapamycin, even when administered after the inciting HIL procedure. Rapamycin inhibited expression of HIF-1α, a marker of cellular hypoxic stress, and led to autophagy induction in association with diminished cellular injury. Rapamycin was also associated with a substantial decrease in microglial activation within the injured brain. Collectively, these results provide pre-clinical evidence for consideration of mTOR inhibitors in the treatment of a subset of infants at risk for CP.

CP is characterized by periventricular white matter injury, accompanied by variable neuronal cell death in the hippocampus, thalamus and cortex which often occurs in late fetal or early neonatal life[13,15,223]. The use of post-natal day 6 mouse pups is intended to model brain injury resulting from lesions at these perinatal time points equivalent 28-32 weeks gestation in humans. The combined insult of hypoxic, ischemic, and inflammatory exposure replicates, in part, the multi-hit etiology that contributes to CP pathogenesis. With 48h of HIL, extensive neuronal death occurs in the hippocampus and cortex in the mouse model as evidenced by increased FJC staining and HIF-1α expression. Enhanced CC3 expression in the periventricular white matter and hippocampus further corroborates the effects of HIL. The pattern of cell death observed in the HIL mouse model closely replicates the regions typically affected in CP, including the periventricular white matter, hippocampus and areas of the thalamus and basal ganglia. Furthermore, these findings demonstrate that maximal cell death occurs within 48h of injury indicating a critical therapeutic window in the mouse during which mTOR

activation may play a pivotal role in brain injury and, more importantly, during which mTOR inhibitors may be implemented. The goal of the presented work was to define the effects of mTOR modulation on cell survival. The significant rapamycin mediated neuroprotection following HIL clearly demonstrates a need for future studies addressing functional motor recovery using a variety of behavioral testing paradigms to prove the efficacy of rapamycin in functional recovery.

Interestingly, changes in mTOR activation (increase or decrease) were not observed acutely following HIL as compared to shams. Instead, there was constitutive level of mTOR activation demonstrated by persistent phosphorylation of downstream mTOR targets S6, S6K and 4EBP1 following HIL. Since prior work has demonstrated that persistent mTOR activity during cell stress (e.g., starvation, hypoxia) can impair cellular stress responses and result in cell death[183,244], the constitutive mTOR signaling in the setting of HIL is biologically inappropriate in the context of diminished oxygen and energy substrates present in the brain induced by HIL. Essentially, persistent mTOR signaling results in discordance between cellular energy available and energy necessary to maintain protein synthesis leading to neuronal death following HIL.

Phosphorylation of S6K and S6 was mTOR, not DAPK, mediated since DAPK and P-DAPK levels were not increased following HIL or decreased with rapamycin treatment. Increased expression of DAPK and decreased expression of phospho-inactivated DAPK following acute neuronal damage (e.g. cerebral ischemia) has been previously reported[245]. Induction of DAPK following injury promotes neuronal death via its kinase activity (reviewed in [246]), which can also phosphorylate S6. However, DAPK does not appear to play a major role in regulating neuronal death following HIL as its

expression levels remained constant irrespective of decrease in neuronal death with rapamycin treatment.

Dysregulation of negative upstream mTOR regulators in the context of HIL may contribute to persistent mTOR signaling. TSC1 and Redd1, upstream regulators of mTOR, are differentially affected by combination of HIL as evidenced by a decrease in Redd1, an indicator of oxygen tension, but no change in TSC1, an indicator of growth factor availability. Furthermore, this dysregulated expression of Redd1 following HIL likely contributes to persistent mTOR signaling observed. Interestingly, the decreased Redd1 expression following HIL is in contrast to previous work demonstrating induction of Redd1 following hypoxic-ischemic insults[238,247,248] emphasizing that HIL is a distinct injury from hypoxia-ischemia and may involve unique alterations to the mTOR and associated signaling cascades. Furthermore, there is a crucial link between Redd1 and cell survival following HIL since decreased Redd1 expression is detected exclusively ipsilateral to the carotid ligation where the most neuronal damage. This supports previous work showing that induction of Redd1 signaling activates pro-survival mechanisms in cells following serum deprivation[249]. Inducing Redd1 expression following HIL may be another therapeutic target to reduce neuronal death in CP.

The decision to use rapamycin was not intended to "normalize" mTOR signaling to non-HIL conditions. Instead, the goal was to readjust the mTOR rheostat in the setting of HIL to create an environment permissive to cell survival. For example, pre-injury administration of rapamycin increases autophagy, and results in decreased cell death and brain damage 24h following neonatal hypoxia-ischemia[186]. Enhancing autophagy with rapamycin reduces infarct size and improves neurological outcome at 48h following

injury in permanent and slow reperfusion stroke models[198]. The addition of inhibitors of autophagy, 3-methyladenine, eliminates rapamycin-mediated neuroprotection[187]. In our results, concomitant treatment of HIL mice with chloroquine, an inhibitor of autophagy, diminished the neuroprotective effects of rapamycin. Thus, constitutive activation of the mTOR signaling cascade in the context of HIL may be detrimental to neuronal survival by inhibiting protective cellular responses to bioenergetic stress, such as autophagy. Logically, by inhibiting mTOR, rapamycin led to early initiation of autophagy as a protective response.

Another obvious effect of rapamycin following HIL was a reduction in the size and number of Iba-1 immunolabeled microglia. Several studies have identified a robust inflammatory response in the brain following hypoxia-ischemia, and a neuroinflammatory mechanism has been proposed as a critical mediator of neuronal death found in CP[250]. A significant increase in the activation and number of microglia was observed ipsilateral to the carotid ligation and coincided with increased mTOR signaling following HIL. Upregulation of mTOR signaling contributes to microglia activation following hypoxia and infectious stimuli, though the exact mechanism remains unknown [209,210]. As such, inhibition of mTOR resulted in a decrease in the both the number and size of activated microglia throughout the brain but especially in the hippocampus, cortex, and thalamus, ipsilateral to the carotid ligation. Of note, there was increased Iba1 labeled microglia, primarily consisting of intermediately activated and resting microglia, at 1 week post-injury in HIL compared to rapamycin treated animals. Increased microglia presence, be it resting microglia, in the absence of on-going cell death or following resolution of inciting injury may explain the presence of increased

proinflammatory molecules in school-aged children with CP[79]. These children also had heightened inflammatory response following exposure to infectious stimuli compared to controls, which may be attributed to increased presence of microglia even after resolution of initial insult. The numbers of activated microglia, a biomarker for neuronal injury and death, may be diminished because of fewer injured and dead neurons, the potent anti-inflammatory effect of rapamycin or a combination of the two.

The transcriptional activation of inflammatory genes in activated microglia is mediated by STAT3 in concert with STAT1[251]. These studies focused on phosphorylation of STAT3 at T705. However, previous work has demonstrated that phosphorylation of STAT3 on S727 is required for maximal transcriptional activity[174,241]. In the HIL model of CP, phospho-activation of STAT3 at S727 was mTOR-dependent with significant reduction in phosphorylation following rapamycin treatment. Of note, increased P-STAT3 in HIL animals demonstrated glial, not neuronal, expression pattern. Thus, this work provides initial evidence of a mechanism for mTOR-mediated microglia activation, and possibly astrogliosis, via increased phosphorylation of STAT3.

Increased HIF-1α expression corresponds with the pattern of neuronal cell death evidenced by FJC staining. Under normoxic conditions, HIF-1α translation is governed by mTOR in a constitutive fashion but it is rapidly degraded under the control of prolyl hydroxylases (PHD) and von Hippel Landau factor (VHL)[252,253]. In the setting of hypoxia, PHD and VHL expression is inhibited via an mTOR-independent mechanism permitting stabilization and expression of HIF-1α, as observed following HIL. Rapamycin treatment drastically reduced HIF-1α expression suggesting that HIF-1α expression following HIL may, at least in part, be mTOR dependent. There is evidence

that the role of HIF-1α following hypoxia, whether promoting cell survival and executing cell death, depends on the phase of injury [188,254,255]. Following neonatal hypoxia-ischemia, the neuroprotective effect hypoxic preconditioning is eliminated in neuron specific HIF-1α knockout mice [254], suggesting a protective role of HIF-1α during preconditioning. However, HIF-1α inhibition following neonatal hypoxic-ischemic injury decreased infarct volume and reduced blood-brain barrier disruption [255] indicating that post-injury HIF-1α promotes cellular injury and death. Further studies are necessary to elucidate whether increased HIF-1α expression following HIL plays a protective or detrimental role in neuronal cell death.

In addition to using rapamycin, we targeted the mTOR signaling cascade by utilizing a highly selective S6K inhibitor (S6KI), PF-4708671[256]. Though it has shown protective effects in an animal model of myocardial infarction[257], S6KI has not been investigated in animal models of cerebral ischemia. We provide the first evidence that treatment with S6KI following HIL is neuroprotective decreasing neuronal death to levels similar to rapamycin. Thus, S6KI-mediated neuroprotection reinforces the integral role of the mTOR signaling cascade in neuronal death following HIL. From a clinical perspective, the beneficial effects of S6KI suggest that it may be an alternative therapeutic option to rapamycin in children with CP.

In conclusion, we have demonstrated that mTOR inhibition following HIL dramatically rescues the cell death phenotype in this model, in association with diminished microglial activation and early induction of autophagy. Our data provide strong support for the hypothesis that modulation of mTOR signaling could provide a novel therapeutic approach to reduce neuronal cell death in CP.

CHAPTER 5: FUTURE DIRECTIONS AND IMPLICATIONS

Potential mechanisms of decreased Redd1 expression

Induction of Redd1 (also known as RTP801) following cellular stress is integral in activation protective mechanisms and promoting survival[249]. For example, recently Redd1 has been shown to limit production of reactive oxygen species[258]. HIL results in decreased Redd1 expression exclusively ipsilateral to the carotid ligation, which may leave cells vulnerable to neuronal cell death. Thus, identifying the mechanism of decreased Redd1 expression in HIL may shed light on additional impaired cell signaling mechanisms in CP. Dysregulated Redd1 expression following HIL may result from impaired activation of Redd1 gene or increased degradation of the Redd1 protein. Redd1 gene (also known as Dig1, DDIT1) contains a hypoxia-response element in the promoter suggesting that it is a hypoxia-inducible protein[238,259]. It follows that HIF-1α and hypoxia mimetic agents such as cobalt chloride induce Redd1 expression which then inhibits mTOR signaling coupling cell proliferation to oxygen tension [259,260]. Furthermore, Redd1 is involved in a negative feedback loop to limit HIF-1α expression since genetic deletion of Redd1 results in increased HIF-1α protein and HIF-1α target gene expression *in vitro* [258]. However, the extent that this feedback loop contributes to HIF-1α expression following hypoxic insults *in vivo* is unknown. Nevertheless, a failure to induce Redd1 following HIL may indicate impaired HIF-1α-dependent regulation and may also contribute to robust increase in HIF-1α ipsilateral to carotid ligation, which co-localizes to areas of cell death.

In addition to enhanced transcription, Redd1 protein expression can be regulated via post-translational modifications. Increased ubiquitination of Redd1 can lead to protein instability and subsequent degradation by the ubiquitin-proteasome system. There are three ubiquitin E3 ligases, CUL4A-DDB1 complex, Parkin and HUWE1/MULE, that target Redd1 (reviewed in [261]). Of these ligases, loss of function in parkin and subsequent over-expression of Redd1 is associated with neurodegeneration in Parkinson's disease, [262]. In the context of HIL, enhanced activity of one or more of these ligases may contribute to decreased Redd1 expression-mediated neuronal death. Indeed, further investigation of Redd1 regulation and function may provide key insights into impaired pathways and new avenues of treatment following HIL.

Differential effects and regulation of S6K and 4EBP1

S6K and 4EBP1 are both downstream targets of mTOR and both regulate protein synthesis. However, these downstream effectors can differentially affect cell growth and proliferation suggesting that they may regulate distinct proteomes [263,264]. Thus, a pathway analysis to determine which proteins in the mTOR phosphoproteome are induced or repressed following HIL may provide help dissect the distinct roles of these downstream mTOR effectors in neuronal death.

In addition, phosphorylation of S6K and 4EBP may be differentially regulated by mTOR. Rapamycin has been shown to differentially inhibit phosphorylation of S6K and 4EBP1 *in vitro*[265]. We also noted greater effect of rapamycin on inhibition of P-S6K compared to P-4EBP1 at 24h and 48h following HIL. The mechanism of differential effects of rapamycin on these two mTOR substrates is not fully understood. Recently, it

was reported that the affinity of the mTOR kinase domain was affected by the characteristics of the mTOR phosphorylation site on downstream effector proteins[266]. Furthermore, the characteristics of mTOR phosphorylation sites on proteins dictated the sensitivity of their responses to changes in nutrient and growth factor availability[266]. Increased phosphorylation by mTOR of downstream effectors, 4E-BP1 and STAT3, following hypoxia *in vitro* was not equivalent[267]. Collectively, this provides initial evidence that a hierarchy of substrate phosphorylation may exist, and could be a potential explanation for differential effects of mTOR inhibition. Differential phosphorylation of mTOR substrates may enable inhibiting translation of certain proteins, for example those mediated by P-4EBP1, while simultaneously promoting others, for example those downstream of P-S6K. Furthermore, this hierarchy may be context and cell type dependent. Thus, different cellular stresses, such as HIL, may initiate a unique pattern of mTOR substrate phosphorylation, which could be used to identify additional mTOR-dependent therapeutic targets in CP.

The role of mTOR in microglia function and polarization

mTOR promotes pro-inflammatory of the peripheral immune system, by inducing differentiation of pro-inflammatory helper T-cells and activation of B-cells [203–205]. With respective to neuroinflammation, previous work demonstrates that mTOR activity is increased in activated microglia and inhibition of mTOR is neuroprotective[209–213,205]. IN support of previous findings, we demonstrate that rapamycin treatment following HIL reduces both microglia number and activation. The drastic effect of rapamycin on neuroinflammation in HIL warrants future studies that will investigate the potential

mechanism responsible for this effect. Specifically, whether diminished microglia activation following rapamycin is due to rapamycin-mediated reduction in neuronal death or a specific effect of rapamycin on microglia. An mTOR-mediated effect on microglia activation independent of neuronal death would be a novel finding suggesting that inhibiting mTOR may have cell specific effects – rapamycin may inhibit cell death in neurons and promote anti-inflammatory activity in microglia following HIL.

Interestingly, recent findings suggest that activated microglia exist on a continuum, with different polarization states similar to those reported in macrophages and analogous to subsets of helper-T cells (reviewed in[268]). Following cerebral ischemia in adult rats, there is a distinct pattern of microglia polarization with a persistence of the M1 or proinflammatory state accompanied by a gradual decrease of the M2 or regenerative state[269]. Furthermore, administration of rapamycin in adult cerebral ischemia reduces the production of pro-inflammatory cytokines by microglia suggesting that mTOR may regulate microglia polarization[205]. However, the effect of rapamycin in polarization of microglia in neonatal mice has not been examined. Thus, investigating the functional profiles of microglia, in terms of cytokine production, following HIL and HIL + Rapamycin treated animals may provide insight as to whether rapamycin mediates a shift in polarization from M1 (pro-inflammatory state) towards M2 (reparative state). In addition, determining the function of microglia observed at 1 week post-injury in HIL animals may elucidate their pro- or anti-inflammatory roles at later time points following HIL.

mTOR-mediated neuronal death may promote white matter damage in CP

Since PVL is a neuropathological hallmark of CP, it is important to consider the consequences of persistent mTOR signaling and subsequent early neuronal death post-HIL in the context of oligodendrocytes and white matter injury. Previously, it has been demonstrated that a significant loss of oligodendrocytes, evidenced by decreased levels of myelin basic protein (MBP) and oligodendrocyte marker 1 (O1), occurs at 96h post-HIL[143,144]. We demonstrate that the maximal period of neuronal loss occurs within 48h post-HIL. Since neuronal loss observed post-HIL occurs prior to reported damage of oligodendrocytes, it may contribute to the white matter loss observed in CP. Neurons provide important growth factors and signaling molecules, such as PDGF, adenosine, neuregulin and BDNF, that promote myelination and oligodendrogenesis (reviewed in [270]). In addition, neuronal activity can promote myelination and oligodendrocyte survival[271–273]. Thus, the loss of neuron-derived growth factors and neuronal activity following neuronal death may impair survival of oligodendrocytes resulting in white matter loss observed in CP.

In addition to the loss of oligodendrocytes and oligodendrocyte progenitor cells, impaired oligodendrocyte differentiation and maturation may also contribute to perinatal white matter injury, such as that observed in CP (reviewed in[274,275]). mTOR signaling cascade plays an integral role in oligodendrocyte maturation and myelination in the developing brain (reviewed in [276]). However, a balanced of mTOR is necessary for myelination since over-activation of mTOR in oligodendrocytes via loss of TSC1 results in hypomyelination[277]. Thus, persistent activation of mTOR signaling may contribute dysregulated oligodendrocyte maturation and subsequent white matter loss in CP. HIF-1α

may mediate mTOR-dependent impaired oligodendrocyte maturation. Recently, it was demonstrated that HIF-1α expression in oligodendrocytes arrests differentiation while promoting angiogenesis coupling maturation and myelination to metabolic demands[278]. Following HIL, HIF-1α expression was increased in the hippocampus, as well as the periventricular white matter. Therefore, impaired oligodendrocyte maturation may result from constitutive activation of HIF-1α, subsequent to persistent mTOR activation following HIL, in oligodendrocytes.

Neuroinflammatory mediators, such as microglia, may exacerbate white matter injury and disrupt oligodendrocyte maturation during development[279,280]. Following HIL, reactive microglia were observed throughout the brain, including the periventricular white matter, at 24h and 48h. These findings are consistent with previous studies suggesting that reactive microglia may contribute to myelination abnormalities in CP. Therefore, inhibiting mTOR in HIL may limit white matter injury by 1) reducing neuronal death, 2) restoring dysregulated HIF-1α expression in oligodendrocytes and 3) reducing microglial activation following HIL. These exciting findings demonstrate a need for future studies to investigate the effect of rapamycin on white matter injury following HIL.

Clinical application of rapamycin as a therapeutic intervention in CP

The data presented provide the first evidence that rapamycin treatment following injury drastically reduces neuronal death in an HIL animal model of CP. These findings necessitate a discussion of the potential clinical applications of mTOR inhibitors in the

treatment of CP. Based on evaluation of ultrasound and MRI findings in children with CP, approximately 80% of CP cases can be attributed to injury during the antenatal period, most likely 23-32 weeks gestation when the white matter is particularly susceptible to injury[20,26]. Thus, one possibility would be to administer a short course of rapamycin to women who present with multiple risk factors for CP (e.g. history of seizures, hypertension, thyroid condition, coagulation disorders, and severe intrauterine infection) during late second and third trimester of their pregnancy. Rapamycin is a lipophilic drug and crosses the placenta[281]. However, rapamycin is categorized by the FDA as a class C drug, which indicates that fetal risk cannot be ruled out due to inadequate studies in humans[281]. However, four organ transplant recipients that received mTOR inhibitors (e.g. sirolimus or everolimus) for part of or their entire pregnancy report no complications during pregnancy and delivery of a healthy baby with no congenital abnormalities[282–285]. One additional liver transplant patient on mTOR inhibitors had an emergency C-section due to breech presentation, but delivered a healthy baby with Apgar score of 10[286]. An additional 3 pregnancies where rapamycin (sirolimus) was part of the original immunosuppressant regiment were reported to the National Transplant Pregnancy Registry of which one was spontaneously aborted and no complications in the remaining two pregnancies[287]. Another pregnancy in which the mother was switched to sirolimus during pregnancy had a cleft lip which had to be surgically repaired[287]. It should be noted that pregnancy in organ transplant recipients are considered high risk pregnancies even in the absence of other complications. These studies demonstrate that mTOR inhibition is not an absolute contraindication during these

high risk pregnancies. However, the clinical feasibility of administering rapamycin during pregnancy in non-transplant recipients needs to be further evaluated.

An additional potential strategy for rapamycin-mediated neuroprotection in CP would be to administer rapamycin to neonates with complicated deliveries (e.g. premature rupture of membranes, fetal placental lesions, maternal fever during labor, chorioamnionitis) or ones that show indications of hypoxia-ischemia (e.g. low Apgar scores, metabolic acidosis in fetal, umbilical arterial cord or early neonatal blood, abnormal fetal heart rate) and/or infection (e.g. recovery of infectious agent from placental or fetal blood, congenital infection, fetal sepsis, fetal infection) shortly following birth. There is limited data for rapamycin use in pediatric population, especially those younger than 13 years age[281]. Recently, everolimus, another mTOR inhibitor, has been approved for pediatric TSC patients ≥ 1 year old with subependymal giant cell astrocytoma[288]. mTOR inhibitor administration in pediatric transplant recipients and pediatric TSC patients demonstrates acceptable adverse effect profile similar to those reported in adult patients[289–291]. The most common side effects reported are peripheral edema, hyperlipidemia, hypercholesterolemia, hypertension, and increased creatinine, but most were self-limiting. Of those reported, hyperlipidemia and increased creatinine resulted in discontinuation of rapamycin therapy in <5% of clinical trials in adults[281]. Of note, most of the adverse effect clinical trials involve chronic treatment with rapamycin, most commonly in post-transplant individuals. Thus, the side effect profile following acute, short-course of rapamycin may be even more favorable and needs to be investigated further.

REFERENCES

1. Kirby, R. S. *et al.* Prevalence and functioning of children with cerebral palsy in four areas of the United States in 2006: A report from the Autism and Developmental Disabilities Monitoring Network. *Res. Dev. Disabil.* **32,** 462–469 (2011).

2. Rosenbaum, P. *et al.* A report: the definition and classification of cerebral palsy April 2006. *Dev Med Child Neurol Suppl* **109,** 8–14 (2007).

3. Pakula, A. T., Van Naarden Braun, K. & Yeargin-Allsopp, M. Cerebral Palsy: Classification and Epidemiology. *Phys. Med. Rehabil. Clin. N. Am.* **20,** 425–452 (2009).

4. Smithers-Sheedy, H. *et al.* What constitutes cerebral palsy in the twenty-first century? *Dev. Med. Child Neurol.* **56,** 323–328 (2014).

5. Odding, E., Roebroeck, M. E. & Stam, H. J. The epidemiology of cerebral palsy: Incidence, impairments and risk factors. *Disabil. Rehabil.* **28,** 183–191 (2006).

6. Yeargin-Allsopp, M. *et al.* Prevalence of cerebral palsy in 8-year-old children in three areas of the United States in 2002: a multisite collaboration. *Pediatrics* **121,** 547–554 (2008).

7. Cans, C. Surveillance of cerebral palsy in Europe: a collaboration of cerebral palsy surveys and registers. *Dev. Med. Child Neurol.* **42,** 816–824 (2000).

8. Palisano, R. *et al.* Development and reliability of a system to classify gross motor function in children with cerebral palsy. *Dev. Med. Child Neurol.* **39,** 214–223 (1997).

9. Graham, H. K., Harvey, A., Rodda, J., Nattrass, G. R. & Pirpiris, M. The functional mobility scale (FMS). *J. Pediatr. Orthop.* **24,** 514–520 (2004).

10. Eliasson, A.-C. *et al.* The Manual Ability Classification System (MACS) for children with cerebral palsy: scale development and evidence of validity and reliability. *Dev. Med. Child Neurol.* **null,** 549–554 (2006).

11. Ashwal, S. *et al.* Practice Parameter: Diagnostic assessment of the child with cerebral palsy Report of the Quality Standards Subcommittee of the American Academy of Neurology and the Practice Committee of the Child Neurology Society. *Neurology* **62,** 851–863 (2004).

12. Towsley, K., Shevell, M. I. & Dagenais, L. Population-based study of neuroimaging findings in children with cerebral palsy. *Eur. J. Paediatr. Neurol.* **15,** 29–35 (2011).

13. Krägeloh-Mann, I. & Horber, V. The role of magnetic resonance imaging in elucidating the pathogenesis of cerebral palsy: a systematic review. *Dev. Med. Child Neurol.* **49,** 144–151 (2007).

14. Robinson, M. N. *et al.* Magnetic resonance imaging findings in a population-based cohort of children with cerebral palsy. *Dev. Med. Child Neurol.* **51,** 39–45 (2008).

15. Bax, M., Tydeman, C. & Flodmark, O. Clinical and MRI correlates of cerebral palsy: the European Cerebral Palsy Study. *Jama* **296,** 1602–1608 (2006).

16. Krägeloh-Mann, I. *et al.* Bilateral lesions of thalamus and basal ganglia: origin and outcome. *Dev. Med. Child Neurol.* **44,** 477–484 (2002).

17. Korzeniewski, S. J., Birbeck, G., DeLano, M. C., Potchen, M. J. & Paneth, N. A Systematic Review of Neuroimaging for Cerebral Palsy. *J. Child Neurol.* **23,** 216–227 (2007).

18. Zubiaurre-Elorza, L. *et al.* Thalamic changes in a preterm sample with periventricular leukomalacia: correlation with white-matter integrity and cognitive outcome at school age. *Pediatr. Res.* **71,** 354–360 (2012).

19. Himmelmann, K. & Uvebrant, P. Function and neuroimaging in cerebral palsy: a population-based study. *Dev. Med. Child Neurol.* **53,** 516–521 (2011).

20. Nguyen, A., Armstrong, E. A. & Yager, J. Y. Evidence for Therapeutic Intervention in the Prevention of Cerebral Palsy: Hope from Animal Model Research. *Semin. Pediatr. Neurol.* **20,** 75–83 (2013).

21. Little, W., J. On The Influence of Abnormal Parturition, Difficult Labours, Premature Birth, and Asphyxia Neonatorum, on the Mental and Physical Condition of the Child, Especially in Relation to Deformities. **3,** 243–344

22. Osler, S. W. *The Cerebral Palsies of Children*. (P. Blakiston, 1889).

23. Accardo, P. J. Freud on Diplegia: Commentary and Translation. *Am. J. Dis. Child.* **136,** 452–456 (1982).

24. Freud, S. Les diplegies cerebrales infantiles. *Rev. Neurol.* **1,** 177–183 (1893).

25. Nelson, K. B. & Grether, J. K. Potentially asphyxiating conditions and spastic cerebral palsy in infants of normal birth weight. *Am. J. Obstet. Gynecol.* **179,** 507–513 (1998).

26. NINDS. Cerebral Palsy: Hope Through Research: National Institute of Neurological Disorders and Stroke (NINDS). *Cerebral Palsy: Hope Through Research* (2013). at <http://www.ninds.nih.gov/disorders/cerebral_palsy/detail_cerebral_palsy.htm>

27. Mcintyre, S. *et al.* A systematic review of risk factors for cerebral palsy in children born at term in developed countries. *Dev. Med. Child Neurol.* **55,** 499–508 (2012).

28. Trønnes, H., Wilcox, A. J., Lie, R. T., Markestad, T. & Moster, D. Risk of cerebral palsy in relation to pregnancy disorders and preterm birth: a national cohort study. *Dev. Med. Child Neurol.* **56,** 779–785 (2014).

29. Wu, Y. W., Croen, L. A., Shah, S. J., Newman, T. B. & Najjar, D. V. Cerebral palsy in a term population: risk factors and neuroimaging findings. *Pediatrics* **118,** 690–697 (2006).

30. Badawi, N. *et al.* Antepartum risk factors for newborn encephalopathy: the Western Australian case-control study. *BMJ* **317,** 1549–1553 (1998).

31. Nelson, K. B. & Ellenberg, J. H. Maternal seizure disorder, outcome of pregnancy, and neurologic abnormalities in the children. *Neurology* **32,** 1247–1247 (1982).

32. McElrath, T. F. *et al.* Maternal Antenatal Complications and the Risk of Neonatal Cerebral White Matter Damage and Later Cerebral Palsy in Children Born at an Extremely Low Gestational Age. *Am. J. Epidemiol.* kwp206 (2009). doi:10.1093/aje/kwp206

33. Badawi, N. *et al.* Cerebral palsy following term newborn encephalopathy: a population-based study. *Dev. Med. Child Neurol.* **47,** 293–298 (2005).

34. Strömberg, B. *et al.* Neurological sequelae in children born after in-vitro fertilisation: a population-based study. *The Lancet* **359,** 461–465 (2002).

35. Hvidtjørn, D. *et al.* Cerebral Palsy Among Children Born After in Vitro Fertilization: The Role of Preterm Delivery—A Population-Based, Cohort Study. *Pediatrics* **118,** 475–482 (2006).

36. Hemminki, K., Li, X., Sundquist, K. & Sundquist, J. High familial risks for cerebral palsy implicate partial heritable aetiology. *Paediatr. Perinat. Epidemiol.* **21,** 235–241 (2007).

37. Petterson, B., Stanley, F. & Henderson, D. Cerebral palsy in multiple births in Western Australia: Genetic aspects. *Am. J. Med. Genet.* **37,** 346–351 (1990).

38. Erkin, G., Delialioglu, S. U., Ozel, S., Culha, C. & Sirzai, H. Risk factors and clinical profiles in Turkish children with cerebral palsy: analysis of 625 cases. *Int. J. Rehabil. Res. Int. Z. Für Rehabil. Rev. Int. Rech. Réadapt.* **31,** 89–91 (2008).

39. al-Rajeh, S. *et al.* Cerebral palsy in Saudi Arabia: a case-control study of risk factors. *Dev. Med. Child Neurol.* **33,** 1048–1052 (1991).

40. Lynex, C. N. *et al.* Homozygosity for a missense mutation in the 67 kDa isoform of glutamate decarboxylase in a family with autosomal recessive spastic cerebral palsy: parallels with Stiff-Person Syndrome and other movement disorders. *BMC Neurol.* **4,** 20 (2004).

41. Lerer, I. *et al.* Deletion of the ANKRD15 gene at 9p24.3 causes parent-of-origin-dependent inheritance of familial cerebral palsy. *Hum. Mol. Genet.* **14,** 3911–3920 (2005).

42. McMichael, G. *et al.* Whole-exome sequencing points to considerable genetic heterogeneity of cerebral palsy. *Mol. Psychiatry* **20,** 176–182 (2015).

43. McMichael, G. *et al.* Rare copy number variation in cerebral palsy. *Eur. J. Hum. Genet.* **22,** 40–45 (2014).

44. Himmelmann, K., Hagberg, G., Beckung, E., Hagberg, B. & Uvebrant, P. The changing panorama of cerebral palsy in Sweden. IX. Prevalence and origin in the birth-year period 1995-1998. *Acta Paediatr.* **94,** 287–294 (2005).

45. Hagberg, B., Hagberg, G., Beckung, E. & Uvebrant, P. Changing panorama of cerebral palsy in Sweden. VIII. Prevalence and origin in the birth year period 1991-94. *Acta Paediatr. Oslo Nor. 1992* **90,** 271–277 (2001).

46. Pharoah, P. O. & Cooke, T. Cerebral palsy and multiple births. *Arch. Dis. Child. Fetal Neonatal Ed.* **75,** F174–F177 (1996).

47. Pharoah, P. O. & Adi, Y. Consequences of in-utero death in a twin pregnancy. *Lancet* **355,** 1597–1602 (2000).

48. Topp, M., Langhoff-Roos, J. & Uldall, P. Preterm birth and cerebral palsy. Predictive value of pregnancy complications, mode of delivery, and Apgar scores. *Acta Obstet. Gynecol. Scand.* **76,** 843–848 (1997).

49. Nelson, K. B., Dambrosia, J. M., Grether, J. K. & Phillips, T. M. Neonatal cytokines and coagulation factors in children with cerebral palsy. *Ann. Neurol.* **44,** 665–675 (1998).

50. Reid, S. *et al.* Factor V Leiden mutation: a contributory factor for cerebral palsy? *Dev. Med. Child Neurol.* **48,** 14–19 (2006).

51. Gibson, C. S. *et al.* Associations between inherited thrombophilias, gestational age, and cerebral palsy. *Am. J. Obstet. Gynecol.* **193,** 1437.e1–1437.e12 (2005).

52. Torres, V. M. & Saddi, V. A. Systematic review: hereditary thrombophilia associated to pediatric strokes and cerebral palsy. *J. Pediatr. (Rio J.)* **91,** 22–29 (2015).

53. Jacobsson, B. *et al.* Cerebral palsy in preterm infants: a population-based case-control study of antenatal and intrapartal risk factors. *Acta Paediatr.* **91,** 946–951 (2002).

54. Redline, R. W. Severe fetal placental vascular lesions in term infants with neurologic impairment. *Am. J. Obstet. Gynecol.* **192,** 452–457 (2005).

55. Redline, R. W. & O'Riordan, M. A. Placental lesions associated with cerebral palsy and neurologic impairment following term birth. *Arch. Pathol. Lab. Med.* **124,** 1785–1791 (2000).

56. Redline, R. W. Placental Pathology and Cerebral Palsy. *Clin. Perinatol.* **33,** 503–516 (2006).

57. Jarvis, S. *et al.* Cerebral palsy and intrauterine growth in single births: European collaborative study. *The Lancet* **362,** 1106–1111 (2003).

58. Nelson, K. B. & Ellenberg, J. H. Antecedents of Cerebral Palsy. *N. Engl. J. Med.* **315,** 81–86 (1986).

59. Blair, E. & Stanley, F. J. Intrapartum asphyxia: A rare cause of cerebral palsy. *J. Pediatr.* **112,** 515–519 (1988).

60. Ellenberg, J. H. & Nelson, K. B. The association of cerebral palsy with birth asphyxia: a definitional quagmire. *Dev. Med. Child Neurol.* **55,** 210–216 (2012).

61. MacLennan, A. A template for defining a causal relation between acute intrapartum events and cerebral palsy: international consensus statement. *BMJ* **319,** 1054–1059 (1999).

62. Grether, J. K. & Nelson, K. B. Maternal Infection and Cerebral Palsy in Infants of Normal Birth Weight. *JAMA* **278,** 207–211 (1997).

63. Lieberman, E. *et al.* Intrapartum Maternal Fever and Neonatal Outcome. *Pediatrics* **105,** 8–13 (2000).

64. Wu, Y. W. *et al.* Chorioamnionitis and Cerebral Palsy in Term and Near-Term Infants. *JAMA* **290,** 2677–2684 (2003).

65. Curry, C. J. *et al.* Risk Factors for Perinatal Arterial Stroke: A Study of 60 Mother-Child Pairs. *Pediatr. Neurol.* **37,** 99–107 (2007).

66. Golomb, M. R., Garg, B. P., Saha, C., Azzouz, F. & Williams, L. S. Cerebral Palsy After Perinatal Arterial Ischemic Stroke. *J. Child Neurol.* **23,** 279–286 (2008).

67. Lee, J. *et al.* Predictors of outcome in perinatal arterial stroke: A population-based study. *Ann. Neurol.* **58,** 303–308 (2005).

68. De Vries, L. S. *et al.* Infarcts in the vascular distribution of the middle cerebral artery in preterm and fullterm infants. *Neuropediatrics* **28,** 88–96 (1997).

69. De Vries, L. *et al.* Correlation Between Neonatal Cranial Ultrasound, MRI in Infancy and Neurodevelopmental Outcome in Infants with a Large Intraventricular Haemorrhage with or without Unilateral Parenchymal Involvement. *Neuropediatrics* **29,** 180–188 (1998).

70. Fitzgerald, K. C., Williams, L. S., Garg, B. P., Carvalho, K. S. & Golomb, M. R. Cerebral Sinovenous Thrombosis in the Neonate. *Arch. Neurol.* **63,** 405–409 (2006).

71. Eastman, N. & DeLeon, M. The etiology of cerebral palsy. *Am. J. Obstet. Gynecol.* **69,** 950–961 (1955).

72. Dammann, O. & Leviton, A. Maternal Intrauterine Infection, Cytokines, and Brain Damage in the Preterm Newborn. *Pediatr. Res.* **42,** 1–8 (1997).

73. O'Shea, Klinepeter, Meis & Dillard. Intrauterine infection and the risk of cerebral palsy in very low-birthweight infants. *Paediatr. Perinat. Epidemiol.* **12,** 72–83 (1998).

74. Neufeld, M. D., Frigon, C., Graham, A. S. & Mueller, B. A. Maternal Infection and Risk of Cerebral Palsy in Term and Preterm Infants. *J. Perinatol.* **25,** 108–113 (2004).

75. Ahlin, K. *et al.* Cerebral Palsy and Perinatal Infection in Children Born at Term: *Obstet. Gynecol.* **122,** 41–49 (2013).

76. Leviton, A. *et al.* Microbiologic and Histologic Characteristics of the Extremely Preterm Infant's Placenta Predict White Matter Damage and Later Cerebral Palsy. The ELGAN Study. *Pediatr. Res.* **67,** 95–101 (2010).

77. Graham, E. M., Holcroft, C. J., Rai, K. K., Donohue, P. K. & Allen, M. C. Neonatal cerebral white matter injury in preterm infants is associated with culture positive infections and only rarely with metabolic acidosis. *Am. J. Obstet. Gynecol.* **191,** 1305–1310 (2004).

78. Kuban, K. C. K. *et al.* Systemic Inflammation and Cerebral Palsy Risk in Extremely Preterm Infants. *J. Child Neurol.* **29,** 1692–1698 (2014).

79. Lin, C.-Y. *et al.* Altered inflammatory responses in preterm children with cerebral palsy. *Ann. Neurol.* **68,** 204–212 (2010).

80. Adinolfi, M. Infectious Diseases in Pregnancy, Cytokines and Neurological Impairment: an Hypothesis. *Dev. Med. Child Neurol.* **35,** 549–553 (1993).

81. Yoon, B. H. *et al.* Amniotic fluid inflammatory cytokines (interleukin-6, interleukin-1beta, and tumor necrosis factor-alpha), neonatal brain white matter lesions, and cerebral palsy. *Am. J. Obstet. Gynecol.* **177,** 19–26 (1997).

82. Yoon, B. H. *et al.* High expression of tumor necrosis factor-α and interleukin-6 in periventricular leukomalacia. *Am. J. Obstet. Gynecol.* **177,** 406–411 (1997).

83. Kadhim, H. *et al.* Inflammatory cytokines in the pathogenesis of periventricular leukomalacia. *Neurology* **56,** 1278–1284 (2001).

84. Deguchi, K., Mizuguchi, M. & Takashima, S. Immunohistochemical expression of tumor necrosis factor alpha in neonatal leukomalacia. *Pediatr. Neurol.* **14,** 13–16 (1996).

85. Leviton, A. Preterm Birth and Cerebral Palsy: Is Tumor Necrosis Factor the Missing Link? *Dev. Med. Child Neurol.* **35,** 553–558 (1993).

86. Elovitz, M. A. *et al.* Intrauterine inflammation, insufficient to induce parturition, still evokes fetal and neonatal brain injury. *Int. J. Dev. Neurosci.* **29,** 663–671 (2011).

87. Stoknes, M. *et al.* The effects of multiple pre- and perinatal risk factors on the occurrence of cerebral palsy. A Norwegian register based study. *Eur. J. Paediatr. Neurol.* **16,** 56–63 (2012).

88. Wheater, M. & Rennie, J. M. Perinatal infection is an important risk factor for cerebral palsy in very-low-birthweight infants. *Dev. Med. Child Neurol.* **null,** 364–367 (2000).

89. Wang, L.-W., Lin, Y.-C., Wang, S.-T., Yeh, T.-F. & Huang, C.-C. Hypoxic/Ischemic and Infectious Events Have Cumulative Effects on the Risk of Cerebral Palsy in Very-Low-Birth-Weight Preterm Infants. *Neonatology* **106,** 209–215 (2014).

90. Nelson, K. B. & Grether, J. K. Selection of neonates for neuroprotective therapies: one set of criteria applied to a population. *Arch. Pediatr. Adolesc. Med.* **153,** 393–398 (1999).

91. Goldenberg, R. L., Culhane, J. F., Iams, J. D. & Romero, R. Epidemiology and causes of preterm birth. *The Lancet* **371,** 75–84 (2008).

92. Kim, C. J. *et al.* The Frequency, Clinical Significance, and Pathological Features of Chronic Chorioamnionitis: A Lesion Associated with Spontaneous Preterm Birth. *Mod. Pathol. Off. J. U. S. Can. Acad. Pathol. Inc* **23,** 1000–1011 (2010).

93. Shevell, A., Wintermark, P., Benini, R., Shevell, M. & Oskoui, M. Chorioamnionitis and cerebral palsy: Lessons from a patient registry. *Eur. J. Paediatr. Neurol.* **18,** 301–307 (2014).

94. Holling, E. E. & Leviton, A. Characteristics of cranial ultrasound white-matter echolucencies that predict disability: a review. *Dev. Med. Child Neurol.* **41,** 136–139 (1999).

95. Ancel, P.-Y. *et al.* Cerebral Palsy Among Very Preterm Children in Relation to Gestational Age and Neonatal Ultrasound Abnormalities: The EPIPAGE Cohort Study. *Pediatrics* **117,** 828–835 (2006).

96. De Vries, L. S., van Haastert, I.-L. C., Rademaker, K. J., Koopman, C. & Groenendaal, F. Ultrasound abnormalities preceding cerebral palsy in high-risk preterm infants. *J. Pediatr.* **144,** 815–820 (2004).

97. Back, S. A. *et al.* Late Oligodendrocyte Progenitors Coincide with the Developmental Window of Vulnerability for Human Perinatal White Matter Injury. *J. Neurosci.* **21,** 1302–1312 (2001).

98. Back, S. A. *et al.* Selective Vulnerability of Late Oligodendrocyte Progenitors to Hypoxia–Ischemia. *J. Neurosci.* **22,** 455–463 (2002).

99. Marret, S., Mukendi, R., Gadisseux, J.-F., Gressens, P. & Evrard, P. Effect of Ibotenate on Brain Development: An Excitotoxic Mouse Model of Microgyria and Posthypoxic-like Lesions. *J. Neuropathol.* **54,** 358–370 (1995).

100. Derrick, M. *et al.* Preterm Fetal Hypoxia-Ischemia Causes Hypertonia and Motor Deficits in the Neonatal Rabbit: A Model for Human Cerebral Palsy? *J. Neurosci.* **24,** 24–34 (2004).

101. Duncan, J. R. *et al.* White Matter Injury after Repeated Endotoxin Exposure in the Preterm Ovine Fetus. *Pediatr. Res.* **52,** 941–949 (2002).

102. Mallard, C., Welin, A.-K., Peebles, D., Hagberg, H. & Kjellmer, I. White Matter Injury Following Systemic Endotoxemia or Asphyxia in the Fetal Sheep. *Neurochem. Res.* **28,** 215–223 (2003).

103. Riddle, A. *et al.* Spatial Heterogeneity in Oligodendrocyte Lineage Maturation and Not Cerebral Blood Flow Predicts Fetal Ovine Periventricular White Matter Injury. *J. Neurosci.* **26,** 3045–3055 (2006).

104. Rees, S., Breen, S., Loeliger, M., McCrabb, G. & Harding, R. Hypoxemia near mid-gestation has long-term effects on fetal brain development. *J. Neuropathol. Exp. Neurol.* **58,** 932–945 (1999).

105. Tan, S. *et al.* Model of cerebral palsy in the perinatal rabbit. *J. Child Neurol.* **20,** 972–979 (2005).

106. Baud, O. *et al.* Gestational Hypoxia Induces White Matter Damage in Neonatal Rats: A New Model of Periventricular Leukomalacia. *Brain Pathol.* **14,** 1–10 (2004).

107. Rice, J. E., Vannucci, R. C. & Brierley, J. B. The influence of immaturity on hypoxic-ischemic brain damage in the rat. *Ann. Neurol.* **9,** 131–141 (1981).

108. Follett, P. L., Rosenberg, P. A., Volpe, J. J. & Jensen, F. E. NBQX Attenuates Excitotoxic Injury in Developing White Matter. *J. Neurosci.* **20,** 9235–9241 (2000).

109. Ferriero, D. M., Holtzman, D. M., Black, S. M. & Sheldon, R. A. Neonatal Mice Lacking Neuronal Nitric Oxide Synthase Are Less Vulnerable to Hypoxic–Ischemic Injury. *Neurobiol. Dis.* **3,** 64–71 (1996).

110. Sheldon, R. A., Sedik, C. & Ferriero, D. M. Strain-related brain injury in neonatal mice subjected to hypoxia–ischemia. *Brain Res.* **810,** 114–122 (1998).

111. Ten, V. S., Bradley-Moore, M., Gingrich, J. A., Stark, R. I. & Pinsky, D. J. Brain injury and neurofunctional deficit in neonatal mice with hypoxic-ischemic encephalopathy. *Behav. Brain Res.* **145,** 209–219 (2003).

112. Lubics, A. *et al.* Neurological reflexes and early motor behavior in rats subjected to neonatal hypoxic–ischemic injury. *Behav. Brain Res.* **157,** 157–165 (2005).

113. Balduini, W., De Angelis, V., Mazzoni, E. & Cimino, M. Long-lasting behavioral alterations following a hypoxic/ischemic brain injury in neonatal rats. *Brain Res.* **859,** 318–325 (2000).

114. Ashwal, S., Cole, D. J., Osborne, S., Osborne, T. N. & Pearce, W. J. L-NAME Reduces Infarct Volume in a Filament Model of Transient Middle Cerebral Artery Occlusion in the Rat Pup. *Pediatr. Res.* **38,** 652–656 (1995).

115. Derugin, N., Ferriero, D. M. & Vexler, Z. S. Neonatal reversible focal cerebral ischemia: a new model. *Neurosci. Res.* **32,** 349–353 (1998).

116. Ashwal, S., Tone, B., Tian, H. R., Chong, S. & Obenaus, A. Comparison of Two Neonatal Ischemic Injury Models Using Magnetic Resonance Imaging. *Pediatr. Res.* **61,** 9–14 (2007).

117. Lai, M.-C. & Yang, S.-N. Perinatal Hypoxic-Ischemic Encephalopathy. *J. Biomed. Biotechnol.* **2011,** 1–6 (2011).

118. Yoon, B. H. *et al.* Experimentally induced intrauterine infection causes fetal brain white matter lesions in rabbits. *Am. J. Obstet. Gynecol.* **177,** 797–802 (1997).

119. Debillon, T. *et al.* Intrauterine Infection Induces Programmed Cell Death in Rabbit Periventricular White Matter. *Pediatr. Res.* **47,** 736–742 (2000).

120. Kannan, S. *et al.* Microglial Activation in Perinatal Rabbit Brain Induced by Intrauterine Inflammation: Detection with 11C-(R)-PK11195 and Small-Animal PET. *J. Nucl. Med.* **48,** 946–954 (2007).

121. Saadani-Makki, F. *et al.* Intrauterine administration of endotoxin leads to motor deficits in a rabbit model: a link between prenatal infection and cerebral palsy. *Am. J. Obstet. Gynecol.* **199,** 651.e1–651.e7 (2008).

122. Duncan, J. R. *et al.* Chronic endotoxin exposure causes brain injury in the ovine fetus in the absence of hypoxemia. *J. Soc. Gynecol. Investig.* **13,** 87–96 (2006).

123. Svedin, P., Kjellmer, I., Welin, A.-K., Blad, S. & Mallard, C. Maturational effects of lipopolysaccharide on white-matter injury in fetal sheep. *J. Child Neurol.* **20,** 960–964 (2005).

124. Rousset, C. I. *et al.* Maternal exposure to LPS induces hypomyelination in the internal capsule and programmed cell death in the deep gray matter in newborn rats. *Pediatr. Res.* **59,** 428–433 (2006).

125. Wang, X., Hagberg, H., Zhu, C., Jacobsson, B. & Mallard, C. Effects of intrauterine inflammation on the developing mouse brain. *Brain Res.* **1144,** 180–185 (2007).

126. Gilles, F. H., Averill, D. R. & Kerr, C. S. Neonatal endotoxin encephalopathy. *Ann. Neurol.* **2,** 49–56 (1977).

127. Eklind, S. *et al.* Bacterial endotoxin sensitizes the immature brain to hypoxic–ischaemic injury. *Eur. J. Neurosci.* **13,** 1101–1106 (2001).

128. Bilbo, S. D. *et al.* Neonatal Infection-Induced Memory Impairment after Lipopolysaccharide in Adulthood Is Prevented via Caspase-1 Inhibition. *J. Neurosci.* **25,** 8000–8009 (2005).

129. Eklind, S. *et al.* Effect of Lipopolysaccharide on Global Gene Expression in the Immature Rat Brain. *Pediatr. Res.* **60,** 161–168 (2006).

130. Wang, X. *et al.* White Matter Damage After Chronic Subclinical Inflammation in Newborn Mice. *J. Child Neurol.* **24,** 1171–1178 (2009).

131. Pang, Y., Cai, Z. & Rhodes, P. G. Disturbance of oligodendrocyte development, hypomyelination and white matter injury in the neonatal rat brain after intracerebral injection of lipopolysaccharide. *Dev. Brain Res.* **140,** 205–214 (2003).

132. Cai, Z., Pang, Y., Lin, S. & Rhodes, P. G. Differential roles of tumor necrosis factor-α and interleukin-1 β in lipopolysaccharide-induced brain injury in the neonatal rat. *Brain Res.* **975,** 37–47 (2003).

133. Ando, M., Takashima, S. & Mito, T. Endotoxin, cerebral blood flow, amino acids and brain damage in young rabbits. *Brain Dev.* **10,** 365–370 (1988).

134. Young, R. S., Hernandez, M. J. & Yagel, S. K. Selective reduction of blood flow to white matter during hypotension in newborn dogs: A possbile mechanism of periventricular leukomalacia. *Ann. Neurol.* **12,** 445–448 (1982).

135. Poltorak, A. Defective LPS Signaling in C3H/HeJ and C57BL/10ScCr Mice: Mutations in Tlr4 Gene. *Science* **282,** 2085–2088 (1998).

136. Kaur, C., Rathnasamy, G. & Ling, E.-A. Roles of Activated Microglia in Hypoxia Induced Neuroinflammation in the Developing Brain and the Retina. *J. Neuroimmune Pharmacol.* **8,** 66–78 (2013).

137. Larouche, A. *et al.* Neuronal Injuries Induced by Perinatal Hypoxic-Ischemic Insults Are Potentiated by Prenatal Exposure to Lipopolysaccharide: Animal Model for Perinatally Acquired Encephalopathy. *Dev. Neurosci.* **27,** 134–142 (2005).

138. Girard, S., Kadhim, H., Beaudet, N., Sarret, P. & Sébire, G. Developmental motor deficits induced by combined fetal exposure to lipopolysaccharide and early neonatal hypoxia/ischemia: A novel animal model for cerebral palsy in very premature infants. *Neuroscience* **158,** 673–682 (2009).

139. Eklind, S., Mallard, C., Arvidsson, P. & Hagberg, H. Lipopolysaccharide Induces Both a Primary and a Secondary Phase of Sensitization in the Developing Rat Brain. *Pediatr. Res.* **58,** 112–116 (2005).

140. Eklind, S., Arvidsson, P., Hagberg, H. & Mallard, C. The Role of Glucose in Brain Injury Following the Combination of Lipopolysaccharide or Lipoteichoic Acid and Hypoxia-Ischemia in Neonatal Rats. *Dev. Neurosci.* **26,** 61–67 (2004).

141. Wang, X. *et al.* Lipopolysaccharide Sensitizes Neonatal Hypoxic-Ischemic Brain Injury in a MyD88-Dependent Manner. *J. Immunol.* **183,** 7471–7477 (2009).

142. Brochu, M.-E., Girard, S., Lavoie, K. & Sébire, G. Developmental regulation of the neuroinflammatory responses to LPS and/or hypoxia-ischemia between preterm and term neonates: An experimental study. *J. Neuroinflammation* **8,** 55 (2011).

143. Shen, Y., Liu, X.-B., Pleasure, D. E. & Deng, W. Axon–glia synapses are highly vulnerable to white matter injury in the developing brain. *J. Neurosci. Res.* **90,** 105–121 (2012).

144. Liu, W., Shen, Y., Plane, J. M., Pleasure, D. E. & Deng, W. Neuroprotective potential of erythropoietin and its derivative carbamylated erythropoietin in periventricular leukomalacia. *Exp. Neurol.* **230,** 227–239 (2011).

145. Shen, Y., Plane, J. M. & Deng, W. Mouse Models of Periventricular Leukomalacia. *J. Vis. Exp. JoVE* (2010). doi:10.3791/1951

146. Lehnardt, S. *et al.* Activation of innate immunity in the CNS triggers neurodegeneration through a Toll-like receptor 4-dependent pathway. *Proc. Natl. Acad. Sci.* **100,** 8514–8519 (2003).

147. Loewith, R. A brief history of TOR. *Biochem. Soc. Trans.* **39,** 437–442 (2011).

148. RAPAMYCIN (AY-22, 989), A NEW ANTIFUNGAL ANTIBIOTIC. *J. Antibiot. (Tokyo)* 727 (2006). doi:10.7164/antibiotics.28.727

149. Eng, C., Sehgal, S. & Vezina, C. Activity of Rapamycin (AY-22.989) Against Transplanted Tumors. *J. Antibiot. (Tokyo)* **37,** 1231–1237 (1984).

150. Martel, R. R., Klicius, J. & Galet, S. Inhibition of the immune response by rapamycin, a new antifungal antibiotic. *Can. J. Physiol. Pharmacol.* **55,** 48–51 (1977).

151. Sabatini, D. M., Erdjument-Bromage, H., Lui, M., Tempst, P. & Snyder, S. H. RAFT1: A mammalian protein that binds to FKBP12 in a rapamycin-dependent fashion and is homologous to yeast TORs. *Cell* **78,** 35–43 (1994).

152. Sabers, C. J. *et al.* Isolation of a Protein Target of the FKBP12-Rapamycin Complex in Mammalian Cells. *J. Biol. Chem.* **270,** 815–822 (1995).

153. Heitman, J., Movva, N. R. & Hall, M. N. Targets for cell cycle arrest by the immunosuppressant rapamycin in yeast. *Science* **253,** 905–909 (1991).

154. Brown, E. J. *et al.* A mammalian protein targeted by G1-arresting rapamycin–receptor complex. *Nature* **369,** 756–758 (1994).

155. Abraham, R. T. & Wiederrecht, G. J. Immunopharmacology of Rapamycin. *Annu. Rev. Immunol.* **14,** 483–510 (1996).

156. Hay, N. & Sonenberg, N. Upstream and downstream of mTOR. *Genes Dev.* **18,** 1926–1945 (2004).

157. Sarbassov, D. D. *et al.* Prolonged Rapamycin Treatment Inhibits mTORC2 Assembly and Akt/PKB. *Mol. Cell* **22,** 159–168 (2006).

158. Lamming, D. W. *et al.* Rapamycin-Induced Insulin Resistance Is Mediated by mTORC2 Loss and Uncoupled from Longevity. *Science* **335,** 1638–1643 (2012).

159. Murakami, M. *et al.* mTOR Is Essential for Growth and Proliferation in Early Mouse Embryos and Embryonic Stem Cells. *Mol. Cell. Biol.* **24,** 6710–6718 (2004).

160. Gangloff, Y.-G. *et al.* Disruption of the Mouse mTOR Gene Leads to Early Postimplantation Lethality and Prohibits Embryonic Stem Cell Development. *Mol. Cell. Biol.* **24,** 9508–9516 (2004).

161. Crino, P. B. mTOR: A pathogenic signaling pathway in developmental brain malformations. *Trends Mol. Med.* **17,** 734–742 (2011).

162. Chong, Z. Z., Shang, Y. C., Wang, S. & Maiese, K. Shedding new light on neurodegenerative diseases through the mammalian target of rapamycin. *Prog. Neurobiol.* **99,** 128–148 (2012).

163. Dennis, P. B., Pullen, N., Kozma, S. C. & Thomas, G. The principal rapamycin-sensitive p70(s6k) phosphorylation sites, T-229 and T-389, are differentially regulated by rapamycin-insensitive kinase kinases. *Mol. Cell. Biol.* **16,** 6242–6251 (1996).

164. Roux, P. P. *et al.* RAS/ERK Signaling Promotes Site-specific Ribosomal Protein S6 Phosphorylation via RSK and Stimulates Cap-dependent Translation. *J. Biol. Chem.* **282,** 14056–14064 (2007).

165. Schumacher, A. M., Velentza, A. V., Watterson, D. M. & Dresios, J. Death-Associated Protein Kinase Phosphorylates Mammalian Ribosomal Protein S6 and Reduces Protein Synthesis†. *Biochemistry (Mosc.)* **45,** 13614–13621 (2006).

166. Gingras, A.-C., Kennedy, S. G., O'Leary, M. A., Sonenberg, N. & Hay, N. 4E-BP1, a repressor of mRNA translation, is phosphorylated and inactivated by the Akt(PKB) signaling pathway. *Genes Dev.* **12,** 502–513 (1998).

167. Gingras, A.-C. *et al.* Regulation of 4E-BP1 phosphorylation: a novel two-step mechanism. *Genes Dev.* **13,** 1422–1437 (1999).

168. Thoreen, C. C. *et al.* A unifying model for mTORC1-mediated regulation of mRNA translation. *Nature* **485,** 109–113 (2012).

169. Jefferies, H. B. J. *et al.* Rapamycin suppresses 5′TOP mRNA translation through inhibition of p70s6k. *EMBO J.* **16,** 3693–3704 (1997).

170. Schwab, M. S. *et al.* p70S6K Controls Selective mRNA Translation during Oocyte Maturation and Early Embryogenesis inXenopus laevis. *Mol. Cell. Biol.* **19,** 2485–2494 (1999).

171. Hsieh, A. C. *et al.* The translational landscape of mTOR signalling steers cancer initiation and metastasis. *Nature* **485,** 55–61 (2012).

172. Meyuhas, O. & Dreazen, A. in *Progress in Molecular Biology and Translational Science* **90,** 109–153 (Elsevier, 2009).

173. Düvel, K. *et al.* Activation of a Metabolic Gene Regulatory Network Downstream of mTOR Complex 1. *Mol. Cell* **39,** 171–183 (2010).

174. Yokogami, K., Wakisaka, S., Avruch, J. & Reeves, S. A. Serine phosphorylation and maximal activation of STAT3 during CNTF signaling is mediated by the rapamycin target mTOR. *Curr. Biol.* **10,** 47–50 (2000).

175. Weichhart, T. *et al.* The TSC-mTOR Signaling Pathway Regulates the Innate Inflammatory Response. *Immunity* **29,** 565–577 (2008).

176. Goncharova, E. A. *et al.* Signal Transducer and Activator of Transcription 3 Is Required for Abnormal Proliferation and Survival of TSC2-Deficient Cells: Relevance to Pulmonary Lymphangioleiomyomatosis. *Mol. Pharmacol.* **76,** 766–777 (2009).

177. Ben-Sahra, I., Howell, J. J., Asara, J. M. & Manning, B. D. Stimulation of de Novo Pyrimidine Synthesis by Growth Signaling Through mTOR and S6K1. *Science* **339,** 1323–1328 (2013).

178. Robitaille, A. M. *et al.* Quantitative Phosphoproteomics Reveal mTORC1 Activates de Novo Pyrimidine Synthesis. *Science* **339,** 1320–1323 (2013).

179. Lee, C.-H. *et al.* Constitutive mTOR activation in TSC mutants sensitizes cells to energy starvation and genomic damage via p53. *EMBO J.* **26,** 4812–4823 (2007).

180. Patel, P. H. & Tamanoi, F. Increased Rheb-TOR signaling enhances sensitivity of the whole organism to oxidative stress. *J. Cell Sci.* **119,** 4285–4292 (2006).

181. Inoki, K., Zhu, T. & Guan, K.-L. TSC2 Mediates Cellular Energy Response to Control Cell Growth and Survival. *Cell* **115,** 577–590 (2003).

182. Choo, A. Y. *et al.* Glucose Addiction of TSC Null Cells Is Caused by Failed mTORC1-Dependent Balancing of Metabolic Demand with Supply. *Mol. Cell* **38,** 487–499 (2010).

183. Ng, S., Wu, Y.-T., Chen, B., Zhou, J. & Shen, H.-M. Impaired autophagy due to constitutive mTOR activation sensitizes TSC2-null cells to cell death under stress. *Autophagy* **7,** 1173–1186 (2011).

184. Papadakis, M. *et al.* Tsc1 (hamartin) confers neuroprotection against ischemia by inducing autophagy. *Nat. Med.* **19,** 351–357 (2013).

185. Xia, D. Y. *et al.* Ischemia preconditioning is neuroprotective in a rat cerebral ischemic injury model through autophagy activation and apoptosis inhibition. *Braz. J. Med. Biol. Res.* **46,** 580–588 (2013).

186. Carloni, S., Buonocore, G. & Balduini, W. Protective role of autophagy in neonatal hypoxia–ischemia induced brain injury. *Neurobiol. Dis.* **32,** 329–339 (2008).

187. Carloni, S. *et al.* Activation of autophagy and Akt/CREB signaling play an equivalent role in the neuroprotective effect of rapamycin in neonatal hypoxia-ischemia. *Autophagy* **6,** 366–377 (2010).

188. Chen, H. *et al.* mTOR activates hypoxia-inducible factor-1α and inhibits neuronal apoptosis in the developing rat brain during the early phase after hypoxia–ischemia. *Neurosci. Lett.* **507,** 118–123 (2012).

189. Xie, R. *et al.* Mammalian Target of Rapamycin Cell Signaling Pathway Contributes to the Protective Effects of Ischemic Postconditioning Against. *Stroke* **45,** 2769–2776 (2014).

190. Xiong, X. *et al.* PRAS40 plays a pivotal role in protecting against stroke by linking the Akt and mTOR pathways. *Neurobiol. Dis.* **66,** 43–52 (2014).

191. Koh, P.-O. *et al.* Estradiol attenuates the focal cerebral ischemic injury through mTOR/p70S6 kinase signaling pathway. *Neurosci. Lett.* **436,** 62–66 (2008).

192. Shi, G. D. *et al.* PTEN deletion prevents ischemic brain injury by activating the mTOR signaling pathway. *Biochem. Biophys. Res. Commun.* **404,** 941–945 (2011).

193. Pattingre, S., Espert, L., Biard-Piechaczyk, M. & Codogno, P. Regulation of macroautophagy by mTOR and Beclin 1 complexes. *Biochimie* **90,** 313–323 (2008).

194. Jung, C. H., Ro, S.-H., Cao, J., Otto, N. M. & Kim, D.-H. mTOR regulation of autophagy. *FEBS Lett.* **584,** 1287–1295 (2010).

195. Jung, C. H. *et al.* ULK-Atg13-FIP200 Complexes Mediate mTOR Signaling to the Autophagy Machinery. *Mol. Biol. Cell* **20,** 1992–2003 (2009).

196. Hosokawa, N. *et al.* Nutrient-dependent mTORC1 Association with the ULK1–Atg13–FIP200 Complex Required for Autophagy. *Mol. Biol. Cell* **20,** 1981–1991 (2009).

197. Kuma, A. *et al.* The role of autophagy during the early neonatal starvation period. *Nature* **432,** 1032–1036 (2004).

198. Buckley, K. M. *et al.* Rapamycin up-regulation of autophagy reduces infarct size and improves outcomes in both permanent MCAL, and embolic MCAO, murine models of stroke. *Exp. Transl. Stroke Med.* **6,** 8 (2014).

199. Miller, J. L. Sirolimus approved with renal transplant indication. *J. Health-Syst. Pharm.* **56,** 2177–2178 (1999).

200. Morice, W. G., Brunn, G. J., Wiederrecht, G., Siekierka, J. J. & Abraham, R. T. Rapamycin-induced inhibition of p34cdc2 kinase activation is associated with G1/S-phase growth arrest in T lymphocytes. *J. Biol. Chem.* **268,** 3734–3738 (1993).

201. Delgoffe, G. M. *et al.* The mTOR Kinase Differentially Regulates Effector and Regulatory T Cell Lineage Commitment. *Immunity* **30,** 832–844 (2009).

202. Delgoffe, G. M. *et al.* The kinase mTOR regulates the differentiation of helper T cells through the selective activation of signaling by mTORC1 and mTORC2. *Nat. Immunol.* **12,** 295–303 (2011).

203. Battaglia, M. Rapamycin selectively expands CD4+CD25+FoxP3+ regulatory T cells. *Blood* **105,** 4743–4748 (2005).

204. Powell, J. D., Pollizzi, K. N., Heikamp, E. B. & Horton, M. R. Regulation of Immune Responses by mTOR. *Annu. Rev. Immunol.* **30,** 39–68 (2012).

205. Xie, L. *et al.* mTOR Signaling Inhibition Modulates Macrophage/Microglia-Mediated Neuroinflammation and Secondary Injury via Regulatory T Cells after Focal Ischemia. *J. Immunol.* **192,** 6009–6019 (2014).

206. Czeh, M., Gressens, P. & Kaindl, A. M. The Yin and Yang of Microglia. *Dev. Neurosci.* **33,** 199–209 (2011).

207. Kaur, C. & Ling, E. A. Periventricular white matter damage in the hypoxic neonatal brain: Role of microglial cells. *Prog. Neurobiol.* **87,** 264–280 (2009).

208. McRae, A., Gilland, E., Bona, E. & Hagberg, H. Microglia activation after neonatal hypoxic-ischemia. *Dev. Brain Res.* **84,** 245–252 (1995).

209. Dello Russo, C., Lisi, L., Tringali, G. & Navarra, P. Involvement of mTOR kinase in cytokine-dependent microglial activation and cell proliferation. *Biochem. Pharmacol.* **78,** 1242–1251 (2009).

210. Lu, D.-Y., Liou, H.-C., Tang, C.-H. & Fu, W.-M. Hypoxia-induced iNOS expression in microglia is regulated by the PI3-kinase/Akt/mTOR signaling pathway and activation of hypoxia inducible factor-1α. *Biochem. Pharmacol.* **72,** 992–1000 (2006).

211. Kjell, J., Codeluppi, S., Josephson, A. & Abrams, M. B. Spatial and Cellular Characterization of mTORC1 Activation after Spinal Cord Injury Reveals Biphasic Increase Mainly Attributed to Microglia/Macrophages. *Brain Pathol. Zurich Switz.* **24,** 557–567 (2014).

212. Park, J. *et al.* Combination therapy targeting Akt and mammalian target of rapamycin improves functional outcome after controlled cortical impact in mice. *J. Cereb. Blood Flow Metab.* **32,** 330–340 (2012).

213. Erlich, S., Alexandrovich, A., Shohami, E. & Pinkas-Kramarski, R. Rapamycin is a neuroprotective treatment for traumatic brain injury. *Neurobiol. Dis.* **26,** 86–93 (2007).

214. Johnston, M. V. & Hoon, A. H. Cerebral Palsy. *NeuroMolecular Med.* **8,** 435–450 (2006).

215. Honeycutt, A. *et al. Economic Costs Associated with Mental Retardation, Cerebral Palsy, Hearing Loss, and Vision Impairment - United States, 2003*. 57–9 (U.S. Center for Disease Control, 2004). at <http://search.proquest.com/docview/203707639>

216. Talos, D. M. *et al.* The Interaction between Early Life Epilepsy and Autistic-Like Behavioral Consequences: A Role for the Mammalian Target of Rapamycin (mTOR) Pathway. *PLoS ONE* **7,** e35885 (2012).

217. Curatolo, P., Seri, S., Verdecchia, M. & Bombardieri, R. Infantile spasms in tuberous sclerosis complex. *Brain Dev.* **23,** 502–507 (2001).

218. Zeng, L.-H., Xu, L., Gutmann, D. H. & Wong, M. Rapamycin prevents epilepsy in a mouse model of tuberous sclerosis complex. *Ann. Neurol.* **63,** 444–453 (2008).

219. Sharma, A. *et al.* Dysregulation of mTOR Signaling in Fragile X Syndrome. *J. Neurosci.* **30,** 694–702 (2010).

220. Goorden, S. M. I., van Woerden, G. M., van der Weerd, L., Cheadle, J. P. & Elgersma, Y. Cognitive deficits in Tsc1+/−mice in the absence of cerebral lesions and seizures. *Ann. Neurol.* **62,** 648–655 (2007).

221. Gu, Q., Schmued, L. C., Sarkar, S., Paule, M. G. & Raymick, B. One-step labeling of degenerative neurons in unfixed brain tissue samples using Fluoro-Jade C. *J. Neurosci. Methods* **208,** 40–43 (2012).

222. Schmued, L. C., Albertson, C. & Slikker, W., Jr. Fluoro-Jade: a novel fluorochrome for the sensitive and reliable histochemical localization of neuronal degeneration. *Brain Res.* **751,** 37–46 (1997).

223. Delaporte, B., Labrune, M., Imbert, M. C. & Dehan, M. Early echographic findings in non-hemorrhagic periventricular leukomalacia of the premature infant. *Pediatr. Radiol.* **15,** 82–84 (1985).

224. Hu, Y. *et al.* A rat pup model of cerebral palsy induced by prenatal inflammation and hypoxia. *Neural Regen. Res.* **8,** (2013).

225. Lein, E. S. *et al.* Genome-wide atlas of gene expression in the adult mouse brain. *Nature* **445,** 168–176 (2007).

226. Shioi, T. *et al.* Rapamycin Attenuates Load-Induced Cardiac Hypertrophy in Mice. *Circulation* **107,** 1664–1670 (2003).

227. Shima, H. *et al.* Disruption of the p70s6k/p85s6k gene reveals a small mouse phenotype and a new functional S6 kinase. *EMBO J.* **17,** 6649–6659 (1998).

228. Houde, V. P. *et al.* Chronic Rapamycin Treatment Causes Glucose Intolerance and Hyperlipidemia by Upregulating Hepatic Gluconeogenesis and Impairing Lipid Deposition in Adipose Tissue. *Diabetes* **59,** 1338–1348 (2010).

229. Auer, R. N., Jensen, M. L. & Whishaw, I. Q. Neurobehavioral deficit due to ischemic brain damage limited to half of the CA1 sector of the hippocampus. *J. Neurosci.* **9,** 1641–1647 (1989).

230. Schmidt-Kastner, R. & Freund, T. F. Selective vulnerability of the hippocampus in brain ischemia. *Neuroscience* **40,** 599–636 (1991).

231. Sugawara, T., Lewén, A., Noshita, N., Gasche, Y. & Chan, P. H. Effects of Global Ischemia Duration on Neuronal, Astroglial, Oligodendroglial, and Microglial Reactions in the Vulnerable Hippocampal CA1 Subregion in Rats. *J. Neurotrauma* **19,** 85–98 (2002).

232. Rees, S. & Inder, T. Fetal and neonatal origins of altered brain development. *Early Hum. Dev.* **81,** 753–761 (2005).

233. Rami, A., Sims, J., Botez, G. & Winckler, J. Spatial resolution of phospholipid scramblase 1 (PLSCR1), caspase-3 activation and DNA-fragmentation in the human hippocampus after cerebral ischemia. *Neurochem. Int.* **43,** 79–87 (2003).

234. Horn, M. & Schlote, W. Delayed neuronal death and delayed neuronal recovery in the human brain following global ischemia. *Acta Neuropathol. (Berl.)* **85,** 79–87 (1992).

235. Fujioka, M. *et al.* Hippocampal Damage in the Human Brain after Cardiac Arrest. *Cerebrovasc. Dis.* **10,** 2–7 (2000).

236. Stevens, C. *et al.* Peptide Combinatorial Libraries Identify TSC2 as a Death-associated Protein Kinase (DAPK) Death Domain-binding Protein and Reveal a Stimulatory Role for DAPK in mTORC1 Signaling. *J. Biol. Chem.* **284,** 334–344 (2009).

237. Lin, Y., Hupp, T. R. & Stevens, C. Death-associated protein kinase (DAPK) and signal transduction: additional roles beyond cell death. *FEBS J.* **277,** 48–57 (2010).

238. Brugarolas, J. *et al.* Regulation of mTOR function in response to hypoxia by REDD1 and the TSC1/TSC2 tumor suppressor complex. *Genes Dev.* **18,** 2893–2904 (2004).

239. Hudson, C. C. *et al.* Regulation of Hypoxia-Inducible Factor 1α Expression and Function by the Mammalian Target of Rapamycin. *Mol. Cell. Biol.* **22,** 7004–7014 (2002).

240. Zhong, H. *et al.* Modulation of hypoxia-inducible factor 1alpha expression by the epidermal growth factor/phosphatidylinositol 3-kinase/PTEN/AKT/FRAP pathway in human prostate cancer cells: implications for tumor angiogenesis and therapeutics. *Cancer Res.* **60,** 1541–1545 (2000).

241. Kim, J.-H., Yoon, M.-S. & Chen, J. Signal Transducer and Activator of Transcription 3 (STAT3) Mediates Amino Acid Inhibition of Insulin Signaling through Serine 727 Phosphorylation. *J. Biol. Chem.* **284,** 35425–35432 (2009).

242. Levine, B. & Klionsky, D. J. Development by Self-Digestion: Molecular Mechanisms and Biological Functions of Autophagy. *Dev. Cell* **6,** 463–477 (2004).

243. Kiffin, R., Bandyopadhyay, U. & Cuervo, A. M. Oxidative Stress and Autophagy. *Antioxid. Redox Signal.* **8,** 152–162 (2006).

244. Wu, Y.-T., Tan, H.-L., Huang, Q., Ong, C.-N. & Shen, H.-M. Activation of the PI3K-Akt-mTOR signaling pathway promotes necrotic cell death via suppression of autophagy. *Autophagy* **5,** 824–834 (2009).

245. Shamloo, M. *et al.* Death-associated Protein Kinase Is Activated by Dephosphorylation in Response to Cerebral Ischemia. *J. Biol. Chem.* **280,** 42290–42299 (2005).

246. Fujita, Y. & Yamashita, T. Role of DAPK in neuronal cell death. *Apoptosis* **19,** 339–345 (2014).

247. DeYoung, M. P., Horak, P., Sofer, A., Sgroi, D. & Ellisen, L. W. Hypoxia regulates TSC1/2-mTOR signaling and tumor suppression through REDD1-mediated 14-3-3 shuttling. *Genes Dev.* **22,** 239–251 (2008).

248. Schwarzer, R. *et al.* REDD1 integrates hypoxia-mediated survival signaling downstream of phosphatidylinositol 3-kinase. *Oncogene* **24,** 1138–1149 (2004).

249. Dennis, M. D., McGhee, N. K., Jefferson, L. S. & Kimball, S. R. Regulated in DNA damage and development 1 (REDD1) promotes cell survival during serum deprivation by sustaining repression of signaling through the mechanistic target of rapamycin in complex 1 (mTORC1). *Cell. Signal.* **25,** 2709–2716 (2013).

250. Fleiss, B. & Gressens, P. Tertiary mechanisms of brain damage: a new hope for treatment of cerebral palsy? *Lancet Neurol.* **11,** 556–566 (2012).

251. Przanowski, P. *et al.* The signal transducers Stat1 and Stat3 and their novel target Jmjd3 drive the expression of inflammatory genes in microglia. *J. Mol. Med.* **92,** 239–254 (2013).

252. Maxwell, P. H. *et al.* The tumour suppressor protein VHL targets hypoxia-inducible factors for oxygen-dependent proteolysis. *Nature* **399,** 271–275 (1999).

253. Jaakkola, P. *et al.* Targeting of HIF-α to the von Hippel-Lindau Ubiquitylation Complex by O2-Regulated Prolyl Hydroxylation. *Science* **292,** 468–472 (2001).

254. Sheldon, R. A., Lee, C. L., Jiang, X., Knox, R. N. & Ferriero, D. M. Hypoxic preconditioning protection is eliminated in HIF-1α knockout mice subjected to neonatal hypoxia-ischemia. *Pediatr. Res.* **76,** 46–53 (2014).

255. Chen, W., Jadhav, V., Tang, J. & Zhang, J. H. in *Acta Neurochirurgica Supplements* 395–399 (Springer, 2009). at <http://link.springer.com/chapter/10.1007/978-3-211-85578-2_77>

256. Pearce, L. R. *et al.* Characterization of PF-4708671, a novel and highly specific inhibitor of p70 ribosomal S6 kinase (S6K1). *Biochem. J.* **431,** 245–255 (2010).

257. Di, R. *et al.* S6K inhibition renders cardiac protection against myocardial infarction through PDK1 phosphorylation of Akt. *Biochem. J.* **441,** 199–207 (2012).

258. Horak, P. *et al.* Negative feedback control of HIF-1 through REDD1-regulated ROS suppresses tumorigenesis. *Proc. Natl. Acad. Sci.* **107,** 4675–4680 (2010).

259. Shoshani, T. *et al.* Identification of a Novel Hypoxia-Inducible Factor 1-Responsive Gene, RTP801, Involved in Apoptosis. *Mol. Cell. Biol.* **22,** 2283–2293 (2002).

260. Jin, H.-O. *et al.* Hypoxic condition- and high cell density-induced expression of Redd1 is regulated by activation of hypoxia-inducible factor-1α and Sp1 through the phosphatidylinositol 3-kinase/Akt signaling pathway. *Cell. Signal.* **19,** 1393–1403 (2007).

261. Canal, M., Romaní-Aumedes, J., Martín-Flores, N., Pérez-Fernández, V. & Malagelada, C. RTP801/REDD1: a stress coping regulator that turns into a

troublemaker in neurodegenerative disorders. *Front. Cell. Neurosci.* **8,** 313 (2014).

262. Romaní-Aumedes, J. *et al.* Parkin loss of function contributes to RTP801 elevation and neurodegeneration in Parkinson's disease. *Cell Death Dis.* **5,** e1364 (2014).

263. Ohanna, M. *et al.* Atrophy of S6K1-/- skeletal muscle cells reveals distinct mTOR effectors for cell cycle and size control. *Nat. Cell Biol.* **7,** 286–294 (2005).

264. Dowling, R. J. O. *et al.* mTORC1-Mediated Cell Proliferation, But Not Cell Growth, Controlled by the 4E-BPs. *Science* **328,** 1172–1176 (2010).

265. Choo, A. Y., Yoon, S.-O., Kim, S. G., Roux, P. P. & Blenis, J. Rapamycin differentially inhibits S6Ks and 4E-BP1 to mediate cell-type-specific repression of mRNA translation. *Proc. Natl. Acad. Sci.* **105,** 17414–17419 (2008).

266. Kang, S. A. *et al.* mTORC1 Phosphorylation Sites Encode Their Sensitivity to Starvation and Rapamycin. *Science* **341,** 1236566 (2013).

267. Dodd, K. M., Yang, J., Shen, M. H., Sampson, J. R. & Tee, A. R. mTORC1 drives HIF-1α and VEGF-A signalling via multiple mechanisms involving 4E-BP1, S6K1 and STAT3. *Oncogene* (2014). doi:10.1038/onc.2014.164

268. Cherry, J. D., Olschowka, J. A. & O'Banion, M. K. Neuroinflammation and M2 microglia: the good, the bad, and the inflamed. *J. Neuroinflammation* **11,** 98 (2014).

269. Hu, X. *et al.* Microglia/Macrophage Polarization Dynamics Reveal Novel Mechanism of Injury Expansion After Focal Cerebral Ischemia. *Stroke* **43,** 3063–3070 (2012).

270. Simons, M. & Trajkovic, K. Neuron-glia communication in the control of oligodendrocyte function and myelin biogenesis. *J. Cell Sci.* **119,** 4381–4389 (2006).

271. Demerens, C. *et al.* Induction of myelination in the central nervous system by electrical activity. *Proc. Natl. Acad. Sci.* **93,** 9887–9892 (1996).

272. Malone, M. *et al.* Neuronal activity promotes myelination via a cAMP pathway. *Glia* **61,** 843–854 (2013).

273. Gary, D. S., Malone, M., Capestany, P., Houdayer, T. & McDonald, J. W. Electrical stimulation promotes the survival of oligodendrocytes in mixed cortical cultures. *J. Neurosci. Res.* **90,** 72–83 (2012).

274. Silbereis, J. C., Huang, E. J., Back, S. A. & Rowitch, D. H. Towards improved animal models of neonatal white matter injury associated with cerebral palsy. *Dis. Model. Mech.* **3,** 678–688 (2010).

275. Back, S. A. & Miller, S. P. Brain injury in premature neonates: A primary cerebral dysmaturation disorder? *Ann. Neurol.* **75,** 469–486 (2014).

276. Wood, T. L. *et al.* mTOR: A Link from the Extracellular Milieu to Transcriptional Regulation of Oligodendrocyte Development. *ASN Neuro* **5,** AN20120092 (2013).

277. Lebrun-Julien, F. *et al.* Balanced mTORC1 Activity in Oligodendrocytes Is Required for Accurate CNS Myelination. *J. Neurosci.* **34,** 8432–8448 (2014).

278. Yuen, T. J. *et al.* Oligodendrocyte-Encoded HIF Function Couples Postnatal Myelination and White Matter Angiogenesis. *Cell* **158,** 383–396 (2014).

279. Favrais, G. *et al.* Systemic inflammation disrupts the developmental program of white matter. *Ann. Neurol.* **70,** 550–565 (2011).

280. Buser, J. R. *et al.* Arrested preoligodendrocyte maturation contributes to myelination failure in premature infants. *Ann. Neurol.* **71,** 93–109 (2012).

281. Rapamune (sirolimus). at <http://www.fda.gov/ohrms/dockets/ac/02/briefing/3832b1_03_FDA-RapamuneLabel.htm>

282. Chu, S.-H., Liu, K.-L., Chiang, Y.-J., Wang, H.-H. & Lai, P.-C. Sirolimus used during pregnancy in a living related renal transplant recipient: a case report. *Transplant. Proc.* **40,** 2446–2448 (2008).

283. Framarino dei Malatesta, M. *et al.* Successful Pregnancy in a Living-Related Kidney Transplant Recipient Who Received Sirolimus Throughout the Whole Gestation: *Transplantation* **91,** e69–e71 (2011).

284. Guardia, O., Rial, M. del C. & Casadei, D. Pregnancy under Sirolimus-Based Immunosuppression: *Transplantation* **81,** 636 (2006).

285. Veroux, M., Corona, D. & Veroux, P. Pregnancy under everolimus-based immunosuppression. *Transpl. Int.* **24,** e115–e117 (2011).

286. Jankowska, I. *et al.* Absence of teratogenicity of sirolimus used during early pregnancy in a liver transplant recipient. *Transplant. Proc.* **36,** 3232–3233 (2004).

287. Armenti, V. *et al.* Report from the National Transplantation Pregnancy Registry (NTPR): outcomes of pregnancy after transplantation. *Clin. Transpl.* 69–83 (2004).

288. Everolimus for Tuberous Sclerosis Complex (TSC). at <http://www.fda.gov/Drugs/InformationOnDrugs/ApprovedDrugs/ucm317490.htm>

289. El-Sabrout, R. *et al.* Rejection-free protocol using sirolimus-tacrolimus combination for pediatric renal transplant recipients. in *Transplantation proceedings* **34,** 1942–1943 (Elsevier, 2002).

290. Lam, C. *et al.* Rapamycin (sirolimus) in tuberous sclerosis associated pediatric central nervous system tumors. *Pediatr. Blood Cancer* **54,** 476–479 (2010).

291. Lobach, N. E., Pollock-Barziv, S. M., West, L. J. & Dipchand, A. I. Sirolimus immunosuppression in pediatric heart transplant recipients: a single-center experience. *J. Heart Lung Transplant. Off. Publ. Int. Soc. Heart Transplant.* **24,** 184–189 (2005).